SOL-GEL-DERIVED MATERIALS FOR ANTIMICROBIAL COATINGS AND ELECTROCHEMICAL NITRIC OXIDE ANALYSIS

Benjamin J. Privett

A dissertation submitted to the faculty of the University of North Carolina at Chapel Hill in the partial fulfillment of the requirements for the degree of Doctor of Philosophy in the Department of Chemistry (Analytical Chemistry).

Chapel Hill
2011

Approved by:

Mark H. Schoenfisch

R. Mark Wightman

J. Michael Ramsey

Linda L. Spremulli

Wei You

ABSTRACT

Benjamin J. Privett: Sol-Gel-Derived Materials for Antimicrobial Coatings and Electrochemical Nitric Oxide Analysis
(Under the direction of Professor Mark H. Schoenfisch)

Sol-gel-derived coatings modified to release nitric oxide (NO), an endogenous broad-spectrum antimicrobial, have been described as highly promising antimicrobial biomaterials. As part of my thesis work, I extended the study of the antimicrobial properties of NO-releasing xerogels against the adhesion, viability, and biofilm formation of the pathogenic fungus, *Candida albicans.* Nitric oxide fluxes as low as 14 pmol cm^{-2} s^{-1} proved sufficient to reduce fungal adhesion by ~49% over controls (non-NO-releasing substrates) after 90 min of exposure. By utilizing a fluorescence live/dead assay and replicate plating, the NO flux was determined to reduce fungal viability in a dose-dependent manner. Likewise, the formation of *C. albicans* biofilms on NO-releasing xerogel-coated silicon rubber (SiR) coupons was impeded when compared to control and bare SiR surfaces.

To begin an examination of the likelihood of exogenous NO fostering NO resistance, bacteria were exposed to NO in long- and short-term mutagenesis assays. Even after 20 d of continuous sub-therapeutic exposure, resistance to NO was not observed for gram-positive and -negative species.

The next phase of my research thus focused on the synthesis of superhydrophobic xerogel coatings from a mixture of nanostructured fluorinated silica colloids,

fluoroalkoxysilane, and a backbone silane. Quantitative bacterial adhesion studies performed using a parallel plate flow cell demonstrated that the adhesion of *Staphylococcus aureus* and *Pseudomonas aeruginosa* were reduced by 2.08 ± 0.25 and 1.76 ± 0.12 log over controls, respectively. The straightforward and mild synthesis of this chemistry enables its application to any surface regardless of geometry making such interfaces ideal as biopassivation strategies.

Along with NO's ability to serve a potent exogenous antimicrobial, endogenous NO serves many important physiological roles (e.g., immune response, vasodilatation, neurotransmission). The final phase of my dissertation research focused on the development of microfluidic NO sensors capable of selectively measuring NO in small volumes (<1 mL). The final device enabled sensitive NO detection in PBS, blood, and simulated wound fluid at concentrations as low as 0.7–2.0 nM. Future studies using this device may prove useful clinically.

DEDICATION

This work is dedicated to Megan, who was always there to listen to my complaints, encourage me after failures, and celebrate with me after successes, and to my family, who always encouraged me to pursue whatever career that would make me happy.

ACKNOWLEDGEMENTS

This work would not have been possible without the assistance of a many colleagues, collaborators, friends, and family members. I would firstly like to thank my adviser, Professor Mark Schoenfisch, for encouraging me to take risks by exploring other fields outside of analytical chemistry and for trying to instill in me an attention to detail in my work. Graduate school was a difficult road, but in retrospect it certainly helped to have someone reminding me to not take myself too seriously, to grow a thicker skin, and to always strive for excellence.

In each project that I undertook, I relied on many collaborators, colleagues, and employees of the Department of Chemistry for their expertise. The superhydrophobic studies were conducted in collaboration with Dr. Jae Ho Shin and his students at Kwangwoon University in Seoul, Korea. I would also like to thank Katey Reighard for her time spent performing AFM measurements on superhydrophobic surfaces. The NO-resistant bacteria studies were the result of collaboration with Dr. Susanne Bauman at Novan, Inc. I am grateful for the time that Dan Riccio spent synthesizing nanoparticles used in the study. Likewise, I am thankful for the significant time Angela Broadnax spent both making therapeutics and performing resistance assays. Microfluidic NO sensor studies were performed in collaboration with Dr. Mike Ramsey and Dr. William H. Henley at the University of North Carolina at Chapel Hill. I am also grateful for having the opportunity to work with three outstanding undergraduates: Chris Chouinard, Steven

Nutz, and Anirudh Gowd. Steven was instrumental in performing adhesion assays for the *C. albicans* project and Anirudh conducted many of the electrochemical sensor experiments for the NO sensor project. Finally, I would like to thank the support staff in the Department of Chemistry for their assistance and training, particularly Bob Geil and Wallace Ambrose at CHANL.

I am very grateful for the friendship and support of my colleagues in the Schoenfisch Lab, and for those who edited my papers and chapters. I am lucky and blessed to be able to consider all of you to be a part of my family.

TABLE OF CONTENTS

LIST OF TABLES ……xii

LIST OF SCHEME …….xiii

LIST OF FIGURES …….xiv

LIST OF ABBREVIATIONS AND SYMBOLS ……..xviii

CHAPTER 1. INTRODUCTION: RECENT ADVANCES IN ANTIMICROBIAL COATINGS AND NITRIC OXIDE DETECTION ……...……...1

1.1 Antimicrobial coatings for biomedical applications ……1

1.1.1 Polymer coatings ……4

1.1.2 Antimicrobial-releasing coatings ……..6

1.1.3 Nitric oxide-releasing coatings …….9

1.1.4 Resistance to antimicrobials ……..…..……11

1.1.5 Superhydrophobic coatings ……..…12

1.2 Nitric oxide detection ……..…..……..15

1.2.1 Indirect detection of NO ……..……...16

1.2.2 Direct detection of NO ……..……..17

1.2.3 Electrode materials ……..……17

1.2.4 Electroactive biological interferences ……...……18

1.2.5 Sensor classification …….……..19

1.2.6 Modes of NO detection …….…….……23

1.2.7 Nitric oxide measurements in biological systems ……..…….....27

1.3 Summary of Dissertation Research …….……..31

1.4 References …….……34

CHAPTER 2. EFFICACY OF SURFACE-GENERATED NITRIC OXIDE AGAINST *CANDIDA ALBICANS* ADHESION AND BIOFILM FORMATION ……...……...……..47

2.1 Introduction ……47

2.2 Materials and Methods ……..…..……..49

2.2.1 Synthesis of AHAP3/BTMOS xerogel-coated films …...……..…...50

2.2.2 Diazeniumdiolate modification of xerogels ……..……..51

2.2.3 Growth of standardized *C. albicans* suspension …...……..……51

2.2.4 Determination of fungal efficacy of AgSD ….……...……52

2.2.5 Flow cell-based fungal adhesion studies …….52

2.2.6 Fluorescence-based qualitative viability studies …….53

2.2.7 Quantitative viability studies ……..54

2.2.8 Efficacy of surface-generated NO against fungal biofilms …….55

2.3 Results and Discussion …….……..55

2.3.1 Nitric oxide release …….55

2.3.2 Flow cell-based fungal adhesion studies ..……...56

2.3.3 Fungal viability studies ……...65

2.3.4 Efficacy of surface-generated NO against fungal biofilms …….72

2.4 Conclusions ..……..……74

2.5 References ……..75

CHAPTER 3. ANTIBACTERIAL FLUORINATED SUPERHYDROPHOBIC SILICA SURFACES ……80

3.1 Introduction ……...80

3.2 Materials and Methods ……..…..……...82

3.2.1 Silica colloid synthesis ……..……..…...82

3.2.2 Sol-gel film synthesis ..……...……..82

3.2.3 Sol-gel film characterization ……..……82

3.2.4 Bacterial adhesion and viability assay ……...……83

3.3 Results and Discussion …….……..84

3.3.1 Coating synthesis ……84

3.3.2 Surface characterization ……..84

3.3.3 Bacterial adhesion and viability assay ……92

3.4 Conclusions ..…….……98

3.5 References ……..99

CHAPTER 4. EXAMINATION OF BACTERIAL RESISTANCE TO EXOGENOUS NITRIC OXIDE ..……...……102

4.1 Introduction ……102

4.2 Materials and Methods ……..…..……103

4.2.1 Strains, media, and chemical reagents …..…….....……..….103

4.2.2 Synthesis of mercaptosilane-based silica particles ……...104

4.2.3 Nitrosation of mercaptosilane-based silica particles ...……..……104

4.2.4 Nitric oxide release characterization …….……...……..……..105

4.2.5 Minimum inhibitory concentration assay …….105

4.2.6 Spontaneous resistance assay ……...105

4.2.7 Serial passage assay ……..106

4.3 Results and Discussion ……..……106

4.3.1 Minimum inhibitory concentration determinations ……109

4.3.2 Spontaneous mutagenesis assay ……..…….109

4.3.3 Serial passage assay ……..……112

4.4 Conclusions ..…….…….…..117

4.5 References ……119

CHAPTER 5. MICROFLUIDIC NITRIC OXIDE SENSOR FOR BIOLOGICAL APPLICATIONS ……..…….125

5.1 Introduction ……..125

5.2 Materials and Methods ……..…..…….128

5.2.1 Preparation of working electrodes ……128

5.2.2 Electrode characterization ……..……..…….129

5.2.3 Membrane synthesis and characterization ……130

5.2.4 Microfluidic device fabrication ……..…….....…..130

5.2.5 Microfluidic device characterization ….……...131

5.3 Results and Discussion ……..……132

5.3.1 Working electrode fabrication and characterization ……132

5.3.2 Membrane deposition and characterization ……..134

5.3.3 Reference electrode fabrication and characterization ……...140

5.3.4 Microfluidic device assembly ……..……...……..143

5.3.5 Microfluidic device characterization ……144

5.3.6 Microfluidic sensor response in physiological fluids ……...151

5.4 Conclusions ..……..…..156

5.5 References ……158

CHAPTER 6. SUMMARY AND FUTURE RESEARCH DIRECTIONS ……...164

6.1 Summary …..……164

6.2 Future research directions ……..…..……166

6.3 Conclusions ……..169

6.4 References ……171

LIST OF TABLES

Table 1.1. Possible interfering species and their physiological concentrations during the electrochemical NO measurements ……...20

Table 2.1. Average (from n=3) nitric oxide release at 25 and 37 ºC 10-40% AHAP3 xerogels (balance BTMOS, v/v) in PBS (pH 7.4). *Total NO release over …..…….58

Table 2.2. *C. albicans* percent surface coverage to AHAP3 xerogels (balance BTMOS) under flowing conditions (0.2 mL/min) and calculated reduction in surface coverages to 10-40% AHAP3 xerogels over controls (non-NO-releasing) ……..…..……...59

Table 3.1. Static water contact angle measurements ……...90

Table 4.1. Minimum inhibitory concentrations of 75 mol% MPTMS/TEOS particles in TSB at 37 °C for 24 h and spontaneous mutation parameters before and after exposure to inhibitory concentrations of NO …….113

Table 4.2. Minimum inhibitory concentrations of 75 mol% MTPMS/TEOS particles after 1 and 20 passages .....……..116

Table 5.1. Electrode sensitivity and limit of detection for NO as a function of widths between bare platinum (Pt) and platinum-black-coated (PtB) electrodes……...…....138

LIST OF SCHEMES

Scheme 5.1. Electrochemical platinization reactions ..……..……137

LIST OF FIGURES

Figure 1.1. Stages of *C. albicans* biofilm development on a substrate ……...3

Figure 1.2. Illustration of *N*-diazeniumdiolate formation on a secondary amine via exposure to high pressure NO and subsequent proton-triggered NO release ……...10

Figure 1.3. Illustration of the "self-cleaning" mechanism of a superhydrophobic surface ……...14

Figure 1.4. Schematic diagrams of (a) Shibuki-style, (b) solid permselective, and (c) solid catalytic NO sensors ……..21

Figure 1.5. Structure of the polymeric cation exchanger Nafion ……..25

Figure 2.1. Illustration of parallel-plate flow cell adhesion assay ……60

Figure 2.2. *C. albicans* adhesion to xerogel-coated glass slides under flowing conditions (0.2 mL/min). Nitric oxide flux was varied by using 10% (●), 20% (▲), 30% (▼), and 40% (♦) AHAP3 xerogels (balance BTMOS, v/v). Control xerogels of all compositions were averaged (■) as surface coverage values at each timepoint were identical (within error) ……61

Figure 2.3. Digitally thresholded phase contrast optical micrographs of *C. albicans* adhesion to control (A), and NO-releasing 20% (B), and 40% (C) AHAP3 xerogels (balance BTMOS, v/v) following 150 minutes of fungal exposure under flowing conditions (flow rate: 0.2 mL/min) ……...62

Figure 2.4. *C. albicans* adhesion to PVC-coated control (■) and NO-releasing (●) 40% AHAP3 xerogels (balance BTMOS, v/v) under flowing conditions (0.2 mL/min) ……..63

Figure 2.5. *C. albicans* adhesion to control (■ and ▲) and NO-releasing (● and ▼) 40% AHAP3 xerogels (balance BTMOS, v/v) under flowing conditions at a flow rate 0.2 mL/min (■ and ●) and 0.6 mL/min (▲ and ▼) …..……...….64

Figure 2.6. Representative brightfield (A and D), syto 9 fluorescence (B and E), and propidium iodide fluorescence (C and F) optical micrographs (10x magnification) of *C. albicans* adhered to control 40% AHAP3 xerogels (balance BTMOS, v/v) taken immediately after preparation (A-C), and after 15 h incubation (D-F) in PBS (pH 7.4) ……...……...66

Figure 2.7. Representative brightfield (A and D), syto 9 fluorescence (B and E), and propidium iodide fluorescence (C and F) optical micrographs (10x magnification) of *C. albicans* adhered to NO-releasing 40% AHAP3 xerogels (balance BTMOS, v/v) taken immediately after preparation (A-C), and after 15 h incubation (D-F) in PBS (pH 7.4) ……68

Figure 2.8. Viable *C. albicans* removed from 10 – 40% AHAP3 xerogels (balance BTMOS, v,v) and 40% AHAP3 xerogels in the presence of a sub-fungicidal concentration of AgSD after 15 h of exposure of adhered fungus in PBS. Initial fungal surface coverage was identical at the start of the assay (20% coverage) …… ……...……70

Figure 2.9. Representative environmental scanning electron micrographs of *C. albicans* biofilms attached to control (A and B) and NO-releasing (C and D) 40% AHAP3-BTMOS xerogels exposed to sterile YPD broth alone (A and C) and 160 μg/mL AgSD in nutrient broth (B and D) …….73

Figure 3.1. Scanning electron microscopy images of 30 mol% 17FTMS-TEOS silica colloids at (A) 15000x, and (B) 36,600x magnification. ……...85

Figure 3.2. Illustration showing silica colloids cast within a thin fluorosilane film …….86

Figure 3.3. Static water contact angles of (A) xerogel films, and (B) silica colloids as a function of the concentration (mol%) of 17FTMS (balance MTMOS and TEOS for films and particles, respectively). Data are represented as means ± SD (n = 15) ……..…….88

Figure 3.4. Static water contact angles of (A) xerogel films, and (B) silica colloids as a function of the concentration (mol%) of 17FTMS (balance MTMOS and TEOS for films and particles, respectively). Data are represented as means ± SD (n = 15) ……...89

Figure 3.5. Scanning electron microscopy images of 30 mol% 17FTMS (balance MTMOS) xerogel films doped with 30 mol% 17FTMS (balance TEOS) silica colloids at (A) 1500x, and (B) 15,000x magnification …….…….91

Figure 3.6. SEM images of A) a fluorinated xerogel (30 mol% 17FTMS-MTMOS) doped with silica colloids (30 mol% 17FTMS-TEOS) and B) a non-fluorinated xerogel (100 mol% MTMOS) doped with silica colloids (30 mol% 17FTMS-TEOS). White arrows indicate examples of s mooth colloid islands ……..93

Figure 3.7. Static water contact angles after immersion in distilled water at 25 ºC. A) Superhydrophobic 30 mol% 17FTMS (balance TEOS) colloid-doped 30 mol% 17FTMS (balance MTMOS) and B) colloid-doped 100 mol% MTMOS xerogels; C) blank (no colloids)

30 mol% 17FTMS (balance MTMOS) xerogels; and, D) MTMOS controls (100 mol%). Data are represented as means ± SD (n = 12) ……..94

Figure 3.8. Reduction in *S. aureus* and *P. aeruginosa* adhesion at (A) blank (no colloids) 30 mol% 17FTMS (balance MTMOS) xerogels; (B) colloid-doped 100 mol% MTMOS xerogels; and, (C) superhydrophobic 30 mol% 17FTMS (balance TEOS) colloid-doped 30 mol% 17FTMS (balance MTMOS) xerogels versus MTMOS controls (100 mol%). Data are represented as means ± SD (n = 9) ……...97

Figure 4.1. Representative NO release from 75 mol% MPTMS/TEOS particles in TSB at 37 °C. [Inset: Enlarged view of NO release during 12–24 h ……108

Figure 4.2. Illustrative overview the spontaneous mutagenesis assay ……111

Figure 4.3. Illustrative overview of the serial passage mutagenesis assay …….115

Figure 4.4. Illustration of nitrosative and oxidative antimicrobial mechanism of NO within a bacterial membrane. Reprinted with permission from ref. 13. Copyright 2008 American Chemical Society ……...118

Figure 5.1. Illustration of a Pt working electrode pattern on a glass substrate ……...135

Figure 5.2. The effect of working electrode width on sensitivity to NO ($R^2 = 0.99$) ……..136

Figure 5.3. Cutaway illustration of reference electrode profile after masking and Ag deposition using A), an S1813 mask only, resulting in "dog ears" after liftoff, and B), a mask composed of both LOR and S1813 ……..142

Figure 5.4. Cutaway illustration of microfluidic channel construction ……..145

Figure 5.5. Top-view illustration of microfluidic device with placement of inlet and outlet reservoirs ……..146

Figure 5.6. Photograph of the microfluidic device with attached sample reservoir ……147

Figure 5.7. Response of bare (gray line) and membrane-coated (black line) microfluidic-based NO sensors to NO in PBS flowing at 15 µL/min. Inset shows NO calibration curves for bare (●) and membrane-coated (■) sensors ……149

Figure 5.8. Response of bare (gray line) and membrane-coated (black line) microfluidic-based NO sensors to interfering species in PBS flowing …….150

Figure 5.9. Response of membrane-coated microfluidic-based NO sensor to 5 μM increases of NO concentrations in whole blood flowing at 15 μL/min ……153

Figure 5.10. Response of membrane-coated microfluidic-based NO sensor to various concentrations of NO in whole blood flowing at 15 μL/min ……154

Figure 5.11. Response of membrane-coated microfluidic-based NO sensor to 50 nM increases of NO concentrations in 10% FBS flowing at 15 μL/min …..155

LIST OF ABBREVIATIONS

~	approximately
°	degree(s)
°C	degree(s) Celsius
%	percentage(s)
Δ	change
±	statistical margin of error
$	dollar(s)
× g	times the force of gravity
[…]	concentration
$[NO]_m$	maximum NO concentration
17FTMS	(Heptadecafluoro-1,1,2,2-tetrahydrodecyl)trimethoxysilane
5-HIAA	5-hydroxyindoleacetic acid
µA	microampere(s)
µg	microgram
µL	microliter(s)
µm	micrometer(s)
µmol	micromole(s)
µM	micromolar
AC	alternating contact
Ach	acetylcholine
AFM	atomic force microscope
Ag	silver

Ag/AgCl	silver/silver chloride
Ag^+	silver ion
$AgNO_3$	silver nitrate
AgSD	silver sulfadiazine
AHAP3	*N*-(6-aminohexyl)aminopropyltrimethoxysilane
Al	aluminum
APACHE	Acute Physiology Age and Chronic Health Examination
Ar	argon gas
ATCC	American Type Culture Collection
Au	gold
BOE	buffered oxide etch
BTMOS	isobutyltrimethoxysilane
C_{con}	percent surface coverage on control substrate
C_{NO}	percent surface coverage on NO releasing substrate
C. albicans	*Candida albicans*
CD14	cluster of differentiation 14
CFU	colony forming unit(s)
Co	cobalt
CO	carbon monoxide
CO_2	carbon dioxide
CRP	C-reactive protein
Cu	copper
CV	cyclic voltammetry
CVC	central venous catheter(s)
d	day(s)

DI	deionized
DNA	deoxyribonucleic acid
DOPAC	3,4-Dihydroxyphenylacetic acid
DPV	differential pulsed voltammetry
DTPA	*diethylene triamine pentaacetic acid*
e^-	*electron*
E. coli	*Escherichia coli*
E. faecalis	*Enterococcus faecalis*
EDTA	ethylenediaminetetraacetic acid
e.g.	for example
eNOS	endothelial nitric oxide synthase
EPR	electron paramagnetic resonance spectroscopy
EPS	exopolysaccharide
et al.	and others
etc.	and so forth
EtOH	ethanol
FBS	fetal bovine serum
FDA	food and drug administration
Fe	iron
g	gram(s)
G5	generation 5
GSED	gaseous secondary electron detector
h	hour(s)
H_2O	water
HCl	hydrochloric acid

i.e.	that is
I.V.	intravenous
IL	interleukin
iNOS	inducible nitric oxide synthase
IVC	intravascular catheter
KCl	potassium chloride
KOH	potassium hydroxide
kg	kilogram(s)
L-NAME	*N*-monomethyl- L-arginine
LOD	limit of detection
LOR	liftoff resist
LPS	lipopolysaccharide
M	molar
MBC	minimum bactericidal concentration
MeOH	methanol
mg	milligram(s)
MIC	minimum inhibitory concentration
MIC_{24}	minimum inhibitory concentration after a 24 h exposure period
min	minute(s)
mL	milliliter(s)
mm	millimeter(s)
mM	millimolar
mmol	milimole(s)
Mn	manganese
mol	mole(s)

MPTMS	mercaptopropyltrimethoxysilane
MRSA	methicillin-resistant *Staphylococcus aureus*
MSSA	methicillin-susceptible *Staphylococcus aureus*
MTMOS	methyltrimethoxysilane
MΩ	megaohm
N_2	nitrogen gas
nA	nanoampere(s)
NaCl	sodium chloride
NADH/NAD^+	nicotinamide adenine dinucleotide
NH_4OH	ammonium hydroxide
nM	nanomolar
nNOS	neuronal nitric oxide synthase
NO	nitric oxide
NO_2	nitrogen dioxide
NO_2^-	nitrite
NO_3^-	nitrate
NO_x	reactive nitrogen species
NOS	nitric oxide synthase
o-PD	*o*-phenylenediamine
O_2	oxygen gas
$OONO^-$	peroxynitrite
P	partial pressure
pA	picoamperes
PAMAM	poly(amidoamine)
P. aeruginosa	*Pseudomonas aeruginosa*

PBS	phosphate buffered saline, pH 7.4
PCT	procalcitonin
Pd	palladium
PEG	poly(ethylene glycol)
PET	poly(ethylene terephthalate)
pH	–log of proton concentration
PI	propidium iodide
PDMS	polydimethylsiloxane
pM	picomolar
ppb	parts per billion
ppm	parts per million
PROLI/NO	*N*-diazeniumdiolated proline
Pt	platinum
PtB	platinum black
RMS	root-mean-squared
PTFE	polytetrafluoroethylene
PVC	poly(vinyl chloride)
PVP	poly(vinyl pyrollidone)
R	percent reduction versus controls
rpm	revolutions per minute
RSNO	*S*-nitrosothiol
RT	room temperature
s	second(s)
S1813	S1813 photoresist
S. aureus	*Staphylococcus aureus*

S. epidermidis	*Staphylococcus epidermidis*
S. salivarius	*Staphylococcus salivarius*
SEM	scanning electron microscopy
SiR	silicone rubber
SIRS	systemic inflammatory response syndrome
SS	stainless steel
SWCNT	single-walled carbon nanotubes
t	time
t[NO]	total concentration of NO
$t_{1/2}$	NO release half life
TEOS	tetraethoxysilane
Ti	titanium
TNF	tumor necrosis factor
TSA	tryptic soy agar
TSB	tryptic soy broth
U.S.	United States
UV	ultraviolet
v:v	volume to volume ratio
V	volt(s)
VREF	vancomycin-resistant *Enterococcus faecalis*
wt	weight
x	times
YPD	yeast peptone dextrose
Zn	zinc

Chapter 1

Introduction: Recent Advances in Antimicrobial Coatings, and Nitric Oxide Detection

1.1 Antimicrobial coatings for biomedical applications

As healthcare providers continue to innovate in the areas of disease diagnosis and treatment techniques, the reliance on medical devices such as catheters, stents, pacemakers, and implanted defibrillators to facilitate improved healthcare has increased drastically.[1, 2] However, medical devices, especially percutaneous and transurethral catheters, are well known for their propensity to foster bacterial colonization and cause sepsis in hospital settings.[3] Roughly 17 million hospital-acquired infections were reported in 2007 in the US alone, resulting in 100,000 deaths.[1, 4] Treatment of such infections typically involves the use of antibiotics and broad-spectrum antimicrobials but even so, eventual device removal is often the only remedy. Left untreated, device infections lead to blood stream infection and ultimately sepsis. Unfortunately, the widespread use of antibiotics in the treatment of infections has resulted in the emergence of antibiotic-resistant bacteria and fungi, further complicating treatment.

Upon implantation of a medical device, proteins and small molecules present in the blood adsorb to the implant surface.[5] Microbes present at the implantation site or from endogenous flora then migrate to the surface, attaching reversibly to the implant surface as a basal layer. Continued microbial colonization results in irreversible

surface attachment to the implant surface. Many species of bacteria and fungi, including *P. aeruginosa* and *S. aureus*, exude an exopolysaccharide matrix, forming a biofilm that increases the structural integrity of this microbial colony.[6, 7] Following biofilm formation, microbes are between 30-2000 times less susceptible to antibiotics, making conventional antimicrobial treatments difficult.[6] In the final stage of biofilm formation, microbes are released and may reattach in other locations, thus establishing new colonies and spreading the infection.[6, 8] Due to the difficulty of treatment and the fastidious nature of biofilms, device removal is often necessary.

The species of microbes implicated in medical device infections is diverse, further complicating prevention and treatment efforts. Both gram-positive and gram-negative bacteria adhere to medical devices, with staphylococci and enterococci being the most common.[9] The species and strain of bacteria encountered in medical device infections depends upon the age of the recipient, the type of device, and preexisting disease. Bacteria most frequently encountered on IVCs include coagulase-negative *staphylococci* and *S. aureus*, which often originate from natural flora or contamination from healthcare workers, although gram-negative bacteria such as *Enterobacter* species are prevalent as well.[10] Most often, single-species IVC infections will eventually result in colonization by multiple species. Pathogenic fungi has also been implicated in medical device infections. *Candida albicans*, the most widely encountered fungus, is found among the natural human microbial flora. This species is more difficult to treat than most bacteria due to the formation of elongated hyphae that enhance the structural rigidity of the biofilm.[9] The stages of colonization and biofilm formation of *C. albicans* are illustrated in Figure 1.1.

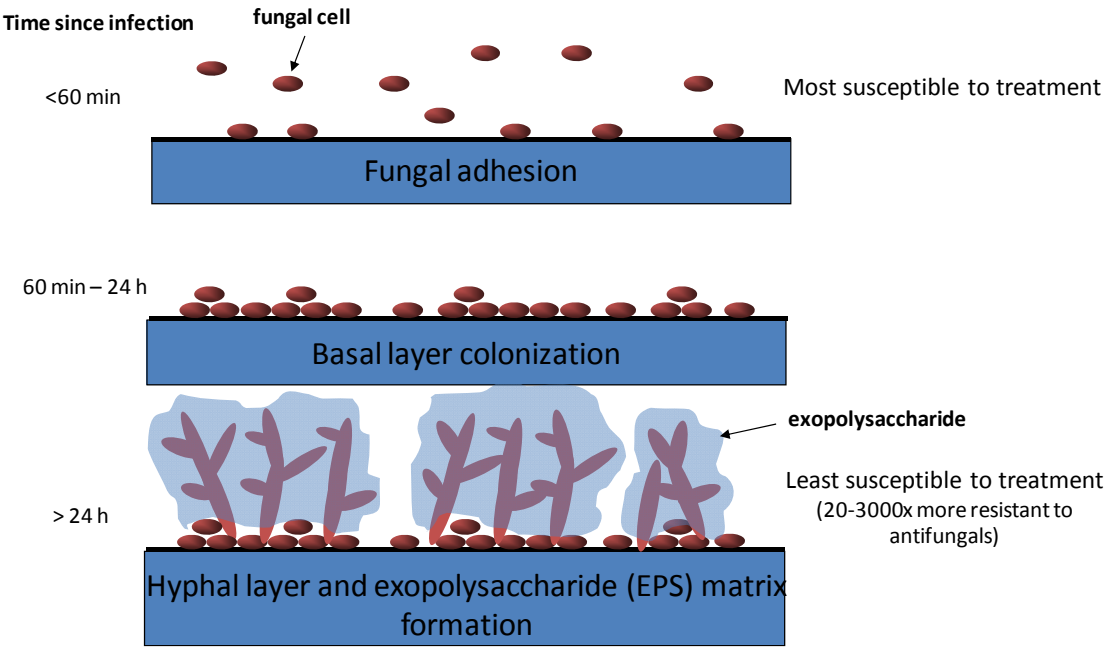

Figure 1.1. Stages of *C. albicans* biofilm development on a substrate.

A method for preventing *C. albicans* adhesion and proliferation on medical device surfaces is described in Chapter 2 of this thesis.

The probability of implant infections is dependent on the materials with which they are constructed. For example, although the reason is not well understood, silicone rubber IVC materials increase the risk of infection when compared to IVCs composed of polytetrafluoroethylene (PTFE), polyvinylchloride (PVC), and polyurethane.[11, 12] Often, ideal polymers used to construct medical devices are limited by the mechanical properties required by the device. A more versatile strategy for developing antimicrobial implant materials is to modify the implant surface with an antimicrobial coating. A wide variety of passive and active-release coatings have been developed for reducing microbial adhesion and viability.

1.1.1 Polymer coatings. The facile nature of polymer synthesis has enabled the development of coatings that resist the adhesion and proliferation of microbes. Polymers such as poly(ethylene glycol) (PEG),[13] poly(vinyl pyrollidone) (PVP),[14] and polyurethane[15] have thus been evaluated as infection-resistant coatings for medical devices. For example, Kingshott et al. fabricated poly(ethylene glycol) coatings grafted to poly(ethyleneimine)-coated poly(ethylene terephthalate) (PET) or stainless steel (SS) substrates to improve antimicrobial efficacy.[13] The authors reported that the adhesion of *Pseudomonas aeruginosa* to the PEG-coated PET was reduced by 2 to 4 orders of magnitude while no reduction in bacterial adhesion was observed to the PEG-coated SS surfaces. Thus, the authors concluded that bacterial adhesion to PEG was highly dependent on the PEG attachment strategy. In another example, Tunney and Gorman evaluated the use of PVP-coated polyurethane for urinary catheters.[14] The reduction of

bacterial adhesion was found to be dependent on the species evaluated, with significantly less *Enterococcus faecalis* adhered to PVP-coated and uncoated polyurethane, but no difference in *E. coli* adhesion.

To enhance the antimicrobial efficacy of their surface, polymers have been modified with "polymer brushes."[16] As bacteria approach the interface or polymer brush, compression and osmotic repulsion create a barrier that discourages attachment. A variety of polymers have been utilized to synthesize polymer brush coatings. For example, Nejadnik et al. synthesized brushes on silicone rubber from polyethylene oxide and polypropylene oxide that resulted in a ~10 fold reduction in the adhesion of *S. aureus* and *S. epidermidis*.[16] Unfortunately, neither a decrease in *P. aeruginosa* biofilm adhesion or viability was observed on the brush-coated surfaces in comparison to the silicone rubber. Polyacrylamide brushes attached to silicon wafers[17] and silicone rubber[18] have also shown some efficacy in reducing microbial adhesion. Cringus-Fundeanu and coworkers reported the synthesis of polyacrylamide brushes on to silicon wafers using atom transfer radical polymerization. [17] Utilizing a flow-cell adhesion assay, the authors found that *S. salivarius, S. aureus, and C. albicans* adhesion was reduced by 70-92% vs. untreated silicon. Although promising, grafting of the brushes to more clinically applicable substrates (e.g., silicone rubber and PVC) has not been demonstrated.

Biomimicry represents a recent innovation in passive polymer coatings for infection control.[19] Phosphorylcholine-based polymers that resemble phospholipid groups on cell membranes have been found to reduce bacterial adhesion. For example, Rose et al. reported that 2-(methacryloyloxyethyl phosphorylcholine)-based coatings resist bacterial adhesion, but only when pre-modified with heparin.[20] Phosphobetaine-modified

polymer coatings have also been evaluated for use in reducing surface fouling. West and coworkers reported that the high wettability resulting from the phosphobetaine moiety prevents protein adsorption and reduces the attachment of *S. aureus* and *S. epidermidis*.[21] However, the synthesis of phosphobetaine-modified polymers is highly complex and cost-prohibitive. Another promising strategy for reducing implant infections is bacterial interference, where a polymer surface is intentionally colonized by benign bacteria, thus preventing the adhesion of pathogenic species. To successfully utilize this method, Lopez and coworkers functionalized a polydimethylsiloxane (PDMS) surface with amine-terminated generation 5 (G5) poly(amidoamine) (PAMAM) dendrimers and then a carboxy-terminated mannose derivative.[22] Benign *E. coli* expressing mannose binding proteins were then colonized on the surface and shown to reduce the adhesion of pathogenic *Enterococcus* by 2 orders of magnitude.

1.1.2 Antimicrobial-releasing coatings. The problem of microbial adhesion to implanted devices has often been addressed by designing surfaces/materials that slowly release antimicrobials from the interface. Large local concentrations of antimicrobials may be achieved by controlled delivery directly at the site where infection is likely. Furthermore, the type of antimicrobial may be tailored to the bacteria likely to be encountered in that environment. While the antibacterial efficacy of polymers doped with antibiotics has been reviewed extensively,[6, 23] significant concern has arisen regarding the emergence of antibiotic-resistant bacteria as the rate of antibiotic delivery from a coating diminishes. Therefore, work has shifted to the design of coatings that release broad-spectrum antimicrobials such as chlorhexidine, silver materials, and other macromolecular agents.

The antimicrobial efficacy of silver (Ag) has been known for hundreds of years, and continues to be evaluated for a variety of applications including in medical device coatings.[24, 25] Silver ions (Ag^+) are believed to target amino acids, disrupting cellular activities and leading to microbial death.[26] Kaali and coworkers utilized the antibacterial nature of zeolites containing Ag^+ for medical device coatings by doping them into polyurethane.[27] The authors exposed the zeolite-loaded polyurethanes to a variety of bacteria and fungi, and found that the antimicrobial effect increased with zeolite concentration. One downside to the use of antimicrobial silver compounds is low light and thermal stability. To address this issue, Gerasimchuk and coworkers synthesized a class of silver compounds known as silver (I) cyanoximates, and evaluated their antimicrobial efficacy as light and heat-insensitive dopants for medical device coatings.[28] By altering the electron withdrawing group on the cyanoximate, the authors found that the compound could be tailored for enhanced efficacy against a wide array of bacteria and fungus. Colloidal and nanoparticle forms of silver have also been used as antimicrobial agents due to their high storage capacity for and controlled release of Ag ions.[29-32] Dair and coworkers evaluated the effect of the substrate material on the antimicrobial efficacy of silver nanoparticle-doped materials.[33] By changing the surface charge, chemical reactivity, or affinity of the surface for the Ag ions, the rate of release and resulting local Ag^+ concentration could be controlled. While the use of silver as an antimicrobial is common in a clinical setting, there is evidence that bacterial resistance to silver is emerging.[34-36] In addition to silver, other metal ions that have been evaluated as antimicrobial dopants for medical device coatings include Cu(II), Zn(II), Al(III), and Fe(III).[37]

Chlorhexidine, a skin and oral antiseptic that works by disrupting bacterial cell membranes, has also been evaluated for use in medical device coatings.[38] Fong et al. incorporated chlorhexidine into polyurethane nanocomposites and found that it reduced the colonization of *S. epidermidis* by two orders of magnitude relative to controls.[39] Chlorhexidine has also been incorporated into medical cements, allowing for prolonged local release and reduced bacterial colonization.[40] However, chlorhexidine has also been reported to have several adverse effects, including cases of anaphylactic shock and bacterial resistance.[41]

Antimicrobial peptides are an integral part of the innate immune defenses and provide potent, broad-spectrum antimicrobial activity by membrane disruption.[42] A number of synthesized peptides are currently being evaluated as potential antimicrobial therapeutics.[43, 44] Strategies have recently been developed for tethering antimicrobial peptides to medical device surfaces.[45] For example, Kazemzadeh-Narbat immobilized antimicrobial peptides to porous calcium phosphate coated on a titanium substrate.[46] The authors reported that the resulting coating reduced the viability of gram-positive and gram-negative bacteria by 6 orders of magnitude after 30 min of incubation with minimal toxicity to human cells. Gao et al. conjugated antimicrobial peptides to hydrophilic polymer brushes via a covalent linkage between a maleimide group and thiol on the cysteine-modified peptide.[47] By attaching multiple peptides on each polymer brush, loading of the antimicrobial peptides was maximized. The authors reported a ~6 order of magnitude reduction in the viability of *P. aeruginosa* exposed to the peptide-modified surfaces versus unmodified controls. While the use of antimicrobial peptides for

antimicrobial surfaces is promising, they are expensive to synthesize and handle, and thus are not yet well suited for clinical use.

1.1.3 Nitric oxide-releasing coatings. As an alternative approach to surface treatments and synthetic antimicrobials, we and others have developed coatings that release nitric oxide (NO), a broad-spectrum antimicrobial that has proven highly effective at reducing bacterial adhesion. In response to pathogens, phagocytes and other immune cells release an oxidative burst of nitric oxide.[48] Both oxidative and nitrosative mechanisms subsequently result in antimicrobial activity, making NO highly effective against a wide variety of microbes.[49, 50] The multi-mechanism activity also reduces the likelihood that a single mutation could result in microbial resistance. Chemical storage of NO is most often accomplished though the formation of a two NO moiety on a secondary amine (*N*-diazeniumdiolate) via exposure to high pressures of NO gas (Figure 1.2). Subsequent NO release is proton-triggered and may be enhanced by heating. Another method of storing NO chemically is the formation of a nitroso NO donor group on a thiol (*S*-nitrosothiol) via nitrosation of the sulfur group.[51, 52] Release of the NO may be triggered by heat, light, or exposure to aqueous copper. Several materials have been devised to chemically store and release NO via *N*-diazeniumdiolate and *S*-nitrosothiol functionalities.[53-62] Biomedical polymers already used for medical device construction such as polyesters[56] and polyurethanes[63] have been modified to release NO and proven effective at reducing colonization of *P. aeruginosa*.[56] The Schoenfisch Group has focused on the synthesis of sol-gel-derived materials for NO storage and release.[53, 61, 62, 64, 65] Nablo et al. evaluated the antimicrobial efficacy of NO-releasing xerogels in a rat

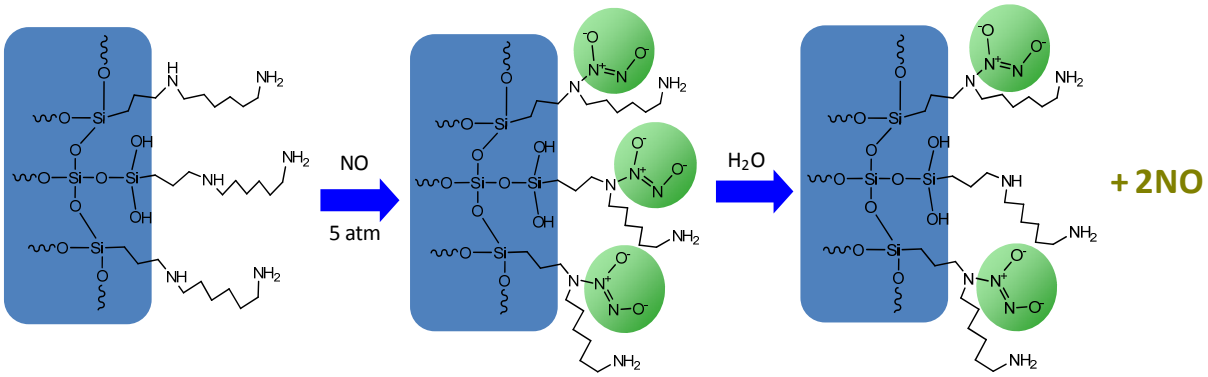

Figure 1.2. Illustration of *N*-diazeniumdiolate formation on a secondary amine via exposure to high pressure NO and subsequent proton-triggered NO release.

infection model by injecting a concentrated suspension of *S. aureus* directly into the implant site.[64] The implants were removed after 8 d and the wound site interrogated. An 82% decrease in the number of infected implants for the NO-releasing group versus non-NO-releasing controls was observed. In a subsequent study, Hetrick et al. reported that aminosilane xerogels modified with NO reduced the adhesion and viability of *P. aeruginosa* in vivo versus non-NO-releasing controls by 65% and >96%, respectively. In Chapter 2 of this thesis, the efficacy of NO-releasing xerogels against the adhesion, viability, and biofilm formation of a highly pathogenic fungus is described as an extension of this research.

1.1.4 Resistance to antimicrobials. The use of antimicrobial- and antibiotic-releasing coatings has become popular, but with questionable efficacy due to the continued emergence of antibiotic-resistant strains.[66, 67] Within many species of bacteria and fungi, the development of resistance to common antimicrobials hinders effective treatment and removal of biofilms.[9, 68] Microbes have evolved to resist many outside stressors (i.e., antimicrobials) through a number of mechanisms including destruction or inactivation of the stressor, the modulation of normal biological processes and pathways (e.g., respiration), and active efflux.[69] For example, only 2 years after the introduction of the antibiotic methicillin, a methicillin-resistant strain of *S. aureus* (MRSA) was identified.[70] By adapting to produce the enzyme β-lactamase, *S. aureus* gained a resistance to a range of β-lactam antibiotics.[71] Evidence of cross-resistance to multiple types of antibiotics has also become prevalent. For example, Vasquez et al. found that the use of nasally-administered mupirocin ointment to prevent MRSA infections resulted in the emergence of high-level mupirocin-resistant strains.[72] Compounding the problem,

antibiotic resistance may be transferred genetically to other bacterial species. In one example, the increased use of *β*-lactam antibiotics resulted in the genetic transfer of *β*-lactamase production to other organisms including *Klebsiella pneumonia* and *Escherichia coli*.[71] Decreased susceptibility to broad-spectrum biocides such as quaternary ammonium compounds, chlorhexidine, and silver-based therapeutics is also becoming prevalent, along with initial evidence of cross-resistance between antibiotics and biocides.[73-76] Contributing to this problem is the significant decrease in antimicrobial susceptibility observed for microbial biofilms.[77, 78]

While researchers are developing novel therapeutics in an attempt to counteract this alarming trend, the pace of the development of effective chemotherapeutic agents has been comparatively slow.[69, 79-81] Indeed, the need for improved passive antimicrobial strategies and/or antimicrobials that are biocidal via multiple mechanisms is significant, thus ensuring a lower likelihood of selecting for resistant microbes.[82, 83] Nitric oxide represents one such antimicrobial that is biocidal via multiple mechanisms. However, no studies to date have examined the propensity of microbes to develop resistance to exogenous NO released from NO donors or macromolecular scaffolds (i.e., particles and polymers). In Chapter 4, both short- and long-term assays are used to evaluate bacteria developing such resistance.

1.1.5 Superhydrophobic coatings. An effective example of non-fouling surfaces in nature is found on the leaves of the lotus plant. A combination of nano- and micro-structured roughness and a low surface energy waxy coating result in a high water contact angle (>150°) that is referred to as superhydrophobic.[84, 85] When a hydrophilic surface is tilted, water droplets slide across, lifting and redepositing any contaminants back on the

surface. Conversely, water acts like an elastic ball on a superhydrophobic surface and instead rolls across the substrate. Any contaminants are picked up by the spherical water droplet and carried away from the surface (Figure 1.3).[85] Thus, superhydrophobic surfaces are often called self-cleaning surfaces. Synthetic superhydrophobic surfaces have been prepared by top-down methods (e.g., chemical etching, micromachining, and templating),[84-88] bottom-up methods (e.g., chemical or layer-by-layer deposition, and colloidal assemblies),[84, 85, 89-92] or a combination of both.

Although researchers have preciously evaluated the efficacy of superhydrophobic surfaces as antifouling coatings for marine hulls,[88, 93] non-wetting coatings for optical surfaces,[89, 92, 94] and anti-icing coatings for aircraft,[93, 95, 96] only a few evaluations of superhydrophobic surfaces as antibacterial coatings for medical use have appeared in the literature.[84, 97, 98] In an early report, Crick and coworkers synthesized superhydrophobic coatings on glass using chemical vapor deposition of a silicone elastomer to study whether such interfaces could reduce the adhesion of bacteria that cause infections. [97] The resulting surface was characterized by a water contact angle of 165°, reducing the adhesion of *E. coli* and *S. aureus* by one order of magnitude. Fadeeva et al. utilized laser ablation, a top-down strategy, to fabricate superhydrophobic surfaces with static water contact angles of ~166°on titanium substrates.[98] While the authors reported that *S. aureus* successfully colonized their surface, the adhesion of *P. aeruginosa* was completely inhibited. Yonghao and coworkers fabricated superhydrophobic coatings by depositing a eutectic liquid composed of tetraethoxysilane and choline chloride-urea on a substrate forming a porous sol-gel.[99]

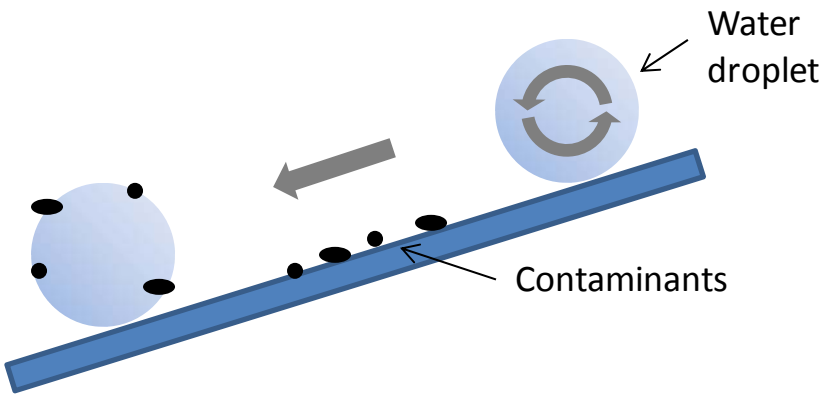

Figure 1.3. Illustration of the "self-cleaning" mechanism of a superhydrophobic surface.

The porous film was then coated with a low surface energy coating of fluoroalkoxysilane. The resulting coating reduced the attachment of *E. coli* while a glass slide control was completely colonized. While these strategies showed some success in vitro, none have been evaluated in a clinical setting. In addition, the aforementioned strategies for synthesizing superhydrophobic surfaces require complex synthesis strategies and equipment, and many are limited in terms of the substrate materials on which they can be employed. In Chapter 3, a simple strategy for synthesizing antimicrobial superhydrophobic surfaces that may be amenable to many substrates is described.

1.2 Nitric oxide detection

Few diatomic molecules have received as much attention as nitric oxide (NO). Although well known as a potent environmental pollutant, it was not until 1987 that Furchgott, Ignarro, and Murad separately identified NO as the endothelium-derived relaxation factor (EDRF) by comparing the effect of NO and EDRF released from arterial and venous strips on adjacent vasculature.[100-102] This discovery would ultimately lead to their shared Nobel prize in physiology in 1998 and spark interest in improved methods for detecting NO. In the years since this discovery, many scientists have continued to unravel the roles of NO in physiology. When produced endogenously from L-arginine by a family of enzymes called nitric oxide synthases (NOSs),[103] NO has been found to be active in the cardiovascular,[104] nervous,[105] and immune[106, 107] system, and in the wound-healing process.[108] Exogenously released NO has been shown to elicit diverse biological

responses such as reduced microbial viability[109] and decreased platelet activation.[61] In a clinical setting, NO has also garnered attention as a biomarker for sepsis.[110-112]

Widespread interest in NO and its biological roles has generated demand for analytical techniques capable of its measurement and quantification. Such technology is not straightforward due to NO's widely varying concentration. In the human body, the effect of NO is dependent on its concentration, ranging from sub-nanomolar to micromolar levels.[113, 114] To complicate matters further, NO has a short half-life (typically <10 s) in biological milieu due to its reactivity with oxygen, thiols, free radicals and hemes.[115] Effective NO detection schemes thus require a wide dynamic range, adequate sensitivity, and fast response time. Furthermore, the method must be highly selective toward NO over interfering species, which is often challenging due to the overwhelming complexity of biological systems.

1.2.1 Indirect detection of NO. One of the earliest examples of the analytical detection of NO was reported by Griess in 1864.[116] In the modern version of this method, now known as the Griess assay, NO is converted to nitrite (NO_2^-), a more stable byproduct of the reaction between NO and oxygen, and then reacted with sulfanilamide and *N*-(1-napthyl)ethylenediamine to form an azo dye. The concentration of the azo dye, typically measured using absorbance spectroscopy, directly relates to the concentration of nitrite, and thus NO in the original sample. Almost 150 years later, the Griess reaction remains the most commonly employed NO detection and quantification scheme. However, the Griess reaction remains poorly suited for measurements in biological systems where quick, real-time detection is necessary, where nitrite may fluctuate due to

other factors (i.e., dietary sources of nitrite), or when samples are opaque (e.g., blood). In addition, proteins present in biological matrices often cause further interfere.[117]

1.2.2 Direct detection of NO. The majority of analytical approaches for measuring NO may be categorized as spectroscopic or electrochemical. Spectroscopic NO detection methods involve either indirect measurement of byproducts of reactions between NO and other chemical species (i.e., Griess reaction and chemiluminescence); or, direct measurement of adducts formed between NO and metal complexes (absorbance), fluorescent dyes (fluorescence), or spin traps (electron paramagnetic resonance spectroscopy).[118] Some spectroscopic methods offer high sensitivity and selectivity for NO. For example, fluorescence detection is widely used for intracellular imaging of NO, enabling NO measurement at concentrations as low as 2 pM.[119] However, most spectroscopic methods present obstacles for *in vivo* NO detection due to complex instrumentation that is difficult to miniaturize. Conversely, electrochemistry allows for direct NO analysis with attractive analytical performance (i.e., sensitivity, selectivity, response time, sensor size, and inexpensive fabrication and operation).

1.2.3 Electrode materials. The materials used to construct an electrochemical NO sensor play a pivotal role in the sensitivity and quality of the ensuing analytical measurement. Materials often chosen as the working electrode include platinum (Pt) and its alloys,[106, 120] carbon fiber,[121] glassy carbon (GC),[122] and gold (Au).[123] By varying the composition and surface characteristics of the electrode material, the sensitivity, selectivity, signal stability, and required oxidation or reduction potential become tunable to varying extent. For example, Meyerhoff's group found that platinum electrodes could be made more stable and sensitive to NO via platinization, a process where platinum

black particles are electrochemically formed on the electrode surface, increasing the roughness and effective surface area.[124] By platinizing the platinum electrode of the NO sensor, 10-fold gains in both the NO detection limit and sensitivity were achieved. The authors surmised that the source of this performance enhancement was a concomitant increase in electron-transfer kinetics with a decrease in the potential required to drive the oxidation of NO.

1.2.4 Electroactive biological interferences. Of the various examples of electrochemical NO sensors intended for biological applications, few have been tested against more than a handful of applicable biological interferences. The extent to which a particular interfering species influences an NO measurement depends on the type of sensor, the applied potential, the characteristics of the permselective membrane (i.e., surface charge, porosity, hydrophobicity, and thickness), and the intended biological location of analysis. For example, interference from gaseous oxygen is only a concern if NO is being measured via electroreduction, since the reduction potential for NO and oxygen are similarly negative. Predicting likely interfering species is further complicated by the dependence of NO and interfering species concentrations on a multitude of outside stimuli (e.g., disease, injury, age, nutrition, and prior medical history). The most commonly encountered interfering species in biological milieu and their typical biological concentration ranges are listed in Table 1.1.[125-128] Nitrite is of particular concern due to its high concentration and similar size and oxidation potential to NO, making it difficult to discriminate between the two. Additionally, nitrite is a stable byproduct of the auto-oxidation of NO by endogenous oxygen and oxyhemoglobin, resulting in a direct dependence between the two species. Carbon monoxide (CO) is

equally problematic because of its similarities to NO in size, hydrophobicity, oxidation potential, and physiological roles.[129] Recent studies have made it apparent that NO and CO regulate each other through various physiological processes.[130] As a result, attempts to exclude CO using a NO selective membrane often fail. Providing selectivity to NO sensors over all of the aforementioned interfering species is clearly challenging and is discussed in more detail in the following sections.

1.2.5 Sensor classification. A wide variety of sensor designs have been developed and adapted for use in the measurement of NO in solution. While the construction of these devices varies widely, sensors are typically composed of a surface capable of the electro-oxidation or -reduction of NO and a mechanism for discriminating against electroactive interferences. A permselective membrane is commonly employed for the latter. In general, sensor styles may be categorized as follows; 1) Shibuki-style, 2) solid permselective, and 3) solid catalytic (Figure 1.4).

Shibuki-style NO sensors are modified versions of the initial oxygen (O_2) sensor first reported by Leland Clark in 1956.[131] This sensor comprises an electrolyte-filled micropipette into which both platinum working and silver reference wires are placed, and covered with a thin gas-permeable rubber membrane. Low molecular weight gases (e.g., NO and O_2) easily diffuse through the membrane to the electrode surface while larger species are excluded. By applying a negative or positive potential at the platinum wire electrode, electroactive species are reduced or oxidized, respectively, at the electrode surface, resulting in current of magnitude proportional to the analyte concentration.

Table 1.1. Possible interfering species and their physiological concentrations during the electrochemical NO measurements.

compound	concentration range	specimen	ref.
nitrite	<20 mM[a]	blood (plasma)	129
ascorbic acid	34 – 114 mM	blood (plasma)	126
uric acid	150 – 470 mM	blood (serum)	126
acetaminophen	66 – 199 mM[b]	blood (serum or plasma)	126
carbon monoxide	0.5 – 1.5 mM[a]	mouse kidney	128
dopamine	<2.0 nM	blood (plasma)	126
norepinephrine	0.35 – 2.96 nM	blood (plasma)	126
serotonin	0.28 – 1.14 mM	whole blood	126
DOPAC[c]	5.88 – 23.10 nM	blood (plasma)	127
5-HIAA[d]	18.31 – 65.91 nM	blood (serum)	126

[a]Basal concentration
[b]Therapeutic concentration
[c]DOPAC, 3,4-dihydroxyphe-nylacetic acid
[d]5-HIAA, 5-hydroxyindole-3-acetic acid

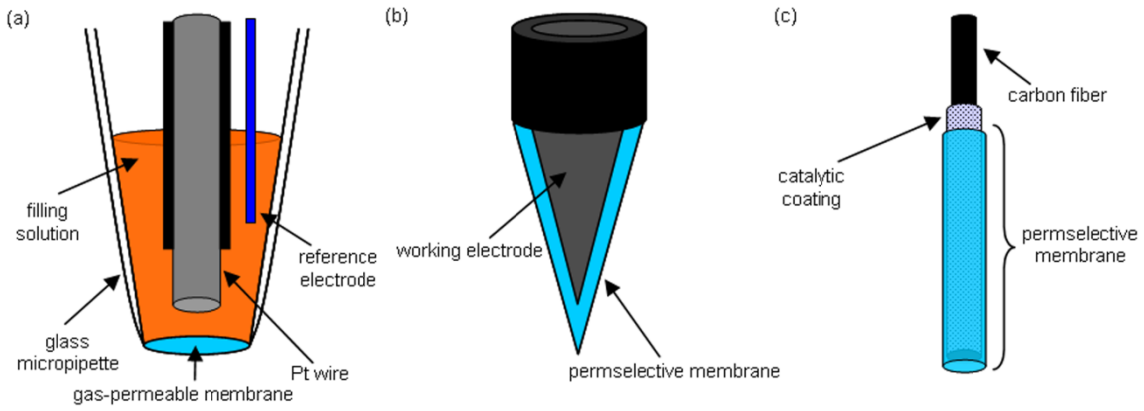

Figure 1.4. Schematic diagrams of (a) Shibuki-style, (b) solid permselective, and (c) solid catalytic NO sensors.

Shibuki reported the fabrication of the first NO-selective sensor in 1990, for which a positive electrode potential (i.e., electrooxidation) was used to oxidize and detect NO.[132] While this type of sensor measures NO with adequate selectivity over nitrite, the sensitivity of the sensor varied over time and between sensors from 2.5–106.3 pA/nM NO, leading to unstable measurements. In addition, the sensor was not readily amenable to miniaturization (>150 μm diameter) due to the complexity of construction and the requirement of an internal filling solution.

Solid permselective NO electrodes have been developed to eliminate the need for an internal filling solution. Fabrication is accomplished by directly modifying a noble metal or carbon electrode with a typically hydrophobic membrane permeable to the analyte of interest but impermeable to other electroactive interferences.[133] The simple design and construction of solid permselective electrodes allows them to be more easily miniaturized than Shibuki-style sensors. By layering multiple types of membranes on the electrode, the sensor selectivity may be tuned to discriminate over a wide variety of interferences including nitrite, dopamine, and acetaminophen, enabling unambiguous NO concentration determination in biological milieu. Nitric oxide is measured directly either by electrooxidation or electroreduction.

Solid catalytic electrodes were developed to further reduce the effect of electroactive interferences on the NO-selective electrode. While similar in construction to solid permselective electrodes, the catalytic electrodes incorporate a mediator (e.g., metalloporphyrins and metal phthalocyanines) either directly on the electrode surface or within a permselective membrane.[133] By including a mediator capable of catalyzing the oxidation or reduction of NO, the magnitude of the required electrochemical potential

(for NO measurement) is decreased, minimizing interference from other electroactive species. When combined with a permselective membrane, solid catalytic electrodes provide unparalleled selectivity. Similar to solid permselective electrodes, NO is measured directly either by catalytic electrooxidation or electroreduction.

1.2.6 Modes of NO detection. While the majority of NO sensor-related publications involve the electrooxidation of NO (direct or catalytic), sensors that measure NO via its electroreduction have been reported.[133-137] Depending on the electrode type and sample solution pH, NO is reduced at negative potentials ranging from -0.5 to -1.4 V (vs. Ag/AgCl).[133] The reaction proceeds via a two electron reduction mechanism:

$$2NO + 2e^- \rightarrow N_2O_2^{2-} \qquad (4)$$

The primary advantage of electroreduction is the avoidance of most interfering species that are commonly troublesome at positive potentials such as nitrite, ascorbic acid, and uric acid. However, electroreductive sensors are often plagued by diminished sensitivity, oxygen interference, and dependence on pH and electrode surface characteristics. With proper optimization, recent reports indicate some utility for specialized biological analysis.[134-136] However, due the limited utility of NO detection via electroreduction, this introduction will not cover the topic in detail.

The electrochemical reaction of NO on metal surfaces at positive electrode potentials (typically 0.6 – 0.9 V vs. Ag/AgCl)[138] proceeds via a three-electron oxidation mechanism:

$$NO \rightarrow NO^{+} + e^{-} \quad (1)$$

$$NO^{+} + OH^{-} \rightarrow HNO_2 \quad (2)$$

$$HNO_2 + H_2O \rightarrow NO_3^{-} + 2e^{-} + 3H^{+} \quad (3)$$

During the third step of the reaction, nitrite is electrochemically oxidized to nitrate. As a result, endogenously produced nitrite presents a significant source of electrochemical interference.[139] As nitrite is typically present in biological tissues at more than an order of magnitude higher concentration than NO, a successful NO electrode via electrooxidation must include a physical contingency for excluding it. Other common interfering species include acetaminophen, ascorbic acid, uric acid, dopamine, and CO. Careful attention thus must be given to understand the type and concentration of such interferences when making NO measurements with bare electrodes.

Since anionic (e.g., ascorbic acid and nitrite) and cationic (e.g., dopamine) species are significant sources of interference for electrooxidative measurements of NO in biological systems, exclusion by electrostatic repulsion is the most common method for imparting selectivity to NO sensors. Nafion, a polymeric cation exchanger (Figure 1.5), has been employed extensively to exclude nitrite via electrostatic repulsion from the sulfonate group present at neutral pH.[123] In an early example of a permselective electrode

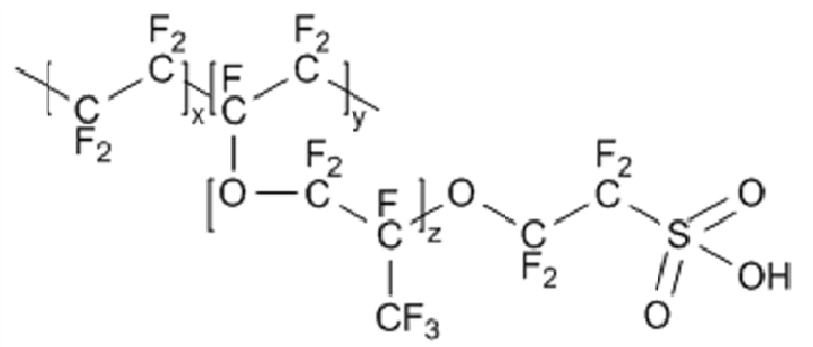

Figure 1.5. Structure of the polymeric cation exchanger Nafion.

that selects against anionic species, Bedioui and coworkers coated gold fiber and microdisk electrodes with a Nafion film. In addition to providing good selectivity for NO, the electrodes exhibited a linear dynamic range for NO from 10–100 μM.[123] While not exceedingly sensitive to NO, the authors noted that by decreasing the thickness of the Nafion membrane, sensitivity to NO was increased at the expense of selectivity over nitrite. Unfortunately, sensors coated with Nafion still respond to cationic and neutral species such as dopamine and acetaminophen, respectively.[140]

The ability to control the degree of hydrophobicity of an NO-selective membrane is important for maximizing sensitivity to NO and selectivity over interfering species. Utilizing multiple fluorinated alkylalkoxysilane precursors, Shin et al. demonstrated the ability to tune the hydrophobicity of NO-selective polymeric xerogel membranes, allowing for optimization of the sensor's response to NO over electroactive interferences.[141] The permeability and selectivity of the sensor to NO were maximized by utilizing a 20% (heptadecafluoro-1,1,2,2-tetrahydrodecyl)trimethoxysilane (v/v, balance methyltrimethoxysilane) xerogel membrane applied to a 5 μm diameter Pt black/Pt-coated conical tungsten microelectrode. The limit of detection and dynamic linear range of the NO sensor were 83 pM and 0.2 nM–4.0 μM, respectively. Furthermore, the sensor had little response to nitrite, ascorbic acid, uric acid, acetaminophen, dopamine, and ammonia.

While the sensitivity and selectivity of direct electrooxidation NO sensors are dependent primarily on the permselective membrane, sensors that operate via catalytic electrooxidation utilize a redox mediator to further improve analytical performance. For example, metalloporphyrins may be immobilized on the electrode surface or incorporated

into a polymer coating to function as catalysts for the oxidation of NO. By increasing the electron transfer kinetics for NO oxidation, the sensitivity to NO is enhanced. The selectivity over interfering species is further improved by employing one or more permselective membranes.

Metalloporphyrins are the most common mediator chosen for fabrication of catalytic NO sensors. Nickel (Ni) is the most frequently employed central metal ion. In their seminal report, Malinski and Taha utilized a Ni-porphyrin electropolymerized on a carbon fiber subsequently modified with a Nafion film.[121] In this configuration, the sensor had a detection limit of 10 nM and linear response up to 300 μM NO. When tested in solutions containing both NO and nitrite, the authors observed only a small increase in current and no change in peak potential indicating minimal interference from nitrite due to the lower oxidation potential employed. An important advantage of utilizing carbon fiber as an electrode is its small size and wide biological applicability. Indeed, the Malinski/Taha sensor was roughly 0.5 μm in diameter, and thus able to measure NO release from single endothelial and smooth muscle cells. In addition to the use of Ni porphyrins, porphyrins containing central metal ions such as iron (Fe) and manganese (Mn) have also been used to construct successful NO sensors.[142-144] For example, Diab and Schuhmann coated platinum electrodes with Mn porphyrin-modified polypyrrole films, resulting in NO sensors with little interference from nitrite or ascorbic acid.[144]

1.2.7 Nitric oxide measurements in biological systems. Evaluation of the NO sensor literature reveals numerous examples of electrochemical NO sensors applied to biological systems. Previous reviews have described the biological applications of NO sensors.[133, 138, 139, 145] A small selection of NO sensors applied to biological measurements

are detailed below as examples of the diversity of problems studied by these devices. Only sensors operating via electrooxidation (direct or catalytic) mode are described due to the interference from O_2 encountered for electroreductive NO sensors.

When making NO measurements in biological systems, it is important to consider the distance of the sensor from the NO source. Due to its rapid diffusion (3300 $\mu m^2\ s^{-1}$) and reactivity in biological milieu, the concentration of NO will decay rapidly with increasing distance from the point of generation.[114] Malinski's group observed an exponential decrease in the NO concentration measured at a porphyrinic sensor with increasing distance from the source via stimulated NO release from a single endothelial cell. The researchers were able to measure, a concentration of roughly 950 nM NO at the cell surface while NO was not measurable at distances >50 μm from the cell.[146]

Size is another important parameter to consider when choosing a NO sensor design for a particular biological purpose. The diameter of most published sensors range from a few hundred nanometers to greater than two millimeters.[138] Since the NO sensitivity of the sensor is directly proportional to the electroactive surface area, larger working electrodes typically offer greater NO sensitivity. However, the size requirement for a sensor depends greatly on the intended measurement location. For example, a micro- or ultramicroelectrode (<1 μm) is suitable for measuring NO in/near a single cell or a cluster of cells, while a larger sensor may be desirable for *in vivo* bulk NO measurements in blood. Ultramicroelectrode sensors offer the additional advantage of minimal perturbation of the surrounding environment upon use. Conversely, larger sensors are more robust and therefore less susceptible to failure over time.

Measurement of NO in blood is of particular interest due to its role in regulating vascular tone.[114] Furthermore, the bioavailability of endothelium-derived NO is an important indicator of cardiovascular risk and has been found to be lower in patients with hypertension and diabetes mellitus.[147] Evaluation of NO bioavailability has often been performed indirectly by observing the extent of vasodilation upon stimulation of NO release by bradykinin or acetylcholine (ACh).[147] With the development of NO sensors, induced NO response is more accurately determined by direct measure of NO. Nevertheless, blood is a challenging environment for quantifying NO due to the presence of both dissolved oxygen and hemoglobin, scavengers of NO that lower circulating NO concentrations. Sensors applied to *in vivo* NO analysis in blood must have excellent sensitivity to and selectivity for NO over its oxidation byproducts (e.g., nitrate and nitrite). In an early example of blood-based electrochemical NO measurements in human vasculature, a Nafion-coated metalloporphyrinic NO sensor was inserted into a hand vein to monitor stimulated NO release via infusions of bradykinin and acetylcholine.[148] The resulting NO measurement revealed a dose-dependent relationship between the concentrations of the stimulating species and NO released. Injection of *N*-monomethyl- L-arginine (L-NAME), a NOS inhibitor, attenuated the release of NO, indicating that the source of the observed signal was NO. Testing of selectivity during calibration indicated that the sensor was unresponsive to the chemical stimulants and inhibitor used during the course of the study. In addition, no signal was detected in response to nitrite or nitrate.

While a continued focus on improving the analytical performance of current electrochemical NO sensors is important, future research must address and improve the ability of NO sensors to resist biofouling for more reliable use in blood (i.e., protein

adsorption, platelet adhesion, and thrombus formation) and tissue (i.e., fibrous encapsulation and infection). Indeed, sensor biofouling often results in diminished analytical performance, poor reproducibility, and even failure. Previously published strategies for reducing biofouling on implantable sensors for other chemical species are reviewed elsewhere.[149, 150] Briefly, current strategies include passive protection of the sensor through the use of sensor membranes that resist biofouling (e.g., polyurethanes, polyethylene glycol, Nafion, and phospholipids) and polymers that actively release antifouling agents.[6] Ironically, a most promising approach for reducing biofouling of implantable sensors is based on NO release from the sensor interface.[6, 151] Clearly, such a strategy would be problematic for NO sensors.

As researchers continue to unravel the complex biological roles of NO and develop therapies based on NO, the need for sensitive, selective, and accurate NO measurement devices will increase. Specifically, the use of clinical NO measurements as diagnostic and prognostic indicators for disease states necessitates inexpensive, small, and simple point-of-care devices. Electrochemical sensors, more than any other type of NO measurement technique, are well suited to fill this role. For practical purposes, electrochemical sensors remain most attractive for real-time *in vivo* NO quantification in biological systems. In addition to their ease of fabrication and miniaturization, the instrumentation required to perform ultrasensitive measurements is both affordable and potentially portable for field use. While few analytical sensors work well for all applications, the most successful designs are characterized by both desirable analytical performance criteria and ruggedness. The emerging development of new approaches

using nano-structured polymers and carbon nanotubes should further enable sensitive, selective, and accurate determinations of NO in challenging environments.

1.3 Summary of dissertation research

The goals of my dissertation research include the synthesis and evaluation of antimicrobial sol-gel-derived coatings and the coupling of sensitive/selective NO measurement to microfluidic devices. Two separate strategies were utilized to explore the efficacy of antimicrobial coatings. In the first, the active release of NO from a sol-gel-derived surface was evaluated for efficacy against the adhesion, viability, and biofilm formation of *C. albicans*. The ability of the superhydrophobic surface to resist bacterial adhesion was evaluated using a modified flow-cell and viability assay. Three separate methods were used to characterize *C. albicans* biofouling including a parallel-plate flow cell adhesion assay, a fluorescence nucleic acid probe viability assay, and electron microscopic evaluation of biofilm formation. A primary advantage of employing multiple assays was that they allowed for the evaluation of the efficacy of NO at all three stages of microbial colonization. In the second strategy, a passive superhydrophobic coating based on a sol-gel doped with fluorinated silica colloids was synthesized. A related study was devoted to understanding the likelihood that exposure to exogenous NO release would cause bacterial resistance to NO. Both high-concentration, short term and low-concentration, long-term exposure assays were utilized to cover the two most common conditions in which resistance is likely to occur. In a separate phase of research, a fluorinated sol-gel was utilized as a selective membrane to fabricate a microfluidic

electrochemical NO sensor. The primary advantages of using a microfluidic device as a platform for the NO sensor include low sample volumes and background noise.

To summarize, the specific aims of my research included:

1) determining the ability of NO-releasing xerogels to resist fungal adhesion under flowing conditions;
2) study of the efficacy of NO-releasing xerogels against fungal biofilm formation;
3) the synthesis and evaluation of sol-gel-derived superhydrophobic surfaces as antimicrobial coatings;
4) evaluating the likelihood that exogenous NO release can foster bacterial resistance to NO; and,
5) fabricating and characterizing a microfluidic electrochemical NO sensor.

The intention of this introduction chapter was to introduce the fields of antimicrobial coatings, discuss the topic of bacterial resistance to antimicrobials, and overview methods for measuring NO. In Chapter 2, an evaluation of the antifungal efficacy of NO-releasing surfaces is reported. In Chapter 3, the synthesis and antimicrobial evaluation of sol-gel-derived superhydrophobic surfaces is presented. Chapter 4 presents an examination of the likelihood of NO resistance emergence upon exposure to exogenous NO release. Chapter 5 presents the fabrication and in vitro evaluation of a sol-gel-based microfluidic NO sensor. Finally, Chapter 6 is a summary of the work contained in this thesis and explains possibilities for future work that would

further develop the field of antimicrobial coatings and electrochemical NO detection, especially in the context of methods for the clinical detection of infection and sepsis.

1.4 References

1. Scott, R. D.; Centers for Disease Control and Prevention, 2009.

2. Francolini, I.; Donelli, G. "Prevention and control of biofilm-based medical-device-related infections," *FEMS Immunol. Med. Microbiol.* 2010, *59*, 227-238.

3. Rivers, E.; Nguyen, B.; Havstad, S.; Ressler, J.; Muzzin, A.; Knoblich, B.; Peterson, E.; Tomlanovich, M. "Early goal-directed therapy in the treatment of severe sepsis and septic shock," *NEJM* 2001, *345*, 1368-1377.

4. Hodgin, K. E.; Moss, M. "The epidemiology of sepsis," *Current Pharmaceutical Design* 2008, *14*, 1833-1839.

5. Duran, L. W. "Preventing medical device related infections.," *Med. Device Technol.* 2000, *11*, 14-17.

6. Hetrick, E. M.; Schoenfisch, M. H. "Reducing implant-related infections: active release strategies," *Chem. Soc. Rev.* 2006, *35*, 780-789.

7. Lynch, A. S.; Robertson, G. T. "Bacterial and fungal biofilm infections," *Annu. Rev. Med.* 2008, *59*, 415-428.

8. Maisel, W. H. "Medical device regulation: An introduction for the practicing physician," *Annals of Internal Medicine* 2004, *140*, 296-302.

9. Douglas, L. J. "Candida biofilms and their role in infection," *Trends in Microbiology* 2003, *11*, 30-36.

10. Zhang, L.; Gowardman, J.; Rickard, C. M. "Impact of microbial attachment on intravascular catheter-related infections," *International Journal of Antimicrobial Agents* 2011, *38*, 9-15.

11. Kaplan, S. S.; Basford, R. E.; Jeong, M. H.; Simmons, R. L. "Biomaterial-neutrophil interactions: dysregulation of oxidative functions of fresh neutrophils induced by prior neutrophil-biomaterial interaction," *J. Biomed. Mater. Res.* 1996, *30*, 67-75.

12. Sherertz, R. J.; Carruth, W. A.; Marosok, R. D.; Espeland, M. A.; Johnson, R. A.; Solomon, D. D. "Contribution of vascular catheter material to the pathogenesis of infection: the enhanced risk of silicone in vivo," *J. Biomed. Mater. Res.* 1995, *29*, 635-645.

13. Kingshott, P.; Wei, J.; Bagge-Ravn, D.; Gadegaard, N.; Gram, L. "Covalent attachment of poly(ethylene glycol) to surfaces, critical for reducing bacterial adhesion," *Langmuir* 2003, *19*, 6912-6921.

14. Tunney, M. M.; Gorman, S. P. "Evaluation of a poly(vinyl pyrollidone)-coated biomaterial for urological use," *Biomaterials* 2002, *23*, 4601-4608.

15. Francois, P.; Vaudaux, P.; Nurdin, N.; Mathieu, H. J.; Descouts, P.; Lew, D. P. "Physical and biological effects of a surface coating procedure on polyurethane catheters," *Biomaterials* 1996, *17*, 667-678.

16. Nejadnik, M. R.; van der Mei, H. C.; Norde, W.; Busscher, H. J. "Bacterial adhesion and growth on a polymer brush-coating," *Biomaterials* 2008, *29*, 4117-4121.

17. Cringus-Fundeanu, I.; Luijten, J.; van der Mei, H. C.; Busscher, H. J.; Schouten, A. J. "Synthesis and characterization of surface-grafted polyacrylamide brushes and their inhibition of microbial adhesion," *Langmuir* 2007, *23*, 5120-5126.

18. Fundeanu, I.; van der Mei, H. C.; Schouten, A. J.; Busscher, H. J. "Polyacrylamide brush coatings preventing microbial adhesion to silicone rubber," *Colloids and Surfaces B-Biointerfaces* 2008, *64*, 297-301.

19. Daculsi, G.; Laboux, O.; Le Geros, R. "Outcome and perspectives in bioactive coatings: What's new, what's coming," *ITBM-RBM* 2002, *23*, 317-325.

20. Rose, S. F.; Okere, S.; Hanlon, G. W.; Lloyd, A. W.; Lewis, A. L. "Bacterial adhesion to phosphorylcholine-based polymers with varying cationic charge and the effect of heparin pre-adsorption," *Journal of Materials Science-Materials in Medicine* 2005, *16*, 1003-1015.

21. West, S. L.; Salvage, J. P.; Lobb, E. J.; Armes, S. P.; Billingham, N. C.; Lewis, A. L.; Hanlon, G. W.; Lloyd, A. W. "The blocompatibility of crosslinkable copolymer coatings containing sulfobetaines and phosphobetaines," *Biomaterials* 2004, *25*, 1195-1204.

22. Lopez, A. I.; Kumar, A.; Planas, M. R.; Li, Y.; Nguyen, T. V.; Cai, C. "Biofunctionalization of silicone polymers using poly(amidoamine) dendrimers and a mannose derivative for prolonged interference against pathogen colonization," *Biomaterials* 2011, *32*, 4336-4346.

23. Zilberman, M.; Elsner, J. J. "Antibiotic-eluting medical devices for various applications," *J. Control. Release* 2008, *130*, 202-215.

24. Chopra, I. "The increasing use of silver-based products as antimicrobial agents: a useful development or a cause for concern?," *J. Antimicrob. Chemother.* 2007, *59*, 587–590.

25. Rai, M.; Yadav, A.; Gade, A. "Silver nanoparticles as a new generation of antimicrobials," *Biotechnol. Adv.* 2009, *27*, 76-83.

26. Privett, B. J.; Deupree, S. M.; Backlund, C. J.; Rao, K. S.; Johnson, C. B.; Coneski, P. N.; Schoenfisch, M. H. "Synergy of nitric oxide and silver sulfadiazine against gram-negative, gram-positive, and antibiotic-resistant pathogens," *Mol. Pharmaceutics* 2010, *7*, 2289-2296.

27. Kaali, P.; Stromberg, E.; Aune, R. E.; Czel, G.; Momcilovic, D.; Karlsson, S. "Antimicrobial properties of Ag(+) loaded zeolite polyester polyurethane and silicone rubber and long-term properties after exposure to in-vitro ageing," *Polymer Degradation and Stability* 2010, *95*, 1456-1465.

28. Gerasimchuk, N.; Gamian, A.; Glover, G.; Szponar, B. "Light Insensitive Silver(I) Cyanoximates As Antimicrobial Agents for Indwelling Medical Devices," *Inorganic Chemistry*, *49*, 9863-9874.

29. Li, D. H.; Diao, J. L.; Zhang, J. T.; Liu, J. C. "Fabrication of new chitosan-based composite sponge containing silver nanoparticles and its antibacterial properties for wound dressing," *Journal of Nanoscience and Nanotechnology* 2011, *11*, 4733-4738.

30. Piwonski, I.; Kadziola, K.; Kisielewska, A.; Soliwoda, K.; Wolszczak, M.; Lisowska, K.; Wronska, N.; Felczak, A. "The effect of the deposition parameters on size, distribution and antimicrobial properties of photoinduced silver nanoparticles on titania coatings," *Applied Surface Science* 2011, *257*, 7076-7082.

31. Samberg, M. E.; Orndorff, P. E.; Monteiro-Riviere, N. A. "Antibacterial efficacy of silver nanoparticles of different sizes, surface conditions and synthesis methods," *Nanotoxicology* 2011, *5*, 244-253.

32. Schwarz, F. P.; Hauser-Gerspach, I.; Waltimo, T.; Stritzker, B. "Antibacterial properties of silver containing diamond like carbon coatings produced by ion induced polymer densification," *Surface & Coatings Technology* 2011, *205*, 4850-4854.

33. Dair, B. J.; Saylor, D. M.; Cargal, T. E.; French, G. R.; Kennedy, K. M.; Casas, R. S.; Guyer, J. E.; Warren, J. A.; Kim, C. S.; Pollack, S. K. "The effect of substrate material on silver nanoparticle antimicrobial efficacy," *Journal of Nanoscience and Nanotechnology* 2010, *10*, 8456-8462.

34. Percival, S. L.; Bowler, P. G.; Russell, D. "Bacterial resistance to silver in wound care," *J. Hosp. Inf.* 2005, *60*, 1-7.

35. Rosenkranz, H. S.; Coward, J. E.; Wlodkowski, T. J.; Carr, H. S. "Properties of silver sulfadiazine-resistant *Enterobacter cloacae*," *Antimicrob. Agents Chemother.* 1973, *5*, 199-201.

36. Silver, S.; Phung, L. T.; Silver, G. "Silver as biocides in burn and wound dressings and bacterial resistance to silver compounds," *J. Ind. Microbiol. Biotechnol.* 2006, *33*, 627-634.

37. Francolini, I.; D'Ilario, L.; Guaglianone, E.; Donelli, G.; Martinelli, A.; Piozzi, A. "Polyurethane anionomers containing metal ions with antimicrobial properties: Thermal, mechanical and biological characterization," *Acta Biomaterialia* 2010, *6*, 3482-3490.

38. Lim, K. S.; Kam, P. C. A. "Chlorhexidine - pharmacology and clinical applications," *Anaesthesia and Intensive Care* 2008, *36*, 502-512.

39. Fong, N.; Simmons, A.; Poole-Warren, L. A. "Antibacterial polyurethane nanocomposites using chlorhexidine diacetate as an organic modifier," *Acta Biomaterialia* 2010, *6*, 2554-2561.

40. Hiraishi, N.; Yiu, C. K. Y.; King, N. M.; Tay, F. R. "Chlorhexidine release and antibacterial properties of chlorhexidine-incorporated polymethyl methacrylate-based resin cement," *J. Biomed. Mater. Res. Part B* 2010, *94B*, 134-140.

41. Kampf, G. "What is left to justify the use of chlorhexidine in hand hygiene?," *J. Hosp. Inf.* 2008, *70*, 27-34.

42. Hancock, R. E. W.; Sahl, H. G. "Antimicrobial and host-defense peptides as new anti-infective therapeutic strategies," *Nature Biotechnology* 2006, *24*, 1551-1557.

43. Batoni, G.; Maisetta, G.; Brancatisano, F. L.; Esin, S.; Campa, M. "Use of antimicrobial peptides against microbial biofilms: advantages and limits," *Current Medicinal Chemistry* 2011, *18*, 256-279.

44. Mohd, A.; Gupta, U. S. "Antimicrobial Peptides and their Mechanism of Action," *Research Journal of Biotechnology* 2011, *6*, 71-79.

45. Costa, F.; Carvalho, I. F.; Montelaro, R. C.; Gomes, P.; Martins, M. C. L. "Covalent immobilization of antimicrobial peptides (AMPs) onto biomaterial surfaces," *Acta Biomaterialia* 2011, *7*, 1431-1440.

46. Kazemzadeh-Narbat, M.; Kindrachuk, J.; Duan, K.; Jenssen, H.; Hancock, R. E. W.; Wang, R. "Antimicrobial peptides on calcium phosphate-coated titanium for the prevention of implant-associated infections," *Biomaterials* 2010, *31*, 9519-9526.

47. Gao, G. Z.; Lange, D.; Hilpert, K.; Kindrachuk, J.; Zou, Y. Q.; Cheng, J. T. J.; Kazemzadeh-Narbat, M.; Yu, K.; Wang, R. Z.; Straus, S. K.; Brooks, D. E.; Chew, B. H.; Hancock, R. E. W.; Kizhakkedathu, J. N. "The biocompatibility and biofilm resistance of implant coatings based on hydrophilic polymer brushes conjugated with antimicrobial peptides," *Biomaterials* 2011, *32*, 3899-3909.

48. Bogdan, C. "Nitric oxide and the immune response," *Nat. Immunol.* 2001, *2*, 907-916.

49. Williams, R. J. P. "Nitric oxide in biology: Its role as a ligand," *Chemical Society Reviews* 1996, *25*, 77-83.

50. Deupree, S. M.; Schoenfisch, M. H. "Morphological analysis of the antimicrobial action of nitric oxide on Gram-negative pathogens using atomic force microscopy," *Acta Biomaterialia* 2009, *5*, 1405-1415.

51. Feelisch, M. "The use of nitric oxide donors in pharmacological studies," *Naunyn-Schmiedebergs Arch. Pharmacol.* 1998, *358*, 113-122.

52. Williams, D. L. H. "The chemistry of S-nitrosothiols," *Accounts of Chemical Research* 1999, *32*, 869-876.

53. Hetrick, E. M.; Schoenfisch, M. H. "Antibacterial nitric oxide-releasing xerogels: Cell viability and parallel plate flow cell adhesion studies," *Biomaterials* 2007, *28*, 1948-1956.

54. Dobmeier, K. P.; Schoenfisch, M. H. "Antibacterial properties of nitric oxide-releasing sol-gel microarrays," *Biomacromolecules* 2004, *5*, 2493-2495.

55. Nablo, B. J.; Schoenfisch, M. H. "Antibacterial properties of nitric oxide-releasing sol-gels," *J. Biomed. Mater. Res., Part A* 2003, *67A*, 1276-1283.

56. Coneski, P. N.; Rao, K. S.; Schoenfisch, M. H. "Degradable Nitric Oxide-Releasing Biomaterials via Post-Polymerization Functionalization of Cross-Linked Polyesters," *Biomacromolecules* 2010, *11*, 3208-3215.

57. Meyerhoff, M. E.; Mowery, K. A.; Schoenfisch, M. H.; Politis, J. K.; Zhang, H. P.; Oh, B.; Batchelor, M. M. "Enhancing the biocompatibility and in vivo performance of intravascular chemical sensors using nitric oxide release polymers.," *Abstracts of Papers of the American Chemical Society* 1999, *218*, U165-U165.

58. Shin, J. H.; Schoenfisch, M. H. "Improving the biocompatibility of in vivo sensors via nitric oxide release," *Analyst* 2006, *131*, 609-615.

59. Schoenfisch, M. H.; Mowery, K. A.; Rader, M.; Meyerhoff, M. E. "Improving the biocompatibility of intravascular amperometric oxygen sensors via nitric oxide release," *Book of Abstracts, 216th ACS National Meeting, Boston, August 23-27 FIELD Full Journal Title:Book of Abstracts, 216th ACS National Meeting, Boston, August 23-27* 1998, ANYL-062.

60. Nablo, B. J.; Schoenfisch, M. H. "In vitro cytotoxicity of nitric oxide-releasing sol-gel derived materials," *Biomaterials* 2005, *26*, 4405-4415.

61. Riccio, D. A.; Dobmeier, K. P.; Hetrick, E. M.; Privett, B. J.; Paul, H. S.; Schoenfisch, M. H. "Nitric oxide-releasing S-nitrosothiol-modified xerogels," *Biomaterials* 2009, *30*, 4494-4502.

62. Charville, G. W.; Hetrick, E. M.; Geer, C. B.; Schoenfisch, M. H. "Reduced bacterial adhesion to fibrinogen-coated substrates via nitric oxide release," *Biomaterials* 2008, *29*, 4039-4044.

63. Coneski, P. N.; Schoenfisch, M. H. "Synthesis of nitric oxide-releasing polyurethanes with S-nitrosothiol-containing hard and soft segments," *Polym. Chem.* 2011, *2*, 906-913.

64. Nablo, B. J.; Prichard, H. L.; Butler, R. D.; Klitzman, B.; Schoenfisch, M. H. "Inhibition of implant-associated infections via nitric oxide," *Biomaterials* 2005, *26*, 6984-6990.

65. Privett, B. J.; Nutz, S. T.; Schoenfisch, M. H. "Efficacy of surface-generated nitric oxide against Candida albicans adhesion and biofilm formation," *Biofouling* 2010, *26*, 973-983.

66. Diefenbeck, M.; Muckley, T.; Hofmann, G. O. "Prophylaxis and treatment of implant-related infections by local application of antibiotics," *Injury-International Journal of the Care of the Injured* 2006, *37*, 95-104.

67. Esposito, S.; Leone, S. "Prosthetic joint infections: microbiology, diagnosis, management and prevention," *Int J Antimicrob Agents* 2008, *32*, 287-293.

68. Chandra, J.; Mukherjee, P. K.; Leidich, S. D.; Faddoul, F. F.; Hoyer, L. L.; Douglas, L. J.; Ghannoum, M. A. "Antifungal resistance of candidal biofilms formed on denture acrylic in vitro," *Journal of Dental Research* 2001, *80*, 903-908.

69. Alanis, A. J. "Resistance to antibiotics: Are we in the post-antibiotic era?," *Archives of Medical Research* 2005, *36*, 697-705.

70. Enright, M. C.; Robinson, D. A.; Randle, G.; Feil, E. J.; Grundmann, H.; Spratt, B. G. "The evolutionary history of methicillin-resistant Staphylococcus aureus (MRSA)," *Proc. Natl. Acad. Sci. U. S. A.* 2002, *99*, 7687-7692.

71. Jacoby, G. A.; Munoz-Price, L. S. "Mechanisms of disease: The new beta-lactamases," *New England Journal of Medicine* 2005, *352*, 380-391.

72. Vasquez, J. E.; Walker, E. S.; Franzus, B. W.; Overbay, B. K.; Reagan, D. R.; Sarubbi, F. A. "The epidemiology of mupirocin resistance among methicillin-resistant Staphylococcus aureus at a veterans' affairs hospital," *Infect. Control Hosp. Epidemiol.* 2000, *21*, 459-464.

73. Suller, M. T. E.; Russell, A. D. "Antibiotic and biocide resistance in methicillin-resistant Staphylococcus aureus and vancomycin-resistant enterococcus," *J. Hosp. Inf.* 1999, *43*, 281-291.

74. Russell, A. D. "Antibiotic and biocide resistance in bacteria: Introduction," *Journal of Applied Microbiology* 2002, *92*, 1S-3S.

75. Russell, A. D.; Suller, M. T. E.; Maillard, J. Y. "Do antiseptics and disinfectants select for antibiotic resistance?," *Journal of Medical Microbiology* 1999, *48*, 613-615.

76. Suller, M. T. E.; Russell, A. D. "Triclosan and antibiotic resistance in Staphylococcus aureus," *J. Antimicrob. Chemother.* 2000, *46*, 11-18.

77. Cos, P.; Tote, K.; Horemans, T.; Maes, L. "Biofilms: An extra hurdle for effective antimicrobial therapy," *Current Pharmaceutical Design* 2010, *16*, 2279-2295.

78. Brooun, A.; Liu, S. H.; Lewis, K. "A dose-response study of antibiotic resistance in Pseudomonas aeruginosa biofilms," *Antimicrob. Agents Chemother.* 2000, *44*, 640-646.

79. Spellberg, B.; Guidos, R.; Gilbert, D.; Bradley, J.; Boucher, H. W.; Scheld, W. M.; Bartlett, J. G.; Edwards, J. "The epidemic of antibiotic-resistant infections: A call to action for the medical community from the infectious diseases society of america," *Clin. Infect. Dis.* 2008, *46*, 155-164.

80. Power, E. "Impact of antibiotic restrictions: the pharmaceutical perspective," *Clinical Microbiology and Infection* 2006, *12*, 25-34.

81. Norrby, S. R.; Nord, C. E.; Finch, R. "Lack of development of new antimicrobial drugs: a potential serious threat to public health," *The Lancet Infectious Diseases* 2005, *5*, 115-119.

82. Eliopoulos, G. M.; Moellering, R. C. "Antibiotic synergism and antimicrobial combinations in clinical infections," *Reviews of Infectious Diseases* 1982, *4*, 282-293.

83. Cottarel, G.; Wierzbowski, J. "Combination drugs, an emerging option for antibacterial therapy," *Trends in Biotechnology* 2007, *25*, 547-555.

84. Furstner, R.; Barthlott, W.; Neinhuis, C.; Walzel, P. "Wetting and self-cleaning properties of artificial superhydrophobic surfaces," *Langmuir* 2005, *21*, 956-961.

85. Li, X. M.; Reinhoudt, D.; Crego-Calama, M. "What do we need for a superhydrophobic surface? A review on the recent progress in the preparation of superhydrophobic surfaces," *Chem. Soc. Rev.* 2007, *36*, 1350-1368.

86. Blossey, R. "Self-cleaning surfaces - virtual realities," *Nature Materials* 2003, *2*, 301-306.

87. Fresnais, J.; Chapel, J. P.; Benyahia, L.; Poncin-Epaillard, F. "Plasma-treated superhydrophobic polyethylene surfaces: Fabrication, wetting and dewetting properties," *J Adhes. Sci. Technol.* 2009, *23*, 447-467.

88. Zhang, H.; Lamb, R.; Lewis, J. "Engineering nanoscale roughness on hydrophobic surface - preliminary assessment of fouling behaviour," *Science and Technology of Advanced Materials* 2005, *6*, 236-239.

89. Bravo, J.; Zhai, L.; Wu, Z. Z.; Cohen, R. E.; Rubner, M. F. "Transparent superhydrophobic films based on silica nanoparticles," *Langmuir* 2007, *23*, 7293-7298.

90. Hikita, M.; Tanaka, K.; Nakamura, T.; Kajiyama, T.; Takahara, A. "Super-liquid-repellent surfaces prepared by colloidal silica nanoparticles covered with fluoroalkyl groups," *Langmuir* 2005, *21*, 7299-7302.

91. Wang, H. X.; Fang, J.; Cheng, T.; Ding, J.; Qu, L. T.; Dai, L. M.; Wang, X. G.; Lin, T. "One-step coating of fluoro-containing silica nanoparticles for universal generation of surface superhydrophobicity," *Chemical Communications* 2008, 877-879.

92. Yang, H. T.; Jiang, P. "Self-cleaning diffractive macroporous films by doctor blade coating," *Langmuir* 2010, *26*, 12598-12604.

93. Genzer, J.; Efimenko, K. "Recent developments in superhydrophobic surfaces and their relevance to marine fouling: a review," *Biofouling* 2006, *22*, 339-360.

94. Gurav, A. B.; Latthe, S. S.; Kappenstein, C.; Mukherjee, S. K.; Rao, A. V.; Vhatkar, R. S. "Porous water repellent silica coatings on glass by sol-gel method," *Journal of Porous Materials* 2011, *18*, 361-367.

95. Mishchenko, L.; Hatton, B.; Bahadur, V.; Taylor, J. A.; Krupenkin, T.; Aizenberg, J. "Design of ice-free nanostructured surfaces based on repulsion of impacting water droplets," *Acs Nano* 2010, *4*, 7699-7707.

96. Saleema, N.; Farzaneh, M.; Paynter, R. W.; Sarkar, D. K. "Prevention of ice accretion on aluminum surfaces by enhancing their hydrophobic properties," *Journal of Adhesion Science and Technology* 2010, *25*, 27-40.

97. Crick, C. R.; Ismail, S.; Pratten, J.; Parkin, I. P. "An investigation into bacterial attachment to an elastomeric superhydrophobic surface prepared via aerosol assisted deposition," *Thin Solid Films* 2011, *519*, 3722-3727.

98. Fadeeva, E.; Truong, V. K.; Stiesch, M.; Chichkov, B. N.; Crawford, R. J.; Wang, J.; Ivanova, E. P. "Bacterial retention on superhydrophobic titanium surfaces fabricated by femtosecond laser ablation," *Langmuir* 2011, *27*, 3012-3019.

99. Yonghao, X.; Hess, D. W.; Wong, C. P., May 29 2007-June 1 2007 2007; 1218-1223.

100. Ignarro, L. J.; Buga, G. M.; Wood, K. S.; Byrns, R. E.; Chaudhuri, G. "Endothelium-derived relaxing factor produced and released from artery and vein Is nitric-oxide," *Proc. Natl. Acad. Sci. U. S. A.* 1987, *84*, 9265-9269.

101. Khan, M. T.; Furchgott, R. F. "Similarities of Behavior of Nitric-Oxide (No) and Endothelium-Derived Relaxing Factor in a Perfusion Cascade Bioassay System," *Fed. Proc.* 1987, *46*, 385-385.

102. Rapoport, R. M.; Murad, F. "Agonist-induced endothelium-dependent relaxation in rat Thoracic Aorta May Be Mediated through Cgmp," *Circ. Res.* 1983, *52*, 352-357.

103. Masters, B. S. In *Nitric Oxide: biology and pathobiology*; Ignarro, L. J., Ed.; Academic Press: San Diego, 2000, pp 3-19.

104. Stamler, J. S. "Nitric oxide in the cardiovascular system," *Coronary Artery Dis.* 1999, *10*, 273-276.

105. Guix, F. X.; Uribesalgo, I.; Coma, M.; Munoz, F. J. "The physiology and pathophysiology of nitric oxide in the brain," *Prog. Neurobiol.* 2005, *76*, 126-152.

106. Bogdan, C. "Nitric oxide and the immune response," *Nat. Immunol.* 2001, *2*, 907-916.

107. MacMicking, J.; Xie, Q. W.; Nathan, C. "Nitric oxide and macrophage function," *Annu. Rev. Immunol.* 1997, *15*, 323-350.

108. Luo, J. D.; Chen, A. F. "Nitric oxide: a newly discovered function on wound healing," *Acta Pharmacol. Sin.* 2005, *26*, 259-264.

109. Hetrick, E. M.; Shin, J. H.; Stasko, N. A.; Johnson, C. B.; Wespe, D. A.; Holmuhamedov, E.; Schoenfisch, M. H. "Bactericidal efficacy of nitric oxide-releasing silica nanoparticles," *ACS Nano* 2008, *2*, 235-246.

110. Dhillon, S. S.; Mahadevan, K.; Bandi, V.; Zheng, Z. L.; Smith, W.; Rumbaut, R. E. "Neutrophils, nitric oxide, and microvascular permeability in severe sepsis," *Chest* 2005, *128*, 1706-1712.

111. Kirkebøen, K. A.; Strand, Ø. A. "The role of nitric oxide in sepsis – an overview," *Acta Anaesthesiol. Scand.* 1999, *43*, 275-288.

112. Vincent, J. L.; Pierrakos, C. "Sepsis biomarkers: a review," *Critical Care* 2010, *14*.

113. Wink, D. A.; Mitchell, J. B. "Chemical biology of nitric oxide: Insights into regulatory, cytotoxic, and cytoprotective mechanisms of nitric oxide," *Free Radical Biol. Med.* 1998, *25*, 434-456.

114. Thomas, D. D.; Ridnour, L. A.; Isenberg, J. S.; Flores-Santana, W.; Switzer, C. H.; Donzelli, S.; Hussain, P.; Vecoli, C.; Paolocci, N.; Ambs, S.; Colton, C. A.; Harris, C. C.; Roberts, D. D.; Wink, D. A. "The chemical biology of nitric oxide: Implications in cellular signaling," *Free Radical Biol. Med.* 2008, *45*, 18-31.

115. Lancaster, J. R. "A tutorial on the diffusibility and reactivity of free nitric oxide," *Nitric Oxide-Biol. Chem.* 1997, *1*, 18-30.

116. Griess, J. P. "Bemerkungen zu der Abhandlung der HH. Weselsky und Benedikt „Ueber einige Azoverbindungen”," *Ber. Dtsch. Chem. Ges.* 1879, *12*, 426-429.

117. Tsikas, D. "Analysis of nitrite and nitrate in biological fluids by assays based on the Griess reaction: Appraisal of the Griess reaction in the l-arginine/nitric oxide area of research," *Journal of Chromatography B* 2007, *851*, 51-70.

118. Hetrick, E. M.; Schoenfisch, M. H. "Analytical chemistry of nitric oxide," *Annu. Rev. Anal. Chem.* 2009, *2*, 409-433.

119. Huang, K. J.; Zhang, M.; Xie, W. Z.; Zhang, H. S.; Feng, Y. Q.; Wang, H. "Sensitive determination of nitric oxide in some rat tissues using polymer monolith microextraction coupled to high-performance liquid chromatography with fluorescence detection," *Anal. Bioanal. Chem.* 2007, *388*, 939-946.

120. Ichimori, K.; Ishida, H.; Fukahori, M.; Nakazawa, H.; Murakami, E. "Practical nitric-oxide measurement employing a nitric oxide-selective electrode," *Rev. Sci. Instrum.* 1994, *65*, 2714-2718.

121. Malinski, T.; Taha, Z. "Nitric-oxide release from a single cell measured insitu by a porphyrinic-based microsensor," *Nature* 1992, *358*, 676-678.

122. Casero, E.; Pariente, F.; Lorenzo, E.; Beyer, L.; Losada, J. "Electrocatalytic oxidation of nitric oxide at 6,17-diferrocenyldibenzo[b,i]5,9,14,18-tetraaza[14]annulen]-nickel(II) modifed electrodes," *Electroanalysis* 2001, *13*, 1411-1416.

123. Bedioui, F.; Trevin, S.; Devynck, J. "The use of gold electrodes in the electrochemical detection of nitric-oxide in aqueous-solution," *J. Electroanal. Chem.* 1994, *377*, 295-298.

124. Lee, Y.; Oh, B. K.; Meyerhoff, M. E. "Improved planar amperometric nitric oxide sensor based on platinized platinum anode. 1. Experimental results and theory when applied for monitoring NO release from diazeniumdiolate-doped polymeric films," *Anal. Chem.* 2004, *76*, 536-544.

125. Burtis, C. A.; Ashwood, E. R.; Tietz, N. W. *Tietz Textbook of Clinical Chemistry*, 3rd ed.; W.B. Saunders Co.: Philadelphia, PA, 1999.

126. Goldstein, D. S.; Stull, R.; Zimlichman, R.; Levinson, P. D.; Smith, H.; Keiser, H. R. "Simultaneous measurement of dopa, dopac, and catecholamines in plasma by liquid-chromatography with electrochemical detection," *Clin. Chem.* 1984, *30*, 815-816.

127. Lee, Y.; Kim, J. "Simultaneous electrochemical detection of nitric oxide and carbon monoxide generated from mouse kidney organ tissues," *Anal. Chem.* 2007, *79*, 7669-7675.

128. Pelletier, M. M.; Kleinbongard, P.; Ringwood, L.; Hito, R.; Hunter, C. J.; Schechter, A. N.; Gladwin, M. T.; Dejain, A. "The measurement of blood and plasma nitrite by chemiluminescence: Pitfalls and solutions," *Free Radical Biol. Med.* 2006, *41*, 541-548.

129. Wu, L. Y.; Wang, R. "Carbon monoxide: Endogenous production, physiological functions, and pharmacological applications," *Pharmacol. Rev.* 2005, *57*, 585-630.

130. Hartsfield, C. L. "Cross talk between carbon monoxide and nitric oxide," *Antioxid. Redox Sign.* 2002, *4*, 301-307.

131. Clark, L. C. "Monitor and control of blood and tissue oxygen tensions," *T. Am. Soc. Art. Int. Org.* 1956, *2*, 41-&.

132. Shibuki, K. "An electrochemical microprobe for detecting nitric-oxide release in brain-tissue," *Neurosci. Res.* 1990, *9*, 69-76.

133. Ciszewski, A.; Milczarek, G. "Electrochemical detection of nitric oxide using polymer modified electrodes," *Talanta* 2003, *61*, 11-26.

134. Liu, X. J.; Shang, L. B.; Pang, J. T.; Li, G. X. "A reagentless nitric oxide biosensor based on haemoglobin/polyethyleneimine film," *Biotechnol. Appl. Biochem.* 2003, *38*, 119-122.

135. Maskus, M.; Pariente, F.; Wu, Q.; Toffanin, A.; Shapleigh, J. P.; Abruna, H. D. "Electrocatalytic reduction of nitric oxide at electrodes modified with electropolymerized films of [Cr(v-tpy)(2)](3+) and their application to cellular NO determinations," *Anal. Chem.* 1996, *68*, 3128-3134.

136. Meulemans, A. "Continuous monitoring of *N*-nitroso-L-arginine using microcarbon electrode in rat-brain," *Neurosci. Lett.* 1993, *157*, 7-12.

137. Zen, J. M.; Kumar, A. S.; Wang, H. F. "A dual electrochemical sensor for nitrite and nitric oxide," *Analyst* 2000, *125*, 2169-2172.

138. Bedioui, F.; Villeneuve, N. "Electrochemical nitric oxide sensors for biological samples - Principle, selected examples and applications," *Electroanalysis* 2003, *15*, 5-18.

139. Davies, I. R.; Zhang, X. J. "Nitric oxide selective electrodes," *Methods in Enzymol.* 2008, *436*, 63-95.

140. Mitchell, K. M.; Michaelis, E. K. "Multimembrane carbon fiber electrodes for physiological measurements of nitric oxide," *Electroanalysis* 1998, *10*, 81-88.

141. Shin, J. H.; Privett, B. J.; Kita, J. M.; Wightman, R. M.; Schoenfisch, M. H. "Fluorinated xerogel-derived microelectrodes for amperometric nitric oxide sensing," *Anal. Chem.* 2008, *80*, 6850-6859.

142. Hayon, J.; Ozer, D.; Rishpon, J.; Bettelheim, A. "Spectroscopic and electrochemical response to nitrogen monoxide of a cationic iron porphyrin immobilized in nafion-coated electrodes or membranes," *J. Chem. Soc., Chem. Commun.* 1994, 619-620.

143. Bedioui, F.; Trevin, S.; Albin, V.; Villegas, M. G. G.; Devynck, J. "Design and characterization of chemically modified electrodes with iron(III) porphyrinic-based polymers: Study of their reactivity toward nitrites and nitric oxide in aqueous solution," *Anal. Chim. Acta* 1997, *341*, 177-185.

144. Diab, N.; Schuhmann, W. "Electropolymerized manganese porphyrin/polypyrrole films as catalytic surfaces for the oxidation of nitric oxide," *Electrochim. Acta* 2001, *47*, 265-273.

145. Bedioui, F.; Trevin, S.; Devynck, J. "Chemically modified microelectrodes designed for the electrochemical determination of nitric oxide in biological systems," *Electroanalysis* 1996, *8*, 1085-1091.

146. Brovkovych, V.; Stolarczyk, E.; Oman, J.; Tomboulian, P.; Malinski, T. "Direct electrochemical measurement of nitric oxide in vascular endothelium," *J. Pharm. Biomed. Anal.* 1999, *19*, 135-143.

147. Neishi, Y.; Mochizuki, S.; Miyasaka, T.; Kawamoto, T.; Kume, T.; Sukmawan, R.; Tsukiji, M.; Ogasawara, Y.; Kajiya, F.; Akasaka, T.; Yoshida, K.; Goto, M. "Evaluation of bioavailability of nitric oxide in coronary circulation by direct measurement of plasma nitric oxide concentration," *Proc. Natl. Acad. Sci. U. S. A.* 2005, *102*, 11456-11461.

148. Vallance, P.; Patton, S.; Bhagat, K.; Macallister, R.; Radomski, M.; Moncada, S.; Malinski, T. "Direct measurement of nitric-oxide in human-beings," *Lancet* 1995, *346*, 153-154.

149. Frost, M.; Meyerhoff, M. E. "In vivo chemical sensors: Tackling biocompatibility," *Anal. Chem.* 2006, *78*, 7370-7377.

150. Li, C. M.; Dong, H.; Cao, X. D.; Luong, J. H. T.; Zhang, X. J. "Implantable electrochemical sensors for biomedical and clinical applications: Progress, problems, and future possibilities," *Curr. Med. Chem.* 2007, *14*, 937-951.

151. Hetrick, E. M.; Prichard, H. L.; Klitzman, B.; Schoenfisch, M. H. "Reduced foreign body response at nitric oxide-releasing subcutaneous implants," *Biomaterials* 2007, *28*, 4571-4580.

Chapter 2

Efficacy of Surface-Generated Nitric Oxide Against *Candida albicans* Adhesion and Biofilm Formation

2.1 Introduction

Despite sterilization and the development of more hydrophilic coatings, invasive microbial infections remain a significant threat to the success of implanted medical devices, including indwelling catheters.[1] Overall, >250,000 catheter-related blood stream infections are reported in the U.S. annually with a mortality rate up to 25% and significant financial burden.[2] *Candida albicans*, a pathogenic fungus found naturally in the human gastrointestinal system, has been identified as the fourth most common pathogen isolated from catheters (behind coagulase-negative staphylococci, *Staphylococcus aureus,* and enterococci).[3] Furthermore, *C. albicans* is characterized by the second highest ratio of colonization to blood stream infection (coagulase-negative staphylococci and *staphylococcus aureus*), highlighting its virulence.[4, 5] Although fungal infections are more common among immunocomprimised patients, the use of broad-spectrum antibiotics in immunocompetent patients often eliminates natural competitive pressure from endogenous bacterial flora, increasing the risk of proliferation of other endogenous microbes and infection.[6-9]

Candida albicans infections typically originate at indwelling medical devices such as central venous catheters (CVCs). Characteristically, pathogenic colonization of medical devices occurs in four stages: adsorption of host proteins, adhesion of single cells

to the surface, formation of multiple basal layers, and growth of biofilm structures (e.g., hyphae, extracellular matrix).[3] Fungal biofilms exhibit a greater resistance to antifungal agents (e.g., fluconazole and amphotericin B) than planktonic cells.[3, 10, 11] Hawser and Douglas observed that the concentrations of five common antifungal agents used to reduce fungal metabolic activity by 50% were five to eight times higher for *C. albicans* in biofilms than planktonic cells.[11] While systemic antifungals may be administered to combat fungal biofilm growth, strains resistant to common antifungals have emerged more recently.[3, 10]

Both passive and active strategies have been employed to mitigate fungal adhesion to medical implants.[12] Passive strategies include surface modifications of polymer brushes,[13] eugenol derivatives,[14] and surface coatings of lauroyl glucose.[15] In vivo, the utility of passive strategies remains limited, particularly in their ability to reduce the viability of attached microbes. Active release of antimicrobials[16, 17] and antibiotics[18] have been shown to effectively reduce both the adhesion and viability of microbes on surfaces, but with increasing concern related to resistant strains,[10, 19-24] necessitating the development of more effective antimicrobial agents.

Recent work has identified nitric oxide (NO), a highly reactive free radical, as an antimicrobial agent that is produced endogenously.[25-28] Macrophages and other immune cells generate NO via inducible nitric oxide synthase (iNOS) in response to pathogens.[29] Restricting iNOS function and thereby limiting endogenous NO was shown by MacMicking et al. to result in greater infection rates.[29, 30] While NO has been demonstrated as an effective antimicrobial, the potential clinical utility of NO-releasing drugs has been confounded by inadequate delivery. Indeed, sustaining effective NO

levels for a given application has proven most challenging.[31] Our lab has employed sol-gel chemistry to produce materials capable of sustained release of NO via diazeniumdiolate NO donors.[27, 28, 32-36] Nitric oxide is stored as two molecule units on secondary amine moieties as a covalently-linked diazeniumdiolate NO donor.[37] Such materials have proven beneficial in reducing bacterial adhesion in both in vitro and in vivo models,[27, 28, 33, 35, 36, 38] and killing surface adhered bacteria.[38] More recently, Hetrick et al. demonstrated that microbial biofilms can be effectively dispersed by NO released from silica particles.[39] While some microbes may decrease their susceptibility to low concentrations of NO and its byproducts by increasing the production of antioxidant enzymes,[29] examples or evidence of bacteria or fungus resistant to high concentrations of NO currently do not exist. Accordingly, interest in the therapeutic applications of NO as an antimicrobial continues to grow.

Although in vitro testing of the efficacy of NO generated by small molecule NO donors against planktonic *Candida albicans* has proven that NO is a potent antifungal,[25, 26] research regarding the effect of NO on the adhesion, viability, and biofilm formation of *C. albicans* remains incomplete. Herein, the effectiveness of surface-generated NO against *Candida albicans* using model xerogel surfaces is evaluated with a parallel plate flow cell (fungal adhesion) assay, fluorescence nucleic acid staining, replicate plating on nutrient agar (viability of adherent fungal cells), and a biofilm growth assay.

2.2 Materials and Methods

Isobutyltrimethoxysilane (BTMOS) was purchased from Aldrich (Milwaukee, WI). *N*-(6-aminohexyl)aminopropyl trimethoxysilane (AHAP3) was purchased from

Gelest (Morrisville, PA). Ethanol (absolute), hydrochloric acid, and tetrahydrofuran were purchased from Fisher Scientific (Pittsburgh, PA). Low molecular weight poly(vinyl chloride) (PVC) and silver sulfadiazine (AgSD) were purchased from Sigma-Aldrich (Tullytown, PA). Nitric oxide (99.5%) and argon (Ar) gases were purchased from National Welders Supply (Durham, NC). Class VI medical grade silicon rubber (0.60" thickness) was purchased from McMaster-Carr (Santa Fe Springs, CA). *C. albicans* (ATCC# 90028) was obtained from the American Type Culture Collection (Manassas, VA). Yeast peptone dextrose broth was purchased from Becton, Dickinson and Company (Sparks, MD). Nucleic acid stains SYTO©9 and propidium iodide (PI) were purchased from Invitrogen (Carlsbad, CA). Distilled water was purified to 18.2 MΩ·cm with a Millipore Milli-Q Gradient A-10 water purification system (Bedford, MA).

2.2.1 Synthesis of AHAP3/BTMOS xerogel-coated films. Nitric oxide-releasing AHAP3/BTMOS xerogel-coated glass slides were synthesized as described previously.[40] Upon mixing ethanol (200 μL), BTMOS (180-120 μL), water (60 μL), and 0.5 M HCl (10 μL) for 1 h, AHAP3 (20-80 μL) was added to the solution and mixed for an additional hour resulting in a sol. The volume percentage of AHAP3 (balance BTMOS) was varied between 10 and 40%. Glass microscope slides were cut to 9 x 24 mm, sonicated in ethanol for 20 min, dried with N_2, and UV-cleaned with a BioForce TipCleaner (Ames, IA) for 20 min. The sol (30 μL) was spread onto the clean glass slides, dried for 30 min in a dessicator, and transferred to a 70 ºC oven for 3 d. Xerogel-coated slides were then stored in a dessicator at room temperature until use. Xerogels formed in this manner are stable upon immersion in solution.[36]

Nitric oxide-releasing 40% AHAP3 (v/v; balance BTMOS) xerogel-coated silicon rubber coupons for use in biofilm studies were synthesized as described previously.[34] Following the mixing of ethanol (1.2 mL), water (640 μL), and 0.5 M HCl (110 μL), BTMOS (1.28 mL) was added dropwise, and the sol mixed for 18 h. AHAP3 (860 μL) was then added and the sol mixed for an additional 30 h. Class VI medical-grade silicon rubber (SiR) was cut into 8 × 6 × 2 mm^3 coupons, cleaned via sonication in ethanol, sterilized in an autoclave at 120 ºC for 20 min, dried for 5 min in a 80 ºC oven, and then immobilized on sterile syringe needles. A xerogel surface was applied to the SiR coupons via dip-coating into the sol. The xerogel-coated SiR coupons were rotated at 1 rev/sec for 3 d to facilitate even curing, then dried in a 50 ºC oven for 1 d. Xerogel-coated SiR squares were then stored in a dessicator at room temperature until use.

2.2.2 Diazeniumdiolate modification of xerogels. Nitric oxide was loaded onto xerogels via exposure of the coated glass slides and SiR coupons to high pressures of NO. The film-coated slides and SiR coupons were placed in a Parr hydrogenation bomb, flushed with Ar at least six times to remove O_2, and pressurized with 5 atm NO gas for 3 d. Unreacted NO was then removed from the vessel by flushing with Ar. The NO donor-modified xerogels were stored in a dessicator at -20 ºC until use to prevent diazeniumdiolate decomposition.

2.2.3 Growth of standardized C. albicans suspension. Candida albicans was cultured in yeast peptone dextrose (YPD) broth at 37 ºC, pelleted by centrifugation, resuspended in 15% glycerol (v/v in PBS) and stored at -80 ºC. Cultures for fungal adhesion, viability, and biofilm studies were grown from a -80 ºC stock in YPD broth overnight. An aliquot of the overnight culture (1 mL) was inoculated into 100 mL sterile

YPD broth, incubated at 37 ºC with gentle agitation, and grown to 1×10^6 colony forming units (CFU) per mL as measured by optical density at 650 nm (OD_{650} ~0.044) and verified by serial 10-fold dilutions in PBS, plating on YPD agar, and enumeration of viable colonies. Cultures for viability and adhesion studies were pelleted by centrifugation (5000 rpm, 15 min) and resuspended in sterile PBS. Cultures for biofilm studies were diluted to 10^4 CFU/mL in YPD broth.

2.2.4 Determination of fungicidal efficacy of AgSD. The efficacy of AgSD against *C. albicans* was determined at 24 h using a standard minimum bactericidal concentration (MBC_{24}) assay. The MBC_{24} is defined as the minimum concentration of AgSD necessary to elicit a 3-log reduction in fungal viability after 24 h in growth conditions. Standardized fungal suspensions were tested against 5 different concentrations of AgSD. Concentrations of AgSD were chosen to bracket the MBC_{24} with a low and high concentration.

A 10^4 CFU/mL suspension of *C. albicans* in YPD broth was diluted to 2×10^4 CFU/mL in YPD broth. A 2x concentration of AgSD in YPD broth was added to an equal volume of fungal suspension, resulting in a 10^4 CFU/mL fungal concentration and the desired final AgSD concentration. The number of viable fungi was determined via serial dilution and replicate plating on YPD agar at the beginning of the assay, and after 6 and 24 h of incubation at 37 °C on an orbital shaker.

2.2.5 Flow cell-based fungal adhesion studies. A parallel plate flow cell assay was employed to examine the effect of surface NO flux on fungal adhesion to xerogel surfaces.[34] Glass slides with control and NO-modified xerogels coated on one side were loaded into a custom-built polycarbonate flow cell device, forming chambers with

dimension 2.1 x 0.6 x 0.08 cm^3. Two sets of three parallel flow chambers were placed in series so that three control xerogels were placed in front of three NO-releasing xerogels, allowing for 3 replicates to be measured in each experiment. A 10^6 CFU/mL *C. albicans* suspension in PBS (25°C) was introduced over the xerogels at 0.2 mL/min using a three-channel peristaltic pump. Fungal coverage to xerogel surfaces was measured by obtaining brightfield micrographs (10x magnification) in real-time at fixed timepoints (5, 20, 40, 60, 90, 120, and 150 min) using a Zeiss Axiovert inverted microscope. Digital images were obtained using a Zeiss Axiocam digital camera (Chester, VA). Fungal adhesion was determined as a function of time using digital thresholding and quantified as percent surface coverage.

2.2.6 Fluorescence-based qualitative viability studies. The viability of *C. albicans* adhered to control and NO-releasing xerogel surfaces was assessed qualitatively using a BacLight fluorescent probe nucleic acid stain assay (propidium iodide and SYTO©9). Fungal viability was measured both immediately following microbial adhesion to xerogel-coated glass slides and after incubation of adhered fungal cells at regular time intervals. By incubating xerogels with adhered fungus for extended periods, the effect of surface-based NO flux on fungal viability was assessed. *Candida albicans* fungi was grown to 10^6 CFU/mL in YPD broth as described above and resuspended in sterile PBS. Glass slides coated on one side with control and NO-releasing xerogels were incubated in the fungal suspension for 1 h at 37 ºC with gentle agitation to evenly adhere cells to the xerogel surface. The substrates were either transferred to a 5 mL solution of fluorescent probes (in PBS) or to 5 mL sterile PBS to maintain NO release. Xerogels incubated in fluorescent probes were removed after 30 min, rinsed in PBS, and dried gently in a N_2

stream. Cell viability was assessed via fluorescence microscopy using a Zeiss Axiovert 200 inverted microscope (Chester, VA) equipped with propidium iodide and cyto 9 filters (λ = 530 and 630 nm, respectively) from Chroma (Battleboro, VT). Digital images were obtained using a Zeiss Axiocam digital camera (Chester, VA). Brightfield and fluorescence micrographs of the xerogel sides of the glass slides were acquired at 10x magnification. Xerogels incubated in PBS for the time-based studies were fluorescently labeled and imaged as described above.

2.2.7 Quantitative viability studies. The number of viable cells adhered to control and NO-releasing xerogels after long-term incubation in PBS was determined by removing cells and plating on nutrient agar. A standardized suspension of *C. albicans* (10^6 CFU/mL) in PBS (25°C) was introduced over the NO-releasing xerogel-coated glass slides at 0.2 mL/min in the parallel plate flow cell. Flow of the fungal suspension was continued until surface coverage of the cells reached 20% as determined by optical microscopy and digital thresholding. Sterile PBS was then exchanged for the fungal suspension without passage of an air-liquid interface at a flow rate of 0.2 mL/min for 5 min to remove non-adhered cells. For AgSD experiments, the fungal suspension was replaced with 160 μg/mL AgSD in sterile PBS. Flow was then stopped and the xerogels were left undisturbed for 15 h at ambient temperature, thus exposing fungal cells to a long-term NO flux. PBS was then removed from the flow cells at a flow rate of 0.2 mL/min, and the slides subsequently removed and imaged at 10x magnification. Each slide was then transferred to 5 mL sterile PBS and sonicated for 15 min to remove adhered cells. Cell viability in the resulting PBS solutions was determined via 10-fold serial dilutions and plating on YPD nutrient agar, followed by enumeration of colony

forming units. Complete removal of cells was confirmed by evaluating the substrate surfaces using phase-contrast optical microscopy.

2.2.8 Efficacy of surface-generated NO against fungal biofilms. Candida albicans was grown in YPD broth to 1×10^6 CFU/mL (OD_{650} ~0.044), and serially diluted to 1×10^4 CFU/mL in YPD broth. Control and NO releasing 40% AHAP3-BTMOS SiR coupons immobilized on needles were sterilized under UV light for 20 min. An aliquot (5 mL) of the 1×10^4 CFU/mL *C. albicans* suspension was added to sterile glass scintillation vials into which control and NO releasing SiR squares were immersed. Vials were incubated at 37 ºC with gentle agitation for 2 h to allow fungal adhesion. Substrates were immersed in sterile YPD broth at 37 ºC for 48 h to initiate biofilm growth, with a fresh supply of YPD broth introduced at 24 h. For AgSD experiments, substrates were incubated in 160 μg/mL AgSD in YPD broth for 24 h, followed by fresh YPD broth. Biofilm-coated substrates were rinsed by immersion in sterile PBS, followed by sterile water to remove salts. Substrates were immediately affixed to a peltier device set at 11.5 ºC in a FEI Quanta 200F scanning electron microscope. Electron micrographs (500 to 1000x magnification) were taken in environmental mode (low vacuum, 5.15 torr) at 50% humidity using a gaseous secondary electron detector (GSED).

2.3 Results and Discussion

2.3.1 Nitric oxide release. Previous studies utilizing NO-releasing aminoalkoxysilane xerogels have demonstrated NO's ability to reduce both bacterial adhesion and viability.[28, 34-36] The optical transparency, stability, and NO release tenability (by varying aminosilane composition) of these materials makes them excellent model substrates for evaluating the effect of surface-generated NO on pathogenic fungus.

The AHAP3/BTMOS xerogel system was selected for this study due to the obtainable NO release at room and physiological temperatures (>48 h) and material stability.[36, 40] Furthemore, previous studies established that the surface properties (i.e., water contact angle) did not change after exposure to high pressure NO.[40] The NO storage capacity was varied by synthesizing a range of compositions with an AHAP3 content from 10-40% (v/v, balance BTMOS). As expected, the flux, total amount, and NO release kinetics (measured as half-life) varied as a function of aminosilane composition and temperature (Table 2.1). For all compositions, NO release was characterized as a low but sustained flux at room temperature. At physiological temperatures (i.e., 37ºC), larger NO fluxes were measured, but at the sacrifice of release longevity. Indeed, the maximum NO flux from 10-40% (v/v) AHAP3 xerogels at room temperature was an order of magnitude lower than at 37 ºC.

2.3.2 Flow cell based fungal adhesion studies. A flow-cell assay[34] was utilized to assess fungal adhesion since the first stage of fungal colonization is the initial adhesion of cells to a substrate. An illustration of the parallel plate flow cell assay is shown in Figure 2.1. As shown in Figure 2.2, lower fungal adhesion to the xerogel films was observed with increasing NO release. Absolute fungal adhesion results are provided in Table 2.2. Percent reduction versus controls, *R*, was calculated using the following equation:

$$R = \frac{c_{con} - c_{NO}}{c_{con}} \times 100 \qquad (3.1)$$

where c_{con} and c_{NO} represent the percent bacterial surface coverage on the control and NO-releasing xerogel, respectively. After only 90 min, a 25% reduction in fungal adhesion was observed for NO-releasing 10% AHAP3 xerogels versus controls,

indicating that an NO flux as low as ~2 pmol cm^{-2} s^{-1} results in a significant reduction in fungal adhesion. Although an increase in the adhesion of *C. albicans* was observed at both control and NO-releasing xerogels at 150 min, the percent reduction in adhesion of all xerogel compositions versus controls remained unchanged. Furthermore, the differences in fungal adhesion between control xerogels were not statistically significant at any timepoint, regardless of aminosilane concentration. In contrast, the % fungal surface coverage observed for controls and all compositions of NO-releasing xerogels was statistically significant at both 120 and 150 min (p value < 0.05). As shown in Figure 2.3 for 150 min, a clear trend of decreased fungal adhesion to NO-releasing xerogels with increasing AHAP3 content is apparent.

To demonstrate that the NO release and not the surface chemistry of the xerogel film resulted in the reduced fungal adhesion, control and NO donor-modified 40% AHAP3/BTMOS xerogels were coated with a thin film of PVC prior to conducting the parallel-plate flow cell assay. As expected, a significant decrease in adhesion was observed for the NO-releasing xerogels versus controls (~28% reduction over controls), confirming that the NO alone leads to decreased fungal adhesion (Figure 2.4). The overall reduction in adhesion at the PVC-coated 40% AHAP3/BTMOS xerogels was lower than the non-PVC-coated xerogel due to the 20% reduction in NO release upon coating with PVC as previously reported.[41] The influence of flow rate through the flow cell was also assessed (Figure 2.5). We expected a decrease in fungal adhesion at higher flow rates due to the increase in shear forces. However, a significant increase in fungal adhesion to control xerogels was observed at the greater flow rate (0.6 mL/min). While

Table 2.1. Average (from n=3) nitric oxide release at 25 and 37 ºC 10-40% AHAP3 xerogels (balance BTMOS, v/v) in PBS (pH 7.4). *Total NO release over 15 h.

% AHAP3	Temperature (ºC)	$[NO]_m$ (pmol cm^{-2} s^{-1})	t[NO] (µmol cm^{-2})*	$t_{1/2}$ (hr)
10	25	1.806 ± 0.715	0.017 ± 0.005	3.872 ± 0.547
	37	8.674 ± 1.579	0.049 ± 0.004	2.450 ± 0.272
20	25	6.117 ± 3.035	0.078 ± 0.026	4.237 ± 1.214
	37	33.31 ± 5.590	0.324 ± 0.055	2.853 ± 0.231
30	25	12.11 ± 4.607	0.206 ± 0.091	5.552 ± 0.941
	37	90.66 ± 26.77	0.852 ± 0.323	2.358 ± 0.274
40	25	14.42 ± 7.689	0.390 ± 0.158	7.615 ± 2.494
	37	146.0 ± 38.22	2.077 ± 0.656	3.936 ± .381

Table 2.2. *C. albicans* percent surface coverage to AHAP3 xerogels (balance BTMOS) under flowing conditions (0.2 mL/min) and calculated reduction in surface coverages to 10-40% AHAP3 xerogels over controls (non-NO-releasing).

	90 min		150 min	
% AHAP3	% surface coverage	% reduction[b]	% surface coverage	% reduction[b]
Control[a]	45±5	N/A	65±4	N/A
10	33±5	27±5	50±5	23±3
20	32±2	29±4	46±3	29±3
30	28±4	38±7	43±2	34±3
40	23±4	49±10	31±7	52±12

[a] Controls are identical to the above xerogel compositions without NO release capabilities. No significant difference was observed between controls of different compositions. Surface coverage values for controls are the average of all compositions.
[b] Over control.

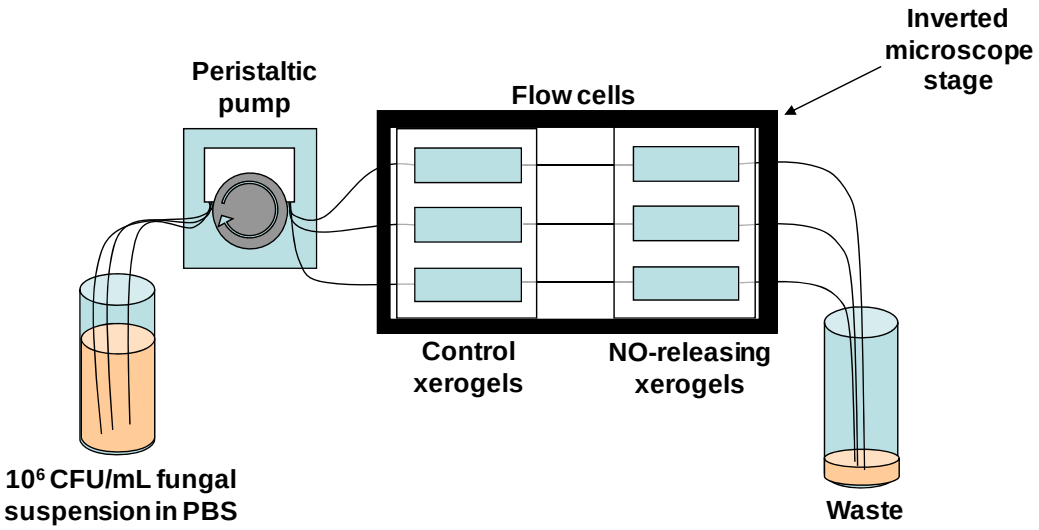

Figure 2.1. Illustration of parallel-plate flow cell adhesion assay.

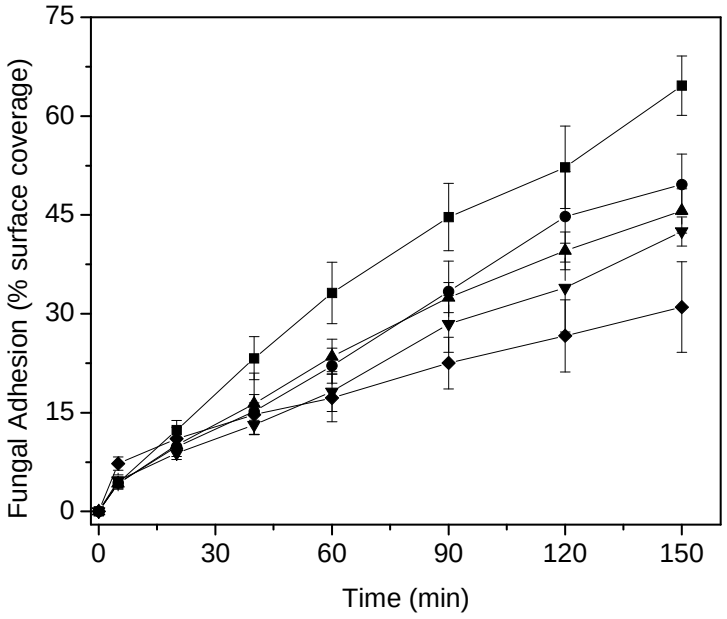

Figure 2.2. *C. albicans* adhesion to xerogel-coated glass slides under flowing conditions (0.2 mL/min). Nitric oxide flux was varied by using 10 (●), 20 (▲), 30 (▼), and 40 (♦) AHAP3 xerogels (balance BTMOS, v/v). Control xerogels of all compositions were averaged (■) as surface coverage values at each timepoint were identical (within error).

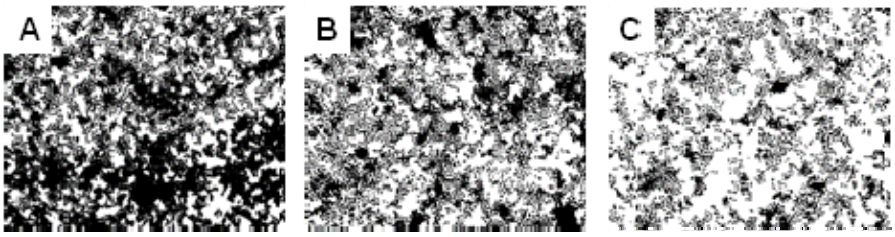

Figure 2.3. Digitally thresholded phase contrast optical micrographs of *C. albicans* adhesion to control (A), and NO-releasing 20% (B), and 40% (C) AHAP3 xerogels (balance BTMOS, v/v) following 150 minutes of fungal exposure under flowing conditions (flow rate: 0.2 mL/min).

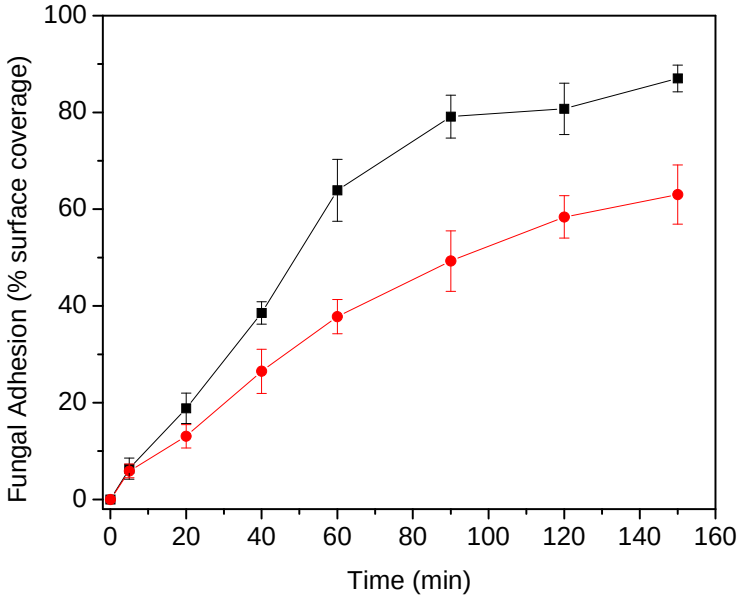

Figure 2.4. *C. albicans* adhesion to PVC-coated control (■) and NO-releasing (●) 40% AHAP3 xerogels (balance BTMOS, v/v) under flowing conditions (0.2 mL/min).

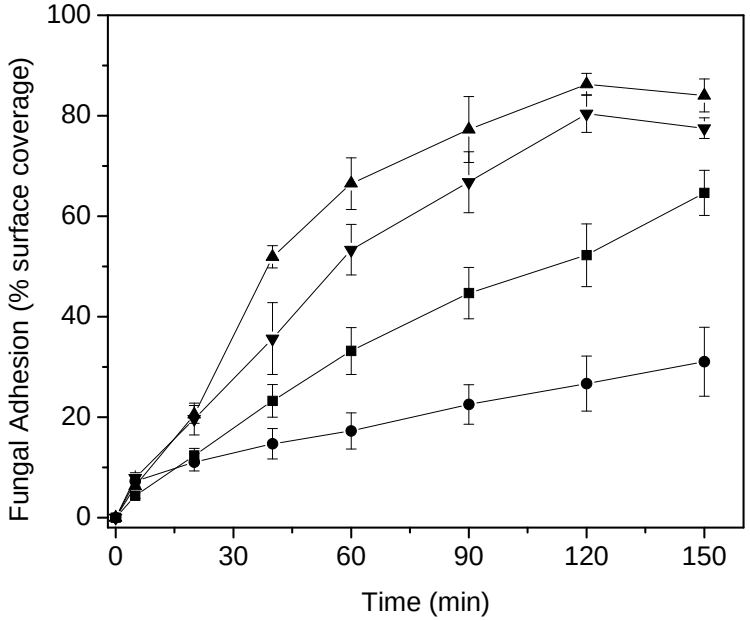

Figure 2.5. *C. albicans* adhesion to control (■ and ▲) and NO-releasing (● and ▼) 40% AHAP3 xerogels (balance BTMOS, v/v) under flowing conditions at a flow rate 0.2 mL/min (■ and ●) and 0.6 mL/min (▲ and ▼).

counterintuitive based on shear forces, we attribute these results to increased transport of *C. albicans* to the substrate. As expected, the NO-mediated reduction in adhesion to NO-releasing xerogels versus controls was less pronounced at the larger flow rate (only ~8% reduction in surface coverage over controls at 0.6 mL/min) due to the more rapid clearance of NO from the xerogel surface. This observation provides further evidence of the primary role of NO in reducing fungal adhesion.

2.3.3 Fungal viability studies. Critical to the success of indwelling catheters is the ability to both resist fungal adhesion and proliferation of adhered cells.[4, 42, 43] To determine the effect of NO on the viability of adhered fungus in situ, a live/dead assay was conducted using a commercially available kit. While this assay has been used primarily to examine the viability of bacterial cells, Jin and coworkers previously validated its use for similar studies of *C. albicans*.[44] We have previously demonstrated that the levels of NO released from xerogel films do not impact the probes (i.e., dyes) used in the assay.[34] *Candida albicans* adhered (by soaking in a fungal suspension) to control and NO-releasing 40% AHAP3/BTMOS xerogels were incubated in PBS for up to 15 h. The fungi were then incubated in a solution containing the two fluorescent probes, SYTO9 and propidium iodide (PI), from a commercially available kit. Since only SYTO9, a green fluorescent dye, enters healthy cells, green fluorescence indicates viable cells. In contrast, red fluorescence suggests significantly compromised cells since PI, a red fluorescent dye, can only penetrate cells with damaged membranes. Example brightfield and fluorescence images of fungi adhered to control and NO-releasing xerogels at 0 and after 11 h incubation are provided in Figures 2.6 and 2.7, respectively.

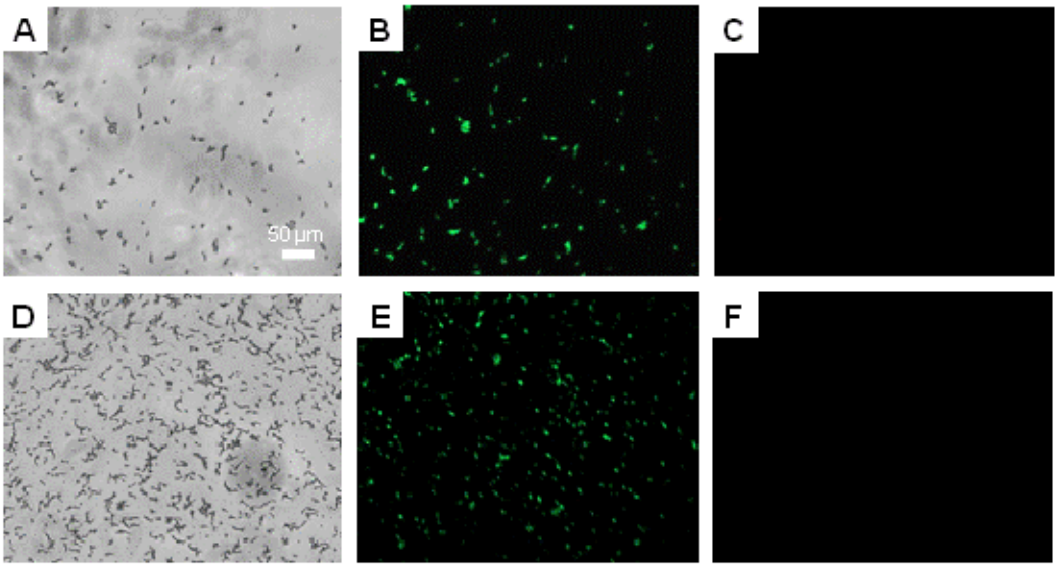

Figure 2.6. Representative brightfield (A and D), syto 9 fluorescence (B and E), and propidium iodide fluorescence (C and F) optical micrographs (10x magnification) of *C. albicans* adhered to control 40% AHAP3 xerogels (balance BTMOS, v/v) taken immediately after preparation (A-C), and after 11 h incubation (D-F) in PBS (pH 7.4).

Fluorescence micrographs of fungus adhered to control xerogels taken both before (Figure 2.6B) and after 11 h of incubation in PBS (Figure 2.6E) exhibited only SYTO9 fluorescence, indicating that cells adhered to controls are initially viable and remain so, even after 11 h in nutrient deficient conditions. In contrast, fungal cells exposed to an NO flux for 15 h had significant red fluorescence due to PI dye penetration (Figure 2.7D-F), even though such cells were viable at t = 0 h (Figure 2.7A-C). The emergence of fluorescence due to PI after 11 h of NO release indicated that the cell envelope was compromised. The PI fluorescence was not observed prior to 11 h incubation, suggesting that at earlier periods the level of total NO remained insufficient to cause cell damage (data not shown). In comparison to results published previously for *P. aeruginosa*, the time required for the appearance of PI was 37% greater.[34]

To gain a more thorough understanding about the relationship between NO flux and fungal viability, we evaluated the viability of adhered fungal cells using a range of NO-releasing xerogels (10, 20, 30 and 40% AHAP3-BTMOS). Viable cells were counted as colony forming units on nutrient agar. *Candida albicans* adhesion was first standardized at 20% coverage on the NO-releasing xerogels in a parallel plate flow cell (as described above) to allow direct comparison of fungal viability between each xerogel composition. After incubation for 15 h in PBS, adherent cells were removed from the xerogel surfaces in an ultrasonic bath, spread on nutrient agar and counted. Previous studies have shown this method of cell removal to be safe removing *C. albicans* from surfaces.[45, 46] Removal of cells was confirmed after sonication by evaluating the surfaces using optical microscopy.

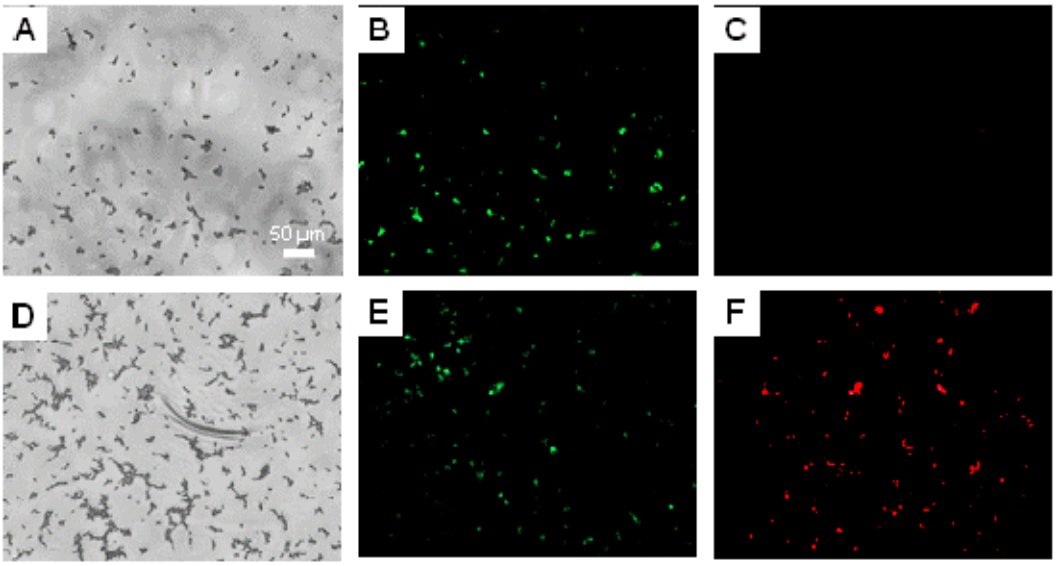

Figure 2.7. Representative brightfield (A and D), syto 9 fluorescence (B and E), and propidium iodide fluorescence (C and F) optical micrographs (10x magnification) of *C. albicans* adhered to NO-releasing 40% AHAP3 xerogels (balance BTMOS, v/v) taken immediately after preparation (A-C), and after 15 h incubation (D-F) in PBS (pH 7.4).

Of note, sonication of control xerogels resulted in incomplete removal of fungus cells, and therefore comparison to NO-releasing xerogels was not possible. Replicate plating experiments confirmed that cells were not killed during this period of sonication (data not shown). As expected, the number of viable cells removed from the xerogel surfaces was inversely proportional to the xerogel's aminosilane content, and therefore the NO flux and total NO released from (Figure 2.8). Optical micrographs taken of each substrate after the 15 hr incubation in PBS but before removal of cells via sonication showed that the majority of cells are in their oval yeast form, rather than growing as hyphae (data not shown). While the total NO release from 10 and 40% AHAP3-BTMOS xerogels was 0.049 and 2.077 μmol cm^{-2}, respectively, the number of viable cells removed from 40% AHAP3 xerogels was ~42% less than that for 10% AHAP3 xerogels. The incomplete removal of fungus from controls further demonstrates the detrimental effect of NO on fungal adhesion. When compared to *P. aeruginosa* (96% decrease in viability between bacteria adhered to 10 and 40% AHAP3 xerogels),[34] the observed reduction is attenuated.

While the data suggests that NO-releasing materials may be effective at reducing fungal adhesion and proliferation, NO alone does not appear to be as potent against *C. albicans* as it is against other biofilm-forming bacteria. Decreased efficacy of NO against *C. albicans* may be attributed to cell size. Indeed, *C. albicans* are up to an order of magnitude larger in diameter than *P. aeruginosa*.[47, 48] As a result, much of the yeast cell would be located further from the source of NO generation, minimizing exposure. Additionally, *C. albicans* are characterized by thick cellular envelopes (200–300 nm)[49] while *P. aeruginosa*, for example, is <50 nm.[48, 49]

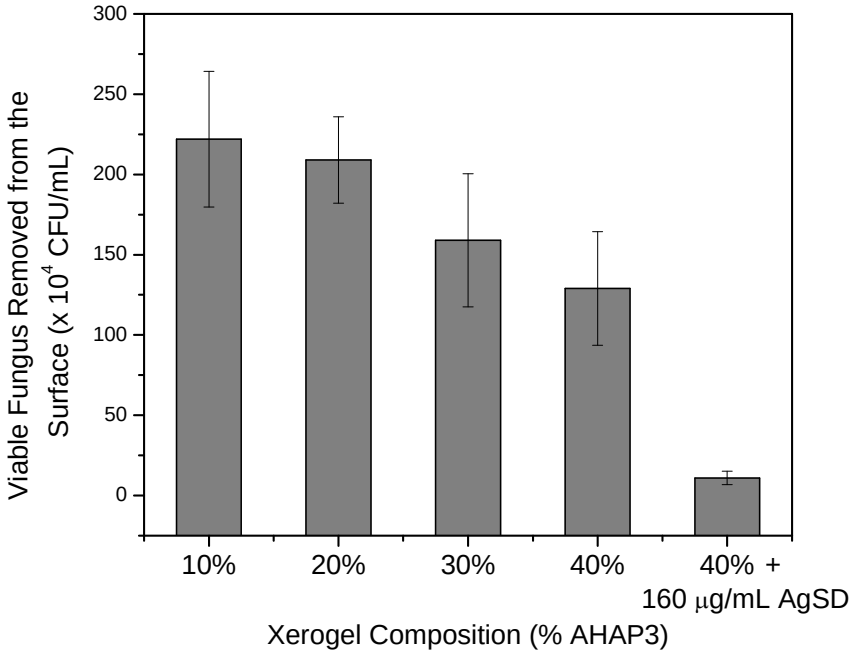

Figure 2.8. Viable *C. albicans* removed from 10 – 40% AHAP3 xerogels (balance BTMOS, v,v) and 40% AHAP3 xerogels in the presence of a sub-fungicidal concentration of AgSD after 15 h of exposure of adhered fungus in PBS. Initial fungal surface coverage was identical at the start of the assay (20% coverage).

The thicker cell envelope may therefore afford *C. albicans* improved protection against NO and its reactive byproducts. Furthermore, a marked difference in the efficacy of broad spectrum antimicrobials such as chlorhexidine and silver sulfadiazine against *C. albicans* and *P. aeruginosa* has been reported by Schierholz and coworkers,[50] suggesting that *C. albicans* may be less susceptible to broad spectrum antimicrobials in general.

To compensate for the decreased NO efficacy, the combination of NO and silver sulfadaziazine (AgSD) was investigated to further reduce colonization of implanted surfaces by *C. albicans*. McElhaney-Feser et al. previously reported that a combination of NO and azole-based antifungal agents resulted in synergistic killing (e.g., improved efficacy in combination than the sum of the efficacy of each individual agent).[25] Following a previous report,[25] the efficacy of AgSD as an antifungal was determined by exposing *C. albicans* to a range of concentrations of AgSD in nutrient broth and measuring viability after 6 and 24 h (data not shown). Exposing C. albicans to a AgSD concentration of 800 μg/mL for 24 h resulted in complete killing (no viable cells). Although some growth inhibition was observed at 200 and 400 μg/mL AgSD, the cells remained completely viable (no inhibition) at a concentration of 100 μg/mL. Of note, no killing was observed at 6 h incubation at AgSD concentrations up to 1.6 mg/mL. To test the surface-localized anti-fungal efficacy of AgSD in combination with NO, fungal cells adhered to an NO-releasing 40% AHAP3-BTMOS xerogel were incubated in a PBS solution containing AgSD at a sub-fungicidal concentration of 160 μg/mL. As shown in Figure 2.8, the combination of NO and AgSD resulted in a ~95% reduction of viable cells compared to the NO release from 10% AHAP3-BTMOS xerogels alone.

2.3.4 Efficacy of surface-generated NO against fungal biofilms. Due to the ability of biofilms to protect microbes from therapeutics,[3] we examined the effect of surface generated NO on the viability of preformed biofilms. Control and NO-releasing (40% AHAP3-BTMOS) xerogel-coated medical grade silicon rubber coupons were exposed to a fungal suspension for 2 h and then transferred to sterile nutrient broth for 2 d (transferring to fresh broth after 1 d) to facilitate biofilm formation. As expected, environmental scanning electron micrographs of each substrate revealed a substantial qualitative difference in the morphology of the biofilm between the control and NO-releasing xerogels (Figure 2.9). Densely packed communities of fungus were found over large areas on control substrates (Figure 2.9A), while only small clusters of cells and hyphae were observed on the NO-releasing substrates (Figure 2.9C). These results suggest that surface-generated NO release alters biofilm growth. To test the effectiveness of the combination of NO and AgSD, biofilms were grown on control and NO-releasing xerogels in the presence of 160 g/mL AgSD. Controls with and without AgSD treatment were indistinguishable, confirming that the AgSD alone had little effect on biofilm growth at the chosen concentration (Figure 2.9B). When AgSD treatment was combined with NO release, only sporadic clusters of cells were present with no hyphal growth (Figure 2.8D). The absence of hyphae suggests that the combination of AgSD and NO release may arrested the growth of planktonic cells that managed to adhere.

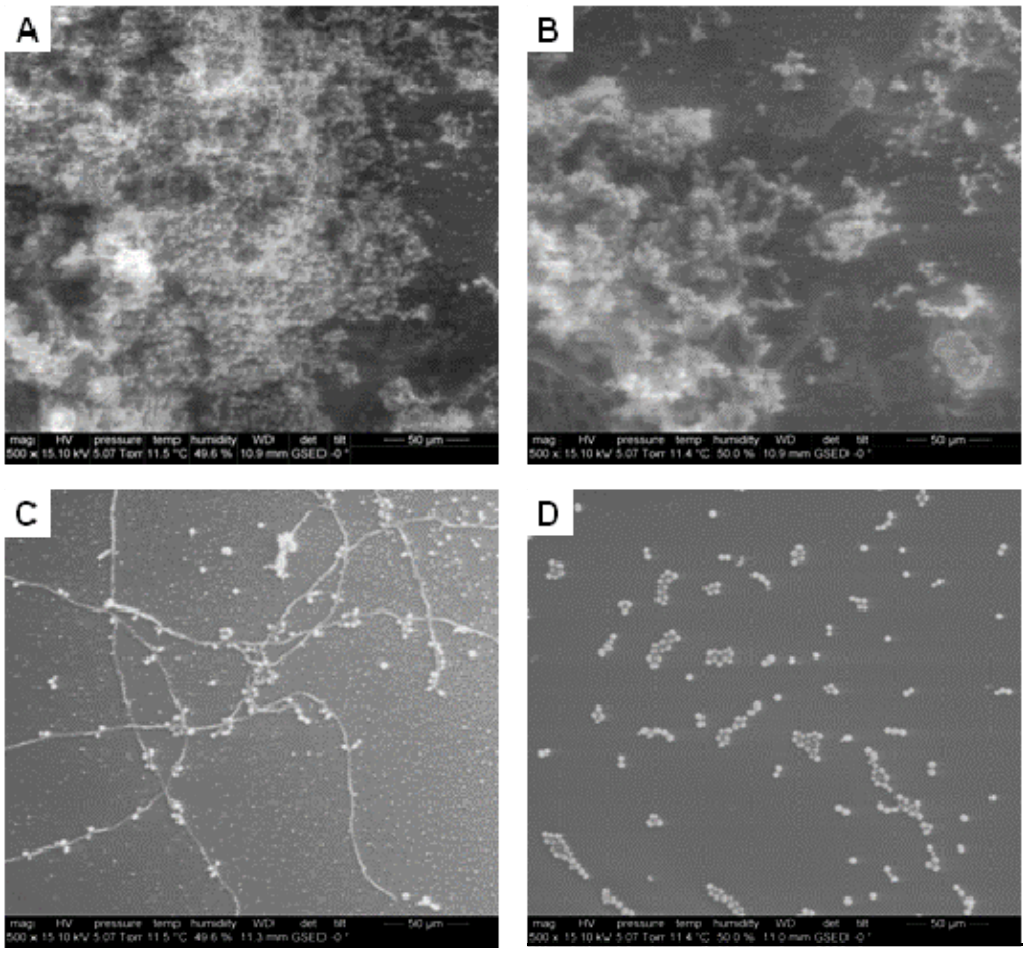

Figure 2.9. Representative environmental scanning electron micrographs of *C. albicans* biofilms attached to control (A and B) and NO-releasing (C and D) 40% AHAP3-BTMOS xerogels exposed to sterile YPD broth alone (A and C) and 160 µg/mL AgSD in nutrient broth (B and D).

2.4 Conclusions

The results described herein demonstrate that surface generated NO is an effective inhibitor of *C. albicans* adhesion at concentrations as low as ~2 pmol cm^{-2} s^{-1}. The majority of adhered cells were killed, with viability dependent on the quantity of NO released. Biofilm formation was reduced when compared to formation on control and blank (bare SiR) substrates. Due to a reduced efficacy against *C. albicans* relative to pathogenic bacteria at similar NO concentrations, future studies will examine both the antifungal and cytotoxic properties of greater NO fluxes. Nevertheless, the synergy study suggests that the combination of surface-generated NO and sub-MBC concentrations of AgSD greatly increases killing over NO alone. Further studies will examine the antimicrobial efficacy effect of broad-spectrum leachable antimicrobials doped into NO-releasing xerogels against *C. albicans* and other biofilm-forming fungus including *C. parapsilosis and C. tropicalis*.

2.5 References

1. Hetrick, E. M.; Schoenfisch, M. H. "Reducing implant-related infections: active release strategies," *Chemical Society Reviews* **2006**, *35*, 780-789.

2. O'Grady, N. P.; Alexander, M.; Dellinger, P.; Gerberding, J. L.; Heard, S. O.; Maki, D. G.; Masur, H.; McCormick, R. D.; Mermel, L. A.; Pearson, M. L.; Raad, II; Randolph, A.; Weinstein, R. A. "Guidelines for the prevention of intravascular catheter-related infections," *Pediatrics* **2002**, *110*.

3. Douglas, L. J. "*Candida* biofilms and thier role in infection," *Trends in Microbiology* **2003**, *11*, 30-36.

4. Crump, J. A.; Collignon, P. J. "Intravascular catheter-associated infections," *Eur. J. Clin. Microbiol. Infect. Dis.* **2000**, *19*, 1-8.

5. Ramage, G.; Saville, S. P.; Thomas, D. P.; Lopez-Ribot, J. L. "Candida biofilms: an update," *Eukaryot. Cell* **2005**, *4*, 633-638.

6. Cole, G. T.; Halawa, A. A.; Anaissie, E. J. "The role of the gastrointestinal tract in hematogenous candidiasis: From the laboratory to the bedside," *Clinical Infectious Diseases* **1996**, *22*, S73-S88.

7. Pfaller, M. A.; Diekema, D. J. "Epidemiology of invasive candidiasis: a persistent public health problem," *Clinical Microbiology Reviews* **2007**, *20*, 133-+.

8. Shin, J. H.; Kee, S. J.; Shin, M. G.; Kim, S. H.; Shin, D. H.; Lee, S. K.; Suh, S. P.; Ryang, D. W. "Biofilm production by isolates of Candida species recovered from nonneutropenic patients: Comparison of bloodstream isolates with isolates from other sources," *Journal of Clinical Microbiology* **2002**, *40*, 1244-1248.

9. Wey, S. B.; Mori, M.; Pfaller, M. A.; Woolson, R. F.; Wenzel, R. P. "Risk factors for hospital-acquired candidemia: A matched case-control study," *Arch Intern Med* **1989**, *149*, 2349-2353.

10. Chandra, J.; Mukherjee, P. K.; Leidich, S. D.; Faddoul, F. F.; Hoyer, L. L.; Douglas, L. J.; Ghannoum, M. A. "Antifungal resistance of candidal biofilms formed on denture acrylic *in vitro*," *J Dent Res* **2001**, *80*, 903-908.

11. Hawser, S. P.; Douglas, L. J. "Resistance of *Candida albicans* biofilms to antifungal agents *in vitro*," *Antimicrobial Agents and Chemotherapy* **1995**, *39*, 2128-2131.

12. Hetrick, E. M.; Schoenfisch, M. H. "Reducing implant-related infections: active release strategies," *Chem. Soc. Rev.* **2006**, *35*, 780-789.

13. Nejadnik, M. R.; van der Mei, H. C.; Norde, W.; Busscher, H. J. "Bacterial adhesion and growth on a polymer brush-coating," *Biomaterials* **2008**, *29*, 4117-4121.

14. Rojo, L.; Barcenilla, J. M.; Vazquez, B.; Gonzalez, R.; Roman, J. S. "Intrinsically antibacterial materials based on polymeric derivatives of eugenol for biomedical applications," *Biomacromolecules* **2008**, *9*, 2530-2535.

15. Dusane, D. H.; Rajput, J. K.; Kumar, A. R.; Nancharaiah, Y. V.; Venugopalan, V. P.; Zinjarde, S. S. "Disruption of fungal and bacterial biofilms by lauroyl glucose," *Lett. Appl. Microbiol.* **2008**, *47*, 374-379.

16. Malcher, M.; Volodkin, D.; Heurtault, B.; Andre, P.; Schaaf, P.; Mohwald, H.; Voegel, J. C.; Sokolowski, A.; Ball, V.; Boulmedais, F.; Frisch, B. "Embedded silver ions-containing liposomes in polyelectrolyte multilayers: Cargos films for antibacterial agents," *Langmuir* **2008**, *24*, 10209-10215.

17. Marini, M.; De Niederhausern, S.; Iseppi, R.; Bondi, M.; Sabia, C.; Toselli, M.; Pilati, F. "Antibacterial activity of plastics coated with silver-doped organic-inorganic hybrid coatings prepared by sol-gel processes," *Biomacromolecules* **2007**, *8*, 1246-1254.

18. Rossi, S.; Azghani, A. O.; Omri, A. "Antimicrobial efficacy of a new antibiotic-loaded poly(hydroxybutyric-co-hydroxyvaleric acid) controlled release system," *Journal of Antimicrobial Chemotherapy* **2004**, *54*, 1013-1018.

19. Freitas, F. I. S.; Guedes-Stehling, E.; Siqueira-Junior, J. P. "Resistance to gentamicin and related aminoglycosides in *Staphylococcus aureus* isolated in Brazil," *Lett. Appl. Microbiol.* **1999**, *29*, 197-201.

20. Chow, V. C. Y.; Hawkey, P. M.; Chan, E. W. C.; Chin, M. L.; Au, T. K.; Fung, D. K. C.; Chan, R. C. Y. "High-level gentamicin resistance mediated by a Tn4001-like transposon in seven nonclonal hospital isolates of *Streptococcus pasteurianus*," *Antimicrobial Agents and Chemotherapy* **2007**, *51*, 2508-2513.

21. De Lencastre, H.; Oliveira, D.; Tomasz, A. "Antibiotic resistant *Staphylococcus aureus*: a paradigm of adaptive power," *Curr. Opin. Microbiol.* **2007**, *10*, 428-435.

22. Witte, W.; Cuny, C.; Klare, I.; Nuebel, U.; Strommenger, B.; Werner, G. "Emergence and spread of antibiotic-resistant Gram-positive bacterial pathogens," *Int. J. Med. Microbiol.* **2008**, *298*, 365-377.

23. Percival, S. L.; Bowler, P. G.; Russell, D. "Bacterial resistance to silver in wound care," *J. Hosp. Infect.* **2005**, *60*, 1-7.

24. Silver, S. "Bacterial silver resistance: molecular biology and uses and misuses of silver compounds," *Fems Microbiol. Rev.* **2003**, *27*, 341-353.

25. McElhaney-Feser, G. E.; Raulli, R. E.; Cihlar, R. L. "Synergy of nitric oxide and azoles against *Candida* species in vitro," *Antimicrobial Agents and Chemotherapy* **1998**, *42*, 2342-2346.

26. Weller, R.; Price, R. J.; Ormerod, A. D.; Benjamin, N.; Leifert, C. "Antimicrobial effect of acidified nitrite on dermatophyte fungi, Candida and bacterial skin pathogens," *Journal of Applied Microbiology* **2001**, *90*, 648-652.

27. Nablo, B. J.; Prichard, H. L.; Butler, R. D.; Klitzman, B.; Schoenfisch, M. H. "Inhibition of implant-associated infections via nitric oxide," *Biomaterials* **2005**, *26*, 6984-6990.

28. Nablo, B. J.; Schoenfisch, M. H. "Antibacterial properties of nitric oxide-releasing sol-gels," *Journal of Biomedical Materials Research Part A* **2003**, *67A*, 1276-1283.

29. MacMicking, J.; Xie, Q. W.; Nathan, C. "Nitric oxide and macrophage function," *Annual Review of Immunology* **1997**, *15*, 323-350.

30. MacMicking, J. D.; Nathan, C.; Hom, G.; Chartrain, N.; Fletcher, D. S.; Trumbauer, M.; Stevens, K.; Xie, Q. W.; Sokol, K.; Hutchinson, N.; Chen, H.; Mudgett, J. S. "Altered responses to bacterial-infection and endotoxic-shock in mice lacking inducible nitric-oxide synthase," *Cell* **1995**, *81*, 641-650.

31. Ghaffari, A.; Miller, C. C.; McMullin, B.; Ghahary, A. "Potential application of gaseous nitric oxide as a topical antimicrobial agent," *Nitric Oxide* **2006**, *14*, 21-29.

32. Charville, G. W.; Hetrick, E. M.; Geer, C. B.; Schoenfisch, M. H. "Reduced bacterial adhesion to fibrinogen-coated substrates via nitric oxide release," *Biomaterials* **2008**, *29*, 4039-4044.

33. Dobmeier, K. P.; Schoenfisch, M. H. "Antibacterial properties of nitric oxide-releasing sol-gel microarrays," *Biomacromolecules* **2004**, *5*, 2493-2495.

34. Hetrick, E. M.; Schoenfisch, M. H. "Antibacterial nitric oxide-releasing xerogels: Cell viability and parallel plate flow cell adhesion studies," *Biomaterials* **2007**, *28*, 1948-1956.

35. Nablo, B. J.; Chen, T. Y.; Schoenfisch, M. H. "Sol-gel derived nitric-oxide releasing materials that reduce bacterial adhesion," *Journal of the American Chemical Society* **2001**, *123*, 9712-9713.

36. Nablo, B. J.; Rothrock, A. R.; Schoenfisch, M. H. "Nitric oxide-releasing sol-gels as antibacterial coatings for orthopedic implants," *Biomaterials* **2005**, *26*, 917-924.

37. Hrabie, J. A.; Keefer, L. K. "Chemistry of the nitric oxide-releasing diazeniumdiolate ("nitrosohydroxylamine") functional group and its oxygen-substituted derivatives," *Chem. Rev.* **2002**, *102*, 1135-1154.

38. Hetrick, E. M.; Shin, J. H.; Stasko, N. A.; Johnson, C. B.; Wespe, D. A.; Holmuhamedov, E.; Schoenfisch, M. H. "Bactericidal efficacy of nitric oxide-releasing silica nanoparticles," *Acs Nano* **2008**, *2*, 235-246.

39. Hetrick, E. M.; Shin, J. H.; Paul, H. S.; Schoenfisch, M. H. "Anti-biofilm efficacy of nitric oxide-releasing silica nanoparticles," *Biomaterials* **2009**, *30*, 2782-2789.

40. Marxer, S. M.; Rothrock, A. R.; Nablo, B. J.; Robbins, M. E.; Schoenfisch, M. H. "Preparation of nitric oxide (NO)-releasing sol-gels for biomaterial applications," *Chemistry of Materials* **2003**, *15*, 4193-4199.

41. Nablo, B. J.; Schoenfisch, M. H. "Poly(vinyl chloride)-coated sol-gels for studying the effects of nitric oxide release on bacterial adhesion," *Biomacromolecules* **2004**, *5*, 2034-2041.

42. Mermel, L. A. "Prevention of intravascular catheter-related infections," *Ann Intern Med* **2000**, *132*, 391-402.

43. Miller, D. L.; O'Grady, N. P. "Guidelines for the prevention of intravascular catheter-related infections: Recommendations relevant to interventional radiology," *J. Vasc. Interv. Radiol.* **2003**, *14*, 133-136.

44. Jin, Y.; Zhang, T.; Samaranayake, Y.; Fang, H.; Yip, H.; Samaranayake, L. "The use of new probes and stains for improved assessment of cell viability and extracellular polymeric substances in *Candida albicans* biofilms," *Mycopathologia* **2005**, *159*, 353-360.

45. Lewis, R. E.; Kontoyiannis, D. P.; Darouiche, R. O.; Raad, II; Prince, R. A. "Antifungal activity of amphotericin B, fluconazole, and voriconazole in an in vitro model of Candida catheter-related bloodstream infection," *Antimicrobial Agents and Chemotherapy* **2002**, *46*, 3499-3505.

46. Sherertz, R. J.; Raad, II; Belani, A.; Koo, L. C.; Rand, K. H.; Pickett, D. L.; Straub, S. A.; Fauerbach, L. L. "3-Year experience with sonicated vascular catheter cultures in a clinical microbiology laboratory," *Journal of Clinical Microbiology* **1990**, *28*, 76-82.

47. Sudbery, P.; Gow, N.; Berman, J. "The distinct morphogenic states of Candida albicans," *Trends in Microbiology* **2004**, *12*, 317-324.

48. Matias, V. R. F.; Al-Amoudi, A.; Dubochet, J.; Beveridge, T. J. "Cryo-transmission electron microscopy of frozen-hydrated sections of Escherichia coli and Pseudomonas aeruginosa," *Journal of Bacteriology* **2003**, *185*, 6112-6118.

49. Chaffin, W. L.; Lopez-Ribot, J. L.; Casanova, M.; Gozalbo, D.; Martinez, J. P. "Cell wall and secreted proteins of *Candida albicans*: Identification, function, and expression," *Microbiology and Molecular Biology Reviews* **1998**, *62*, 130-180.

50. Schierholz, J. M.; Fleck, C.; Beuth, J.; Pulverer, G. "The antimicrobial efficacy of a new central venous catheter with long-term broad-spectrum activity," *J. Antimicrob. Chemother.* **2000**, *46*, 45-50.

Chapter 3

Antibacterial Fluorinated Silica Colloid Superhydrophobic Surfaces

3.1 Introduction

The development of non-fouling coatings remains an important objective for the next generation of marine hulls, optical surfaces, and medical devices. Indeed, microbial fouling of biomedical devices (i.e., catheters, artificial joints) often results in blood stream infections (BSI) that have long plagued the healthcare industry. In 2002, 17 million cases of hospital acquired infections were reported in the United States resulting in roughly 100,000 deaths and $45 billion in direct medical costs.[1, 2] The increasing prevalence of these devices and the concomitant rise in associated infections have led to widespread dissemination of antibiotics, resulting in the emergence and rapid spread of drug-resistant microbes.[3]

As such, the development of device coatings capable of resisting microbial colonization has become a major thrust of research with recent activity focusing on the active release of antibiotics[4] or broad-spectrum antimicrobials such as silver ions or nitric oxide.[5, 6] To date, concerns about toxicity,[7] microbial resistance,[3, 8] and finite release lifetime[9] have limited the use and effectiveness of such coatings. Passive strategies including the physical or chemical modification of surfaces have been developed to resist bacterial adhesion in the absence of antimicrobial release, although such approaches have been pursued for decades with limited success.[1] For example, polymers including

polyurethane[10] and poly(ethylene glycol) have been shown to reduce in vitro bacterial adhesion,[11] but their in vivo effectiveness varies widely with surface chemistry, polymer composition and bacterial species.

Ideal non-fouling coatings not only resist adhesion of fouling agents (i.e., microorganisms), but allow for easy removal of contamination that may occur. Examples of "self-cleaning" surfaces that exist in nature include lotus leaves and water strider legs. These surfaces are referred to as "superhydrophobic," and exhibit static water contact angles >150º.[12, 13] The preparation of synthetic superhydrophobic surfaces generally involves surface modification via nanoparticles, photolithography, mesoporous polymers or surface etching resulting in nanoscale surface roughness, sometimes in conjunction with additional chemical modifications to reduce surface energy.[12, 14-16] The latter often require harsh synthetic conditions (e.g., etching and high temperature)[17, 18] and complex fabrication techniques,[19, 20] thus limiting the substrate type and geometry that may be coated.[18, 19, 21] While previous reports have highlighted the utility of superhydrophobic surfaces for reducing fouling, few have evaluated the ability of such surfaces to resist the adhesion of medically-relevant bacteria.[22-24] Of those evaluations published, assays were non-quantitative[22] or did not evaluate the viability of attached bacteria.[23, 24] Herein, we describe the synthesis of a superhydrophobic fluoroalkoxysilane coating that unlike previous reports makes use of mild reaction and curing conditions, and should enable modification of any substrates regardless of size or geometry. Using a quantitative bacterial adhesion/viability assay, we demonstrate the utility of this coating to reduce bacterial adhesion.

3.2 Materials and Methods

3.2.1 Silica colloid synthesis. Silica colloids were synthesized by sonicating a mixture of (heptadecafluoro-1,1,2,2-tetrahydrodecyl)trimethoxysilane (17FTMS) and tetraethylorthosilicate (TEOS) for 5 min. The amount of 17FTMS in the silane mixture was varied between 0 and 70 mol% (6.23 mmol total silane). The silane mixture was then added dropwise to a stirred solution of 30 mL ethanol (absolute) and 12 mL ammonium hydroxide (28%, w:w) over 30 min to form silica colloids. After an additional 20 min of mixing at room temperature, a white precipitate was collected via centrifugation at 4500 × g, washed twice with ethanol, and dried overnight under ambient conditions.

3.2.2 *Sol-gel film synthesis.* Silica colloid-doped 17FTMS/methyltrimethoxysilane (MTMOS) films were prepared via dispersing 400 mg silica colloids in 9.4 mL cold ethanol via sonication, and then adding 17FTMS and MTMOS. The amount of 17FTMS in the silane mixture was varied between 0 and 40 mol% (1 mmol total silane). Following 5 min of additional sonication, the mixture was added to a flask containing 2 mL H_2O and 200 μL 0.1 M HCl and stirred for 1 h. The sol solution was spread-cast onto ozone/UV-treated glass slides (69.4 μL sol solution per cm^2) and dried overnight, resulting in an opaque white film or xerogel. The control sols without colloids were spincast onto 9 × 24 mm glass substrates (200 μL at 3000 rpm for 10 s) as simple spread-casting resulted in non-uniform coatings.

3.2.3 Sol-gel film characterization. The wettability of the resulting surfaces was characterized via static water contact angle goniometry. Reported results are an average of 12 measurements. Surface morphology was characterized via electron microscopy

after coating with 2.5 nm Au/Pd and imaging using a Hitachi S-4700 scanning electron microscope. Root-mean-square (RMS) roughness of the substrates was measured via atomic force microscopy, and were calculated from 20 μm^2 images of three different substrates obtained in AC mode in air using an Asylum MFP-3D AFM and Olympus AC240TS silicon beam cantilevers (spring constant of 2 Nm^{-1}). MFP-3D software was used for calculation of RMS values. The stability of the coatings was assessed via daily contact angle measurements while soaking the substrates in water at 25 ºC for 15 d.

3.2.4 Bacterial adhesion and viability assay. Bacterial adhesion to the substrates was characterized using a parallel-plate flow cell. *S. aureus* and *P. aeruginosa* were grown overnight from a frozen (-80 ºC) stock in tryptic soy broth (TSB) at 37 ºC, reinoculated in fresh TSB (37 ºC), and grown to 10^8 colony forming units (CFU)/mL as determined by optical density at 600 nm and verified by replicate plating on nutrient agar. The bacteria were pelleted via centrifugation (4500 × g, 15 min) and resuspended in an equivalent volume of PBS. The bacterial suspension was flowed over the xerogel substrates at 0.2 mL/min in a custom-machined polycarbonate parallel-plate flow cell (chamber dimensions = 2.1 × 0.6 × 0.08 cm^3) for 90 min. The bacterial suspension was then exchanged with sterile PBS without passage of an air-water interface and flowed for another 20 min to rinse away any non-adherent bacteria. The substrates were removed, immersed in 5 mL sterile PBS, and subjected to ultrasonication for 15 min to remove adhered bacteria from the substrates. Bacterial suspensions were then serially diluted, plated on tryptic soy agar, and enumerated after incubation at 37 ºC for 24 h.

3.3 Results and Discussion

3.3.1 Coating synthesis. Silica colloids were synthesized from 17FTMS (0 – 70 mol% total silane) and TEOS via base-catalyzed hydrolysis and condensation. The resulting silica colloids were composed of agglomerated silica particles with both micro-scale particle agglomerates (Figure 3.1A) and nano-scale individual particle definition (Figure 3.1B). While agglomeration of irregularly-sized colloids would not be ideal for use as a therapeutic delivery vehicle, the varied structure was advantageous in for the use in a superhydrophobic coating. Xerogel coatings with and without added colloids were synthesized from 17FTMS (0 – 40 mol% total silane) and MTMOS via acid-catalyzed hydrolysis and condensation. The xerogel served as a low surface energy chemical modification to hold the silica colloids in place, as illustrated in Figure 3.2. Control surfaces consisted of 1) 17FTMS colloids without the additional 17FTMS xerogel coating (i.e., 100 mol% MTMOS); 2) 30 mol% 17FTMS/MTMOS xerogel coating without colloids; and, 3) a 100 mol% MTMOS xerogel coating without colloids.

3.3.2 Surface Characterization. Contact angle goniometry (CAG) was used to measure static water contact angles of the control and silica colloid-doped xerogels. As shown in Figure 3.3, the optimal 17FTMS concentrations for both silica colloids alone and the xerogel blanks (without doped silica colloids) was 20-30 mol%. Increasing the 17FTMS concentration above 30 mol% 17FTMS did not significantly increase the water contact angles, but negatively impacted the quality of the resulting films (data not shown).

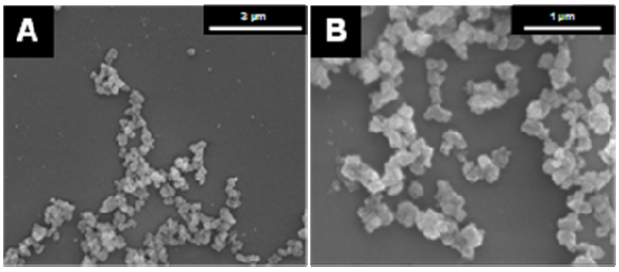

Figure 3.1. Scanning electron microscopy images of 30 mol% 17FTMS-TEOS silica colloids at (A) 15000x, and (B) 36,600x magnification.

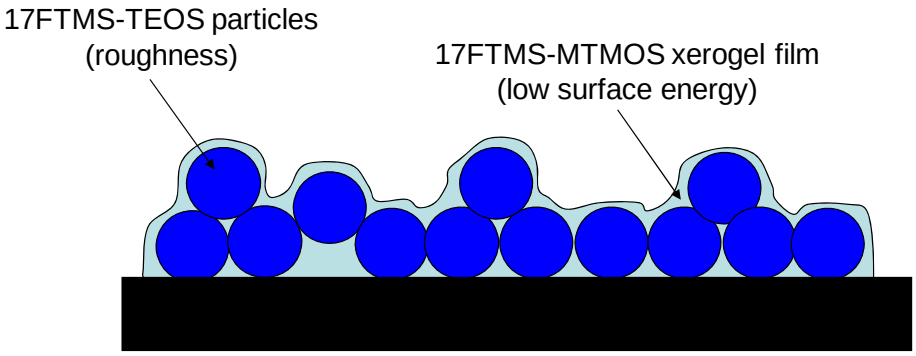

Figure 3.2. Illustration showing silica colloids cast within a thin fluorosilane film.

Thus, 30 mol% 17FTMS was used for all fluorinated colloid and xerogel film compositions. Static water contact angle images of the silica colloid-modified xerogels (superhydrophobic films) and controls, and blanks are shown in Table 3.1. The term "superhydrophobic" is typically given to any surface with a static water contact angle >150°, while the terms "hydrophobic" and "hydrophilic" are >90° and <90°, respectively (Figure 3.4). Doping the silica colloids into 17FTMS xerogels resulted in a superhydrophobic interface that was not achievable with silica colloids or 17FTMS xerogels alone. Scanning electron microscopy (SEM) images of the resulting silica colloid-containing fluorinated xerogel surfaces revealed a dense assembly of agglomerated particles consisting of both micro- and nano-scale features (Figure 3.5), which are prerequisite surface properties for obtaining superhydrophobicity.[12] The 17FTMS/MTMOS xerogel film was not apparent in the SEM images as it was spread as a thin coating on the high surface area created by the colloids. Both fluorinated and non-fluorinated blank substrates (without colloids) were characterized with a slight surface roughness of 11.7 ± 0.3 and 1.5 ± 1.3 nm, respectively. As expected, the surface roughness of the 17FTMS colloid-doped substrates was much greater (898.5 ± 84.8 and 573.8 ± 154 nm for fluorinated and non-fluorinated xerogels, respectively). The substantially greater surface roughness for the silica colloid-containing fluorinated substrates may be attributed to the assembly of the hydrophobic silica colloids within the hydrophobic 17FTMS.

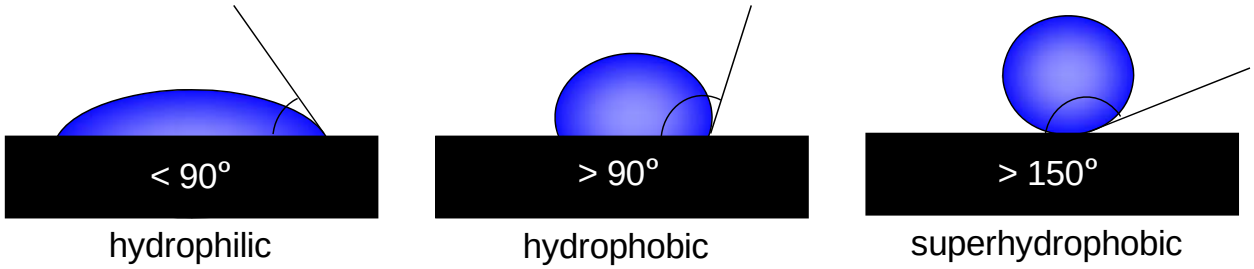

Figure 3.3. Static water contact angles of (A) xerogel films, and (B) silica colloids as a function of the concentration (mol%) of 17FTMS (balance MTMOS and TEOS for films and particles, respectively). Data are represented as means ± SD (n = 15).

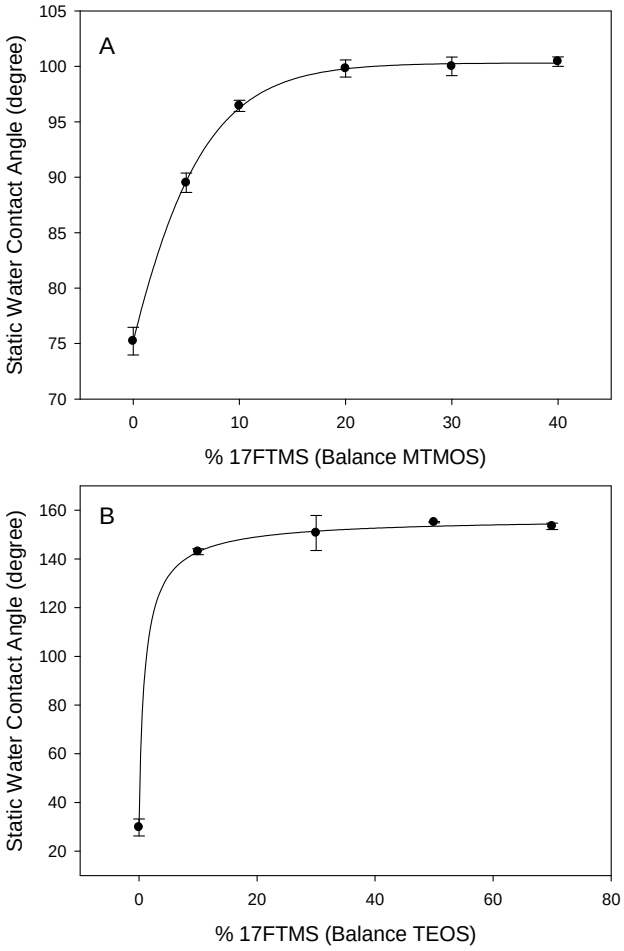

Figure 3.4. Static water contact angles of (A) xerogel films, and (B) silica colloids as a function of the concentration (mol%) of 17FTMS (balance MTMOS and TEOS for films and particles, respectively). Data are represented as means ± SD (n = 15).

Table 3.1. Static water contact angle measurements.

	Silica colloid-doped xerogel		Xerogel blanks	
Surface	100 mol% MTMOS	30 mol% 17FTMS-MTMOS	100 mol% MTMOS	30 mol% 17FTMS-MTMOS
	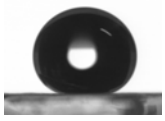	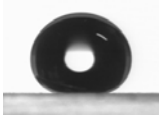	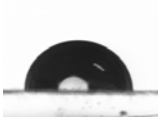	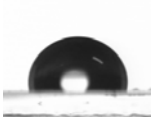
Static water contact angle (degrees)	151.0 ± 0.5	167.7 ± 1.8	88.3 ± 5.5	104.7 ± 0.8

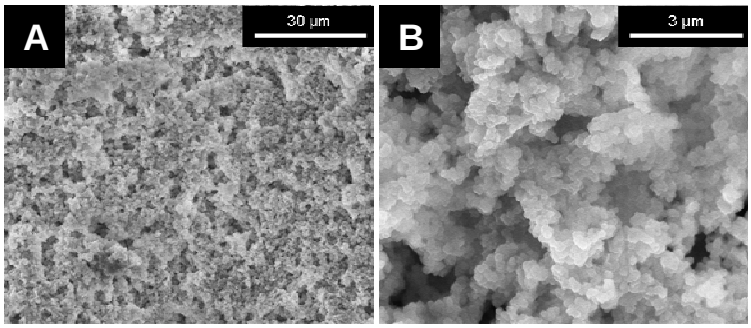

Figure 3.5. Scanning electron microscopy images of 30 mol% 17FTMS (balance MTMOS) xerogel films doped with 30 mol% 17FTMS (balance TEOS) silica colloids at (A) 1500x, and (B) 15,000x magnification.

Indeed, comparison of scanning electron micrographs of both fluorinated and non-fluorinated colloid doped substrates revealed flat islands of colloids on non-fluorinated surfaces but no such features on the fluorinated interface (Figure 3.6). The presence of the smoother colloid islands would be expected to reduce both the measured surface roughness and resulting superhydrophobic character of the films. The stability of the coatings was evaluated by soaking substrates in distilled water for 15 days while measuring the static water contact angle each day. Contact angles were maintained for all four substrates over this period (Figure 3.7), indicating that these xerogel-modified interfaces are sufficiently stable in aqueous solutions. Furthermore, the static water contact angle for the fluorinated superhydrophobic substrate (~167º) remained constant under the conditions of the bacteria experiment (25 ºC in phosphate buffered saline) over the course of the bacterial adhesion assay.

2.3.3 Bacterial adhesion and viability assay. Bacterial infection of pin tracts represents the most common complication associated with external fixation of orthopedic biomaterials.[25-27] We evaluated the adhesion of Gram-positive *Staphylococcus aureus* and Gram-negative *Pseudomonas aeruginosa*, strains common to pin tract infections, to control and superhydrophobic surfaces using a modified version of a conventional flow cell assay.

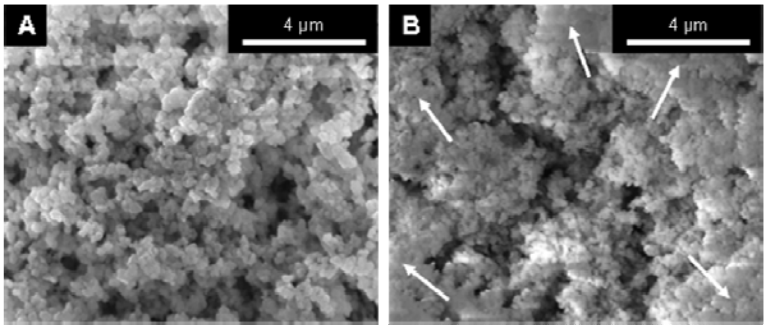

Figure 3.6. SEM images of A) a fluorinated xerogel (30 mol% 17FTMS-MTMOS) doped with silica colloids (30 mol% 17FTMS-TEOS) and B) a non-fluorinated xerogel (100 mol% MTMOS) doped with silica colloids (30 mol% 17FTMS-TEOS). White arrows indicate examples of smooth colloid islands.

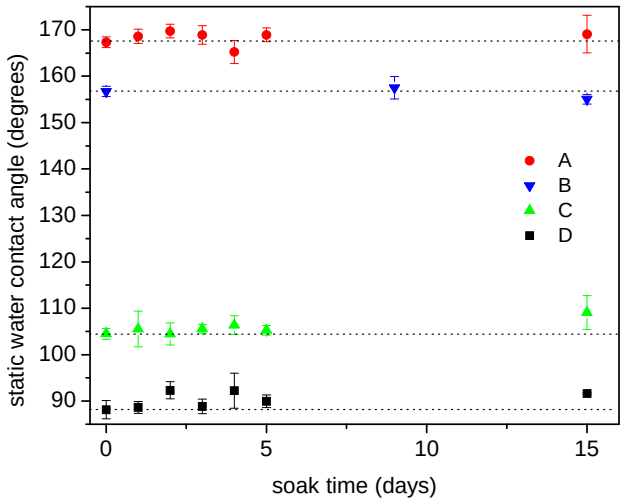

Figure 3.7. Static water contact angles after immersion in distilled water at 25 ºC. A) Superhydrophobic 30 mol% 17FTMS (balance TEOS) colloid-doped 30 mol% 17FTMS (balance MTMOS) and B) colloid-doped 100 mol% MTMOS xerogels; C) blank (no colloids) 30 mol% 17FTMS (balance MTMOS) xerogels; and, D) MTMOS controls (100 mol%). Data are represented as means ± SD (n = 12).

Many assays have been developed to evaluate bacterial adhesion and viability on surfaces. The most straightforward of these techniques is a static adhesion assay, where a coated substrate is incubated in a solution containing bacteria for a prescribed period. The extent of bacterial adhesion is then evaluated either qualitatively (i.e., bright field or electron microscopy) or quantitatively (i.e., ultrasonic removal of bacteria and plating on nutrient agar). Static adhesion assays are not ideal models for in vivo bacterial adhesion because the repeated passage of an air-water interface during substrate removal and rinsing often dislodges adhered bacteria before evaluation. Adhesion assays utilizing flow cells are a better model as exposure and rinsing steps may be performed without the passage of an air-water interface. In addition, flow may be controlled to mimic a particular biological environment. Although bacterial adhesion may be evaluated in real-time using optical microscopy, quantification requires a transparent, relatively smooth substrate. Both static and flow techniques may be utilized to obtain semi-quantitative viability data by coupling the assay with fluorescent nucleic acid stains such as propidium iodide (enters only dead cells) and Syto 9 (enters both living and dead cells). To properly evaluate the superhydrophobic films in this study, a combination of a static and flow cell assay was utilized. Although the minimization of air-water interfaces afforded by the flow cell assay was necessary, the films were neither optically-transparent nor microscopically smooth precluding the use of optical microscopy for quantification. Evaluation of bacterial adhesion was performed by removing the substrates from the flow cell prior to the rinse step, sonicating briefly in sterile PBS to remove adhered cells, and quantifying by plating on nutrient agar. An added advantage to this procedure is that unlike for optical microscopy, only viable bacteria were quantified.

As shown in Figure 3.8, the adhesion of *S. aureus* and *P. aeruginosa* to the silica colloid-doped fluorinated substrates was reduced by 99.0 and 98.2% (2.08 and 1.76 logs, respectively) versus the MTMOS blank. For silica colloid-coated substrates lacking the additional fluorosilane film modification, the reduction in *S. aureus* and *P. aeruginosa* adhesion versus MTMOS was an order of magnitude less at 87.4 (0.93 log) and 91.3% (1.10 log), respectively. Bacterial adhesion to fluorinated and non-fluorinated controls (without colloids) were identical within error as shown at A in Figure 3.8, indicating that the low surface energy of the fluorinated surface alone does not reduce bacterial adhesion. While these results suggest that the surface roughness of the silica colloid coatings alone may reduce bacterial adhesion, the low surface energy fluorosilane modification further improves the non-fouling nature of the surfaces as observed previously.[28] Although the increase in static water contact angle upon fluorine modification was similar (~16º), only the colloid-containing substrates showed a measurable decrease in bacterial adhesion (1-log reduction for fluorinated versus non-fluorinated). These results suggest that the greater surface roughness observed for the colloid-containing fluorinated surfaces plays a major role in the observed bacterial adhesion, compared to the 17FTMS coating alone.

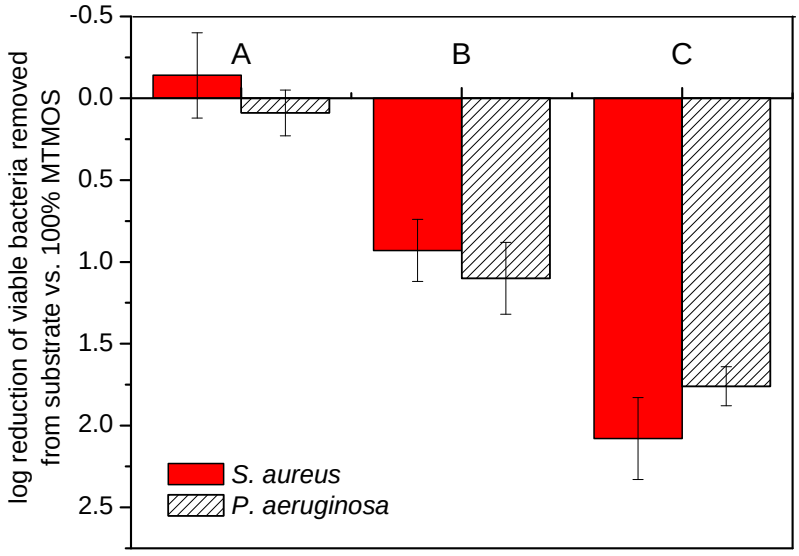

Figure 3.8. Reduction in *S. aureus* and *P. aeruginosa* adhesion at (A) blank (no colloids) 30 mol% 17FTMS (balance MTMOS) xerogels; (B) colloid-doped 100 mol% MTMOS xerogels; and, (C) superhydrophobic 30 mol% 17FTMS (balance TEOS) colloid-doped 30 mol% 17FTMS (balance MTMOS) xerogels versus MTMOS controls (100 mol%). Data are represented as means ± SD (n = 9).

2.4 Conclusions

The simple and flexible synthesis of silica colloid-based superhydrophobic surfaces has been reported and represents an important advance in developing non-fouling surface coatings. The combination of micro- and nanostructured features from silica colloids and a low surface energy fluorinated silane xerogel resulted in surfaces that reduce the adhesion of highly pathogenic *S. aureus* and *P. aeruginosa* by ~2 orders of magnitude vs. controls, making these surfaces excellent candidates for further study as medical device coatings. By utilizing well-defined sol-gel chemistry for colloid and xerogel synthesis, the surface chemistry and physical properties of the resulting coatings may be tuned and optimized depending on the applications. Future studies will focus on the effect of colloid size, surface roughness, backbone silane structure and concentration, and protein preconditioning on bacterial adhesion. Furthermore, the bacterial adhesion of the superhydrophobic surfaces may be further reduced with additional silane precursor modifications that enable the active release of biocidal agents. For example, we have previously reported on silica nanoparticles and xerogels capable of releasing antimicrobial concentrations of nitric oxide.[5, 29]

2.5 References

1. Francolini, I.; Donelli, G. "Prevention and control of biofilm-based medical-device-related infections," *FEMS Immunol. Med. Microbiol.* **2010**, *59*, 227-238.

2. Scott, R. D.; Centers for Disease Control and Prevention, March 2009.

3. Andersson, D. I.; Hughes, D. "Antibiotic resistance and its cost: is it possible to reverse resistance?," *Nat. Rev. Microbiol.* **2010**, *8*, 260-271.

4. Zilberman, M.; Elsner, J. J. "Antibiotic-eluting medical devices for various applications," *J. Control. Release* **2008**, *130*, 202-215.

5. Hetrick, E. M.; Schoenfisch, M. H. "Antibacterial nitric oxide-releasing xerogels: Cell viability and parallel plate flow cell adhesion studies," *Biomaterials* **2007**, *28*, 1948-1956.

6. Kumar, R.; Munstedt, H. "Silver ion release from antimicrobial polyamide/silver composites," *Biomaterials* **2005**, *26*, 2081-2088.

7. Rai, M.; Yadav, A.; Gade, A. "Silver nanoparticles as a new generation of antimicrobials," *Biotechnol. Adv.* **2009**, *27*, 76-83.

8. Chopra, I. "The increasing use of silver-based products as antimicrobial agents: a useful development or a cause for concern?," *J. Antimicrob. Chemother.* **2007**, *59*, 587–590.

9. Hetrick, E. M.; Schoenfisch, M. H. "Reducing implant-related infections: active release strategies," *Chem. Soc. Rev.* **2006**, *35*, 780-789.

10. Dickinson, R. B.; Nagel, J. A.; Proctor, R. A.; Cooper, S. L. "Quantitative comparison of shear-dependent Staphylococcus aureus adhesion to three polyurethane ionomer analogs with distinct surface properties," *J. Biomed. Mater. Res.* **1997**, *36*, 152-162.

11. Kingshott, P.; Wei, J.; Bagge-Ravn, D.; Gadegaard, N.; Gram, L. "Covalent attachment of poly(ethylene glycol) to surfaces, critical for reducing bacterial adhesion," *Langmuir* **2003**, *19*, 6912-6921.

12. Li, X. M.; Reinhoudt, D.; Crego-Calama, M. "What do we need for a superhydrophobic surface? A review on the recent progress in the preparation of superhydrophobic surfaces," *Chem. Soc. Rev.* **2007**, *36*, 1350-1368.

13. Blossey, R. "Self-cleaning surfaces - virtual realities," *Nat. Mater.* **2003**, *2*, 301-306.

14. Sarkar, D. K.; Saleema, N. "One-step fabrication process of superhydrophobic green coatings," *Surf. Coat. Tech.*, *204*, 2483-2486.

15. Zhang, H.; Lamb, R.; Lewis, J. "Engineering nanoscale roughness on hydrophobic surface - preliminary assessment of fouling behaviour," *Science and Technology of Advanced Materials* **2005**, *6*, 236-239.

16. Wang, H. X.; Fang, J.; Cheng, T.; Ding, J.; Qu, L. T.; Dai, L. M.; Wang, X. G.; Lin, T. "One-step coating of fluoro-containing silica nanoparticles for universal generation of surface superhydrophobicity," *Chem. Commun.* **2008**, 877-879.

17. Fresnais, J.; Chapel, J. P.; Benyahia, L.; Poncin-Epaillard, F. "Plasma-treated superhydrophobic polyethylene surfaces: Fabrication, wetting and dewetting Properties," *J Adhes. Sci. Technol.* **2009**, *23*, 447-467.

18. Hikita, M.; Tanaka, K.; Nakamura, T.; Kajiyama, T.; Takahara, A. "Super-liquid-repellent surfaces prepared by colloidal silica nanoparticles covered with fluoroalkyl groups," *Langmuir* **2005**, *21*, 7299-7302.

19. Yang, H. T.; Jiang, P. "Self-Cleaning diffractive macroporous films by doctor blade coating," *Langmuir* **2010**, *26*, 12598-12604.

20. Bravo, J.; Zhai, L.; Wu, Z. Z.; Cohen, R. E.; Rubner, M. F. "Transparent superhydrophobic films based on silica nanoparticles," *Langmuir* **2007**, *23*, 7293-7298.

21. Furstner, R.; Barthlott, W.; Neinhuis, C.; Walzel, P. "Wetting and self-cleaning properties of artificial superhydrophobic surfaces," *Langmuir* **2005**, *21*, 956-961.

22. Crick, C. R.; Ismail, S.; Pratten, J.; Parkin, I. P. "An investigation into bacterial attachment to an elastomeric superhydrophobic surface prepared via aerosol assisted deposition," *Thin Solid Films* **2011**, *519*, 3722-3727.

23. Fadeeva, E.; Truong, V. K.; Stiesch, M.; Chichkov, B. N.; Crawford, R. J.; Wang, J.; Ivanova, E. P. "Bacterial retention on superhydrophobic titanium surfaces fabricated by femtosecond laser ablation," *Langmuir* **2011**, *27*, 3012-3019.

24. Yonghao, X.; Hess, D. W.; Wong, C. P. "A novel method to prepare superhydrophobic, self-cleaning and transparent coatings for biomedical applications," *Electronic Components and Technology Conference* **2007**, 1218-1223.

25. Mahan, J.; Seligson, D.; Henry, S. L.; Hynes, P.; Dobbins, J. "Factors in pin tract infections," *Orthopedics* **1991**, *14*, 305-308.

26. Duran, L. W. "Preventing medical device related infections.," *Med. Device Technol.* **2000**, *11*, 14-17.

27. Coester, L. M.; Nepola, J. V.; Allen, J.; Marsh, J. L. "The effects of silver coated external fixation pins.," *Iowa Orthop J.* **2006**, *26*, 48-53.

28. Ma, M. L.; Hill, R. M. "Superhydrophobic surfaces," *Curr. Opin. Colloid Interface Sci.* **2006**, *11*, 193-202.

29. Hetrick, E. M.; Shin, J. H.; Stasko, N. A.; Johnson, C. B.; Wespe, D. A.; Holmuhamedov, E.; Schoenfisch, M. H. "Bactericidal efficacy of nitric oxide-releasing silica nanoparticles," *Acs Nano* **2008**, *2*, 235-246.

Chapter 4

Examination of Bacterial Resistance to Exogenous Nitric Oxide

4.1 Introduction

Nitric oxide (NO) is an endogenous diatomic free radical implicated in several physiological processes including vasodilation, immune response, neurotransmission, and wound healing.[1] During infection, NO is released by macrophages and other immune cells at >1 μM concentrations where it serves as a broad spectrum biocidal agent.[1-6] Nitric oxide induces both nitrosative and oxidative stress that results in numerous toxic effects on bacteria, including direct modification of membrane proteins, lipid peroxidation, and DNA cleavage.[1, 6-8] As such, the exogenous application of NO as a therapy has been the subject of intense interest during the past decade.[9-14]

Controlled NO storage and delivery using chemical NO donors has led to several pharmacological applications.[15, 16] Example antimicrobial NO delivery vehicles include low molecular weight compounds (e.g., sodium nitroprusside, *N*-diazeniumdiolated proline, and *S*-nitroso-*N*-acetylpenicillamine),[17-19] macromolecular vehicles,[13, 14, 20-23] and polymeric coatings.[9, 11, 24-32] We have previously reported the bactericidal activity of NO-releasing silica nanoparticles and sol-gel-derived xerogel films against *Pseudomonas aeruginosa* at concentrations of minimal toxicity to mammalian cells.[9, 13]

It is known that bacteria possess mechanisms for reducing the pharmacological effects of drugs such as antibiotics by decreasing their diffusion (i.e., efflux pumps),

overproduction or alterations of drug target sites, and enzymatic drug degradation.[33-38] Recent research also indicates that select bacteria are capable of up-regulating NO scavengers[39-43] and/or altering respiration in response to endogenous NO.[44] An example is NO detoxification by flavohemoglobin, a protein that is up-regulated in *E. coli* in response to macrophage-produced NO.[45] Enzymes including reductases and superoxide dismutase have been implicated to serve similar functions.[45, 46] With respect to cellular respiration, Husain et al. reported arrested respiration in *Salmonella* with concomitant accumulation of NADH, thereby increasing the ability of the bacteria to resist oxidative stress.[47]

While the antimicrobial action of NO-releasing materials is established,[9, 12, 13, 27, 48-50] knowledge about the bacterial resistance to exogenous concentrations of NO remains scarce.[39-44, 51] Miller et al. reported that *S. aureus* was not capable of developing resistance to exogenous gaseous NO; however, NO exposure was intermittent with discontinuous selective pressure against the NO-susceptible bacteria.[52-55] Herein, we report a thorough bacterial resistance study using both spontaneous mutation and serial passage mutagenesis assays with continuous exposure to physiologically relevant concentrations of NO from NO-releasing silica nanoparticles. Representative gram positive and gram negative bacteria were selected to provide preliminary resistance information as a function of bacteria classification and structure.

4.2 Materials and Methods

4.2.1 Strains, media, and chemical reagents. 3-Mercaptopropyltrimethoxysilane (MPTMS) and tetraethoxysilane (TEOS) were purchased from Gelest (Tullytown, PA).

Bacteria were propagated at 37 °C in tryptic soy broth (TSB) and agar (TSA, Becton, Dickinson, Franklin Lakes, NJ). Sodium chloride, potassium chloride, sodium phosphate monobasic, methanol, ethanol, ammonium hydroxide, and hydrochloric acid were obtained from Fisher Scientific (Pittsburgh, PA). Sodium phosphate dibasic and sodium nitrite were obtained from Sigma Aldrich (St. Louis, MO). *Escherichia coli* O157:H7 (35150), *Pseudomonas aeruginosa* (19143), methicillin-susceptible *Staphylococcus aureus* (MSSA) (29213), methicillin-resistant *Staphylococcus aureus* (MRSA) (33591), and *Staphylococcus epidermidis* (35983) were obtained from American Type Culture Collection (ATCC, Manassas, VA). Distilled water was purified to 18.2 MΩ·cm with a Millipore Milli-Q Gradient A-10 water purification system (Bedford, MA).

4.2.2 Synthesis of mercaptosilane-based silica particles. Nitrosothiol particles (75 mol% MPTMS/TEOS) were synthesized following a procedure reported previously.[20] Briefly, 3-mercaptopropyltrimethoxysilane (MPTMS, 424 μL) and tetraethoxysilane (TEOS, 169 μL) were mixed and added dropwise via a Kent Scientific Genie Plus syringe pump at a flow rate of 0.5 mL min^{-1} through an 18.5 gauge needle to a solution of ethanol (16.3 mL), water (1.4 mL), and ammonium hydroxide (11 mL). The reaction was stirred for 2 h at room temperature and the particles collected by centrifugation at 3645g (10 min), washed twice with 40 mL EtOH, recollected, and dried overnight at ambient conditions.

4.2.3 Nitrosation of mercaptosilane-based silica particles. Thiols within the particles were nitrosated upon reaction with nitrous acid as follows. Particles (~200 mg) were first added to 4 mL methanol (MeOH). While stirring, 2 mL of hydrochloric acid (5 M) was added to the suspension. A 2 mL aqueous solution containing sodium nitrite (2x

molar excess to thiol) and DTPA (500 μM) was then added to the particle suspension, and the mixture was stirred for 2 h in the dark on ice. Particles were collected by centrifugation at 3645g (5 min), washed with 40 mL chilled 500 μM $DTPA_{(aq)}$, recollected, washed with 40 mL chilled MeOH, recollected, and vacuum dried in the dark for 30 min. Particles were stored at –20 °C in vacuo until used.

4.2.4 Nitric oxide release characterization. Real-time NO release from 75 mol% MPTMS/TEOS particles was measured at 1 s intervals using a Sievers Chemiluminescence Nitric Oxide Analyzer (Boulder, CO). Particles were added to 25 mL deoxygenated TSB (37 °C) containing 50 μL antifoaming agent B (Sigma-Aldrich) to prevent frothing. The solution was sparged with nitrogen (80 mL/min) with additional nitrogen was supplied to the reaction flask to match the collection rate of the NOA (200 mL min^{-1}). The apparatus was covered with aluminum foil to prevent light-initiated nitrosothiol decomposition.

4.2.5 Minimum inhibitory concentration assay. Bacterial cultures were grown from an overnight stock in TSB to 10^8 colony forming units (cfu) mL^{-1} and diluted to 2 × 10^6 cfu ml^{-1}. Bacteria were added to serial dilutions of nitrosothiol particles in a 96-well plate resulting in a final concentration of 10^6 cfu mL^{-1} bacteria. After incubating by shaking for 24 h at 37 °C, MIC values were determined as the lowest particle concentration not supporting bacterial growth (i.e., not turbid).

4.2.6 Spontaneous resistance assay. Bacterial cultures were grown from an overnight stock in TSB to ~10^{10} cfu mL^{-1}. A 1-mL aliquot of the 10^9 cfu mL^{-1} culture was added to NO-releasing particles at 2–8× the MIC. Following a 24 h incubation at 37 °C in the dark with agitation, 1 mL of each concentration was plated on TSA (200 μL on 5

separate plates) and incubated overnight at 37 °C. Surviving colonies were propagated overnight at 37 °C in TSB, reinoculated and grown to 10^8 cfu mL^{-1}. The MICs for propagated strains were determined using the above procedure and compared to the parent strain. Surviving colonies on TSA that could not be propagated in TSB were passaged on TSA for three days and then grown in TSB overnight at 37 °C. If overnight growth in TSA was successful, the MIC was then evaluated and compared to the parent strain. Otherwise, formation and settling of a bacterial precipitate did not allow an MIC assay to be performed.

4.2.7 Serial passage assay. Bacterial cultures were grown from an overnight stock in TSB to 10^8 cfu mL^{-1} and diluted to 2×10^6 cfu mL^{-1}. The bacterial suspensions were then added to serial dilutions of nitrosothiol particles in a 96-well plate resulting in wells containing 10^6 cfu mL^{-1} bacteria and nitrosothiol particle concentrations of 2, 1, 0.5, 0.25, and 0.125× the MIC (n=3). After incubating by shaking for 24 h at 37 °C, MIC values were recorded, and an aliquot from the well containing the highest particle concentration that supported bacterial growth was diluted to 2×10^6 cfu mL^{-1}. The MIC assay was performed using this bacterial suspension. The entire process was repeated for 20 exposure cycles.

4.3 Results and Discussion

The bacterial species used in these studies were selected because they are frequently found in a clinical environment. While gaseous NO has proven useful for pulmonary treatment, it is generally not a good candidate for an antimicrobial therapeutic. The short half-life (<10 s) of NO in physiological milieu prevents its delivery to common

infection sites such as an indwelling medical device (i.e., catheter) or deep wound. As such, nanoparticles chemically modified to store and release NO have been studied widely as candidate antimicrobials.[12-14] We have previously described particles that release NO over extended periods (from minutes to days), allowing more targeted NO delivery, thus ensuring more lethal concentrations of NO. Indeed, Hetrick and coworkers reported excellent efficacy of NO-releasing particles against both planktonic and biofilm-based bacteria.[12, 13] To date, the only studies that have examined bacterial resistance to exogenous NO have used NO gas from cylinders.[52-55] Martinez and Baquero demonstrated that the development of resistant bacteria depends on antibiotic exposure parameters (i.e., concentration and kinetics).[56] Thus, we utilized chemically-stored NO release for these studies to more fully evaluate resistance potential. In particular, nitrosothiol-based NO-releasing particles were selected because their extended NO release capabilities (>24 h) facilitate continuous selective pressure for resistant mutants whereas low molecular weight *N*-diazeniumdiolate NO donors tend to release their NO payload more quickly, especially in aqueous media.[13, 20]

The NO release profile of 75 mol% MPTMS-TEOS particles (635 ± 63 nm diameter) in TSB at 37 °C is shown in Figure 4.1. To mimic the conditions used during the bacteria assays, NO release measurements were conducted in the absence of light such that NO production was limited to thermal decomposition and not photolytic cleavage. Upon addition to the assay media (2 mg mL^{-1} final particle concentration) (TSB,37 °C), a bolus of NO was released at ~740 ppb mg^{-1} s^{-1}. This level of NO decreased with time, ultimately dropping to ~11 ppb mg^{-1} s^{-1} after 24 h. Over the course of the assay, a total of 0.90 μmol mg^{-1} was released per mg of particles. Both the

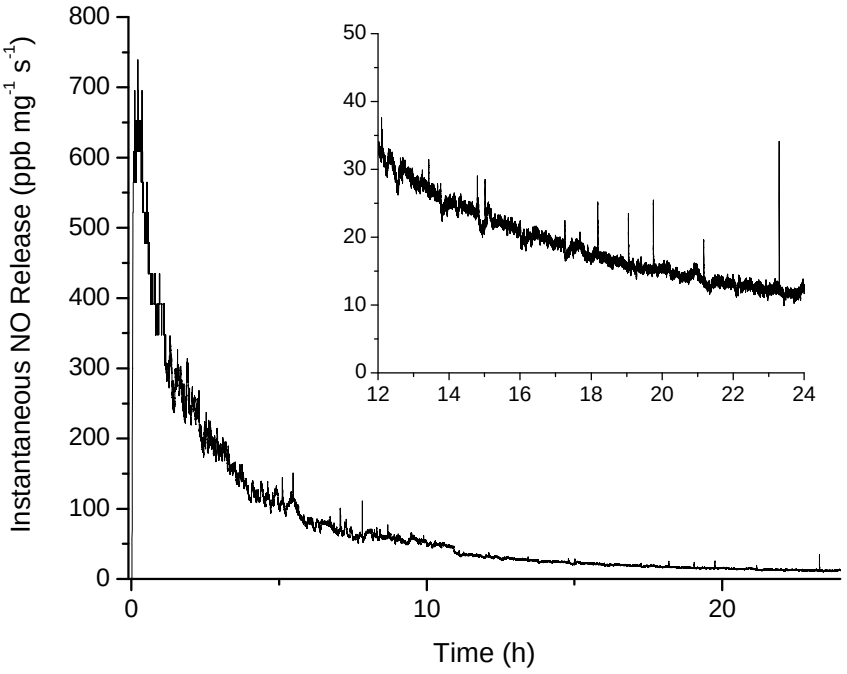

Figure 4.1. Representative NO release from 75 mol% MPTMS/TEOS particles in TSB at 37 °C. [Inset: Enlarged view of NO release during 12–24 h.

maximum instantaneous and the total NO released from the particles in TSB were slightly lower than reported previously in PBS (1205 ppb mg^{-1} s^{-1} and 1.17 μmol mg^{-1}, respectively), which is likely due to reactions between NO and proteins present in TSB.[20]

4.3.1 Miniminum inhibitory concentration determinations. Minimum inhibitory concentrations were used to rapidly determine the efficacy of the NO release and monitor for the emergence of resistance.[56-59] As shown in Table 4.1, the MICs were used for both the spontaneous and serial passage mutagenesis assays. The MIC of 75 mol% MPTMS/TEOS particles for each bacterial species was determined under growth conditions (TSB, 37 °C) over 24 h. The measured MICs ranged from 3.13 to 6.25 mg mL^{-1} across all bacterial species (Table 4.1).Of note, the MICs for both methicillin-susceptible and -resistant *S. aureus* were half that of *S. epidermidis* and the two Gram negative species, *E. coli* and *P. aeruginosa*.

4.3.2 Spontaneous mutagenesis assay. Even after exposure to bactericidal doses of an antimicrobial, some microbes may survive depending on the antimicrobial concentration, environmental conditions, and microbial species.[56] In the case of antibiotics, some of the surviving microbes are the result of a spontaneous mutation that confers greater resistance to future treatment.[56] Thus, the rate of spontaneous mutations occurring at inhibitory NO concentrations was evaluated for each bacterial species to address the possibility of NO-resistance. Nitric oxide-releasing particle concentrations ranging from 2 to 8 times the MIC were utilized to provide adequate selective pressure against NO-susceptible bacteria. Surviving colonies were isolated and propagated in TSB, and the MIC assays were repeated to observe if the microbes were more or less susceptible to NO treatment. Exposure of *E. coli* to NO-releasing particles at 2 times the

MIC resulted in 19 surviving colonies in 1 mL. Each colony was reinoculated in TSB, and all resulted in a cloudy suspension after overnight incubation. An MIC assay was performed individually on each colony and the susceptibility of all 19 colonies was unchanged from the parent strain (6.25 mg mL^{-1}). An illustrative overview of the spontaneous mutation assay is shown in Figure 4.2. Nanoparticle exposure to MRSA at 7 times the MIC resulted in one surviving colony in 1 mL. Although the MIC of this survivor was increased by 2 times to 6.25 mg mL^{-1}, this increase is considered to be within the experimental variation and is thus not significant. After exposure of *P. aeruginosa* to 2 times the MIC, 7 surviving colonies were isolated and propagated successfully in TSB. The MIC of all *P. aeruginosa* survivors was increased two fold to 12.5 mg mL^{-1}, but again this increase is within the experimental variation and not significant.

Some colonies that were able to survive NO treatment were not able to grow successfully in TSB. These colonies were instead propagated three times on TSA to assess if the mutation that limited growth in broth was stable. After exposure of *S. epidermidis* to 4 times the MIC, two of the three surviving colonies could not be propagated further in TSB, even after three successful passages on TSA. Regrowth of the bacterial precipitate was possible on TSA. However, the lack of growth to turbidity in TSB prevented the determination of the MIC. The spontaneous mutation that resulted in this NO tolerance seemed to have prevented regrowth in nutrient broth. Others have observed similar behavior where mutations conferring resistance to a therapeutic also result in a fitness cost to the bacteria, sometimes preventing further propagation.[60, 61] A third colony of *S. epidermidis* was successfully regrown in TSB, but viability was not

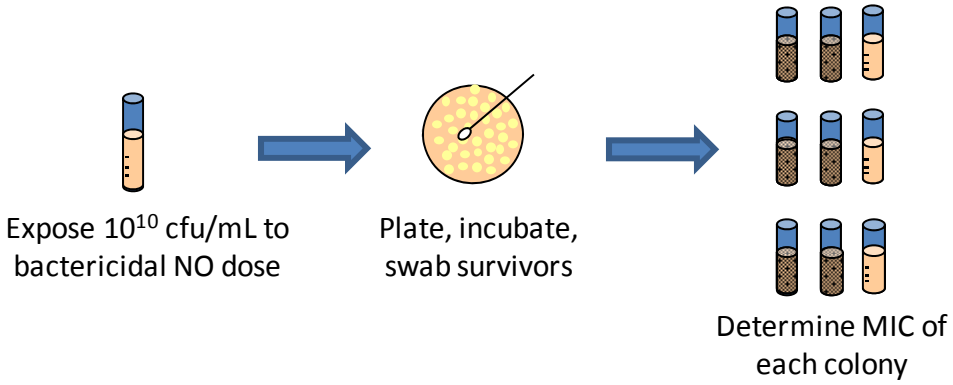

Figure 4.2. Illustrative overview of the spontaneous mutagenesis assay.

evident following NO exposure even at 1/8 of the MIC. To assess the fitness of this colony, it was propagated three times in succession on TSA and then inoculated in TSB. The solution again grew to a cloudy suspension overnight. An MIC assay was successfully completed and found to be identical to the parent strain (~6.25 mg mL^{-1}). These results indicate that for one mutant, the growth defect preventing propagation in TSB in the absence of NO was resolved, possibly due to a second mutation that also abolished the observed increase in NO resistance.

Methicillin-susceptible *S. aureus* exposed to 8 times the MIC resulted in 12 surviving colonies on TSA. Reinoculation of each colony in TSB produced a precipitate similar to that of the *S. epidermidis* colonies described above. Similarly, the colony failed to successfully grow to a cloudy suspension in TSB after regrowth on TSA three times in succession. Therefore, no MIC assay was performed. However, propagation of the bacteria aggregate on TSA was successful. A comparison of all parameters (initial and final MIC, survivors, and colonies propagated in TSB) is shown in Table 4.1.

4.3.3 Serial passage assay. Repeated exposure to sub-therapeutic concentrations of antibiotics often hastens the development of antibiotic-resistant bacteria.[62, 63] Genetic mutations may result, leading to an increased resistance to the antibiotic that the microbes were exposed to at subcidal or subinhibitory doses. Repeated or prolonged exposure to sub-therapeutic antibiotic concentrations would further enrich the resistant strain. To investigate possible resistance, the susceptibility to NO treatment following exposure to sub-inhibitory NO doses was examined using the NO-releasing nitrosothiol-modified particles. Bacterial cultures were treated with a range of concentrations both above and

Table 4.1. Minimum inhibitory concentrations of 75 mol% MPTMS/TEOS particles in TSB at 37 °C for 24 h and spontaneous mutation parameters before and after exposure to inhibitory concentrations of NO.

species	ATCC #[a]	MIC_{24h} ($mg\ mL^{-1}$)	Exposure concentration ($mg\ mL^{-1}$)[b]	Survivors after >MIC NO exposure	Colonies propagated in TSB	Final MIC_{24h} ($mg\ mL^{-1}$)
S. aureus	29213	3.13	25.0	12	0	N/A[c]
MRSA	33591	3.13	21.9	1	1	6.25
S. epidermidis	35983	6.25	25.0	3	1	6.25
E. coli (0157:H7)	35150	6.25	12.5	19	19	6.25
P. aeruginosa	19143	6.25	12.0	3	6	12.5

[a]ATCC, American Type Culture Collection.

[b]Starting bacterial concentrations were ~10^{10} cfu mL^{-1}.

[c]Regrowth in broth did not result in turbidity, thus an MIC could not be performed.

below the MIC for 24 h in nutrient growth conditions employing a serial passage mutagenesis assay described previously.[58, 59] The assay was repeated by propagating the bacteria exposed to the highest concentration of particles that did not inhibit growth. An illustrative overview of the serial passage mutagenesis assay is shown in Figure 4.3. After the completion of 20 passages of NO exposure in this manner, no sustained increases in the MIC for any of the bacterial species were observed versus the parent strains (Table 4.2). The two-fold increase in susceptibility observed for S. aureus and S. epidermidis was not significant and is considered normal inter-experimental variation.

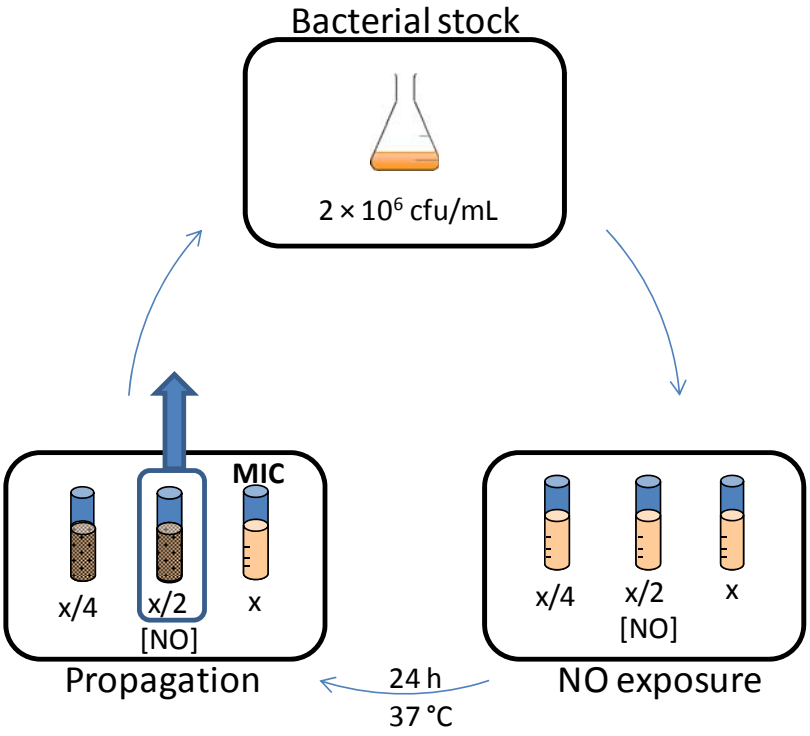

Figure 4.3. Illustrative overview of the serial passage mutagenesis assay.

Table 4.2. Minimum inhibitory concentrations of 75 mol% MTPMS/TEOS particles after 1 and 20 passages in 1×10^6 cfu/mL bacterial stock.

		MIC_{24h} ($mg\,mL^{-1}$)		
species	ATCC #	Day 1	Day 20	ΔMIC
S. aureus	29213	3.13	3.13	0
MRSA	33591	3.13	1.65	-50%
S. epidermidis	35983	6.25	3.13	-50%
E. coli (0157:H7)	35150	6.25	6.25	0
P. aeruginosa	19143	6.25	6.25	0

4.4 Conclusions

The inability of bacteria to develop resistance to exogenous NO delivered from a silica vehicle was not surprising primarily because of the multiple mechanisms by which NO presents toxicity towards microbes.[2, 9, 12, 13, 16, 48] The hydrophobicity and small size of NO allows it to rapidly migrate across bacterial lipid membranes where a number of nitrosative and oxidative reactions may occur (Figure 4.4).[13] The diversity of NO's antimicrobial mechanisms thus would require multiple mutations to occur simultaneously for microbial survival, hindering resistance development. Nevertheless, it would be naïve to conclude that bacteria absolutely cannot develop increased resistance to exogenous NO. Spellberg et al. points out the fallacy of assuming that we (humans) can win a war against bacteria that have been "creating and defeating antibiotics for 20 million times longer than *Homo sapiens* have known that antibiotics existed."[63] It is likely that the emergence of resistance to exogenous NO will depend heavily on environmental conditions such as nutrient availability, temperature, exposure duration/intensity, the presence of other bacterial species, and infection location (i.e., in vivo vs. in vitro). Clearly, it is imperative that future studies examining the efficacy of NO-releasing therapeutics also consider the ability of bacteria to develop resistance, especially as such therapeutics are applied clinically.

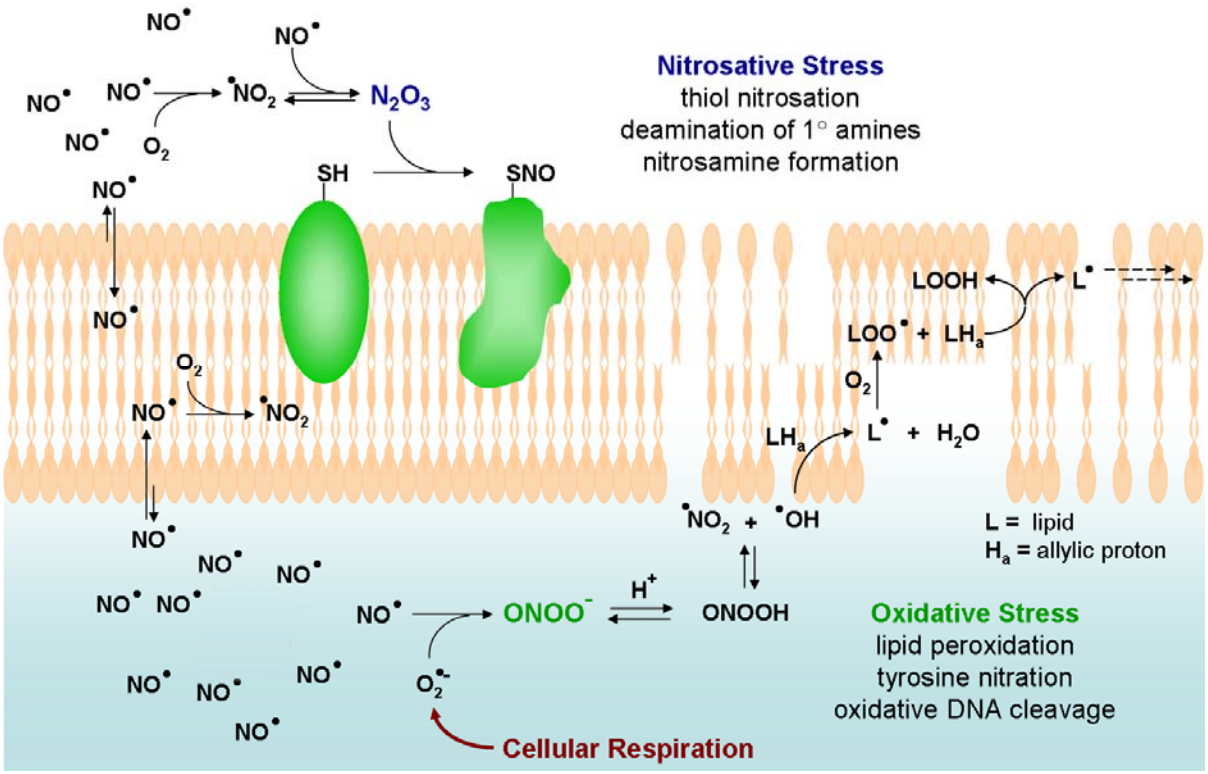

Figure 4.4. Illustration of nitrosative and oxidative antimicrobial mechanism of NO within a bacterial membrane. Reprinted with permission from ref. 13. Copyright 2008 American Chemical Society.

4.5 References

1. Wink, D. A.; Mitchell, J. B. "Chemical biology of nitric oxide: Insights into regulatory, cytotoxic, and cytoprotective mechanisms of nitric oxide," *Free Radic. Biol. and Med.* **1998**, *25*, 434-456.

2. Bogdan, C. "Nitric oxide and the immune response," *Nat. Immunol.* **2001**, *2*, 907-916.

3. Fang, F. C. "Host/pathogen interactions: Mechanisms of nitric oxide-related antimicrobial activity," *J. Clin. Invest.* **1997**, *99*, 2818-2825.

4. Foley, E.; O'Farrell, P. H. "Nitric oxide contributes to induction of innate immune responses to gram-negative bacteria in Drosophila," *Genes Dev.* **2003**, *17*, 115-125.

5. MacMicking, J.; Xie, Q. W.; Nathan, C. "Nitric oxide and macrophage function," *Annu. Rev. Immunol.* **1997**, *15*, 323-350.

6. Mannick, J. B. "Immunoregulatory and antimicrobial effects of nitrogen oxides," *Proc. Am. Thorac. Soc.* **2006**, *3*, 161-165.

7. Moller, M. N.; Li, Q.; Lancaster, J. R. J.; Denicola, A. "Acceleration of nitric oxide autooxidation and nitrosation by membranes," *Life* **2007**, *59*, 243-248.

8. Zaki, M. H.; Akuta, T.; Akaike, T. "Nitric oxide-induced nitrative stress involved in microbial pathogenesis," *J. Pharmacol. Sci.* **2005**, *98*, 117-129.

9. Hetrick, E. M.; Schoenfisch, M. H. "Antibacterial nitric oxide-releasing xerogels: Cell viability and parallel plate flow cell adhesion studies," *Biomaterials* **2007**, *28*, 1948-1956.

10. Keefer, L. K. "Progress toward clinical application of the nitric oxide-releasing diazeniumdiolates," *Annu. Rev. Pharmacol. Toxicol.* **2003**, *43*, 585-607.

11. Nablo, B. J.; Rothrock, A. R.; Schoenfisch, M. H. "Nitric oxide-releasing sol-gels as antibacterial coatings for orthopedic implants," *Biomaterials* **2005**, *26*, 917-924.

12. Hetrick, E. M.; Shin, J. H.; Paul, H. S.; Schoenfisch, M. H. "Anti-biofilm efficacy of nitric oxide-releasing silica nanoparticles," *Biomaterials* **2009**, *30*, 2782-2789.

13. Hetrick, E. M.; Shin, J. H.; Stasko, N. A.; Johnson, C. B.; Wespe, D. A.; Holmuhamedov, E.; Schoenfisch, M. H. "Bactericidal efficacy of nitric oxide-releasing silica nanoparticles," *ACS Nano* **2008**, *2*, 235-246.

14. Shin, J. H.; Metzger, S. K.; Schoenfisch, M. H. "Synthesis of nitric oxide-releasing silica nanoparticles," *J. Am. Chem. Soc.* **2007**, *129*, 4612-4619.

15. Ghaffari, A.; Miller, C. C.; McMullin, B.; Ghahary, A. "Potential application of gaseous nitric oxide as a topical antimicrobial agent," *Nitric Oxide* **2006**, *14*, 21-29.

16. Feelisch, M. "The use of nitric oxide donors in pharmacological studies," *Naunyn-Schmiedebergs Arch. Pharmacol.* **1998**, *358*, 113-122.

17. Muscará, M. N.; Wallace, J. L. "V. Therapeutic potential of nitric oxide donors and inhibitors," *Am. J. Physiol. - Gastrointestinal and Liver Physiology* **1999**, *276*, G1313-G1316.

18. Artz, J. D.; Toader, V.; Zavorin, S. I.; Bennett, B. M.; Thatcher, G. R. J. "In vitro activation of soluble guanylyl cyclase and nitric oxide release: A comparison of NO donors and NO mimetics," *Biochemistry* **2001**, *40*, 9256-9264.

19. Barraud, N.; Hassett, D. J.; Hwang, S. H.; Rice, S. A.; Kjelleberg, S.; Webb, J. S. "Involvement of nitric oxide in biofilm dispersal of Pseudomonas aeruginosa," *Journal of Bacteriology* **2006**, *188*, 7344-7353.

20. Riccio, D. A.; Nugent, J. L.; Schoenfisch, M. H. "Stöber synthesis of nitric oxide-releasing *S*-nitrosothiol-modified silica particles," *Chemistry of Materials* **2010**, *23*, 1727-1735.

21. Stasko, N. A.; Fischer, T. H.; Schoenfisch, M. H. "S-nitrosothiol-modified dendrimers as nitric oxide delivery vehicles," *Biomacromolecules* **2008**, *9*, 834-841.

22. Stasko, N. A.; Schoenfisch, M. H. "Dendrimers as a scaffold for nitric oxide release," *J. Am. Chem. Soc.* **2006**, *128*, 8265-8271.

23. Rothrock, A. R.; Donkers, R. L.; Schoenfisch, M. H. "Synthesis of nitric oxide-releasing gold nanoparticles," *J. Am. Chem. Soc.* **2005**, *127*, 9362-9363.

24. Marxer, S. M.; Rothrock, A. R.; Nablo, B. J.; Robbins, M. E.; Schoenfisch, M. H. "Preparation of nitric oxide (NO)-releasing sol-gels for biomaterial applications," *Chemistry of Materials* **2003**, *15*, 4193-4199.

25. Coneski, P. N.; Schoenfisch, M. H. "Synthesis of nitric oxide-releasing polyurethanes with S-nitrosothiol-containing hard and soft segments," *Polym. Chem.* **2011**, *2*, 906-913.

26. Coneski, P. N.; Nash, J. A.; Schoenfisch, M. H. "Nitric oxide-releasing electrospun polymer microfibers," *ACS Appl. Mater. Interfaces* **2011**, *3*, 426-432.

27. Privett, B. J.; Nutz, S. T.; Schoenfisch, M. H. "Efficacy of surface-generated nitric oxide against Candida albicans adhesion and biofilm formation," *Biofouling* **2010**, *26*, 973-983.

28. Coneski, P. N.; Rao, K. S.; Schoenfisch, M. H. "Degradable nitric oxide-releasing biomaterials via post-polymerization functionalization of cross-linked polyesters," *Biomacromolecules* **2010**, *11*, 3208-3215.

29. Riccio, D. A.; Dobmeier, K. P.; Hetrick, E. M.; Privett, B. J.; Paul, H. S.; Schoenfisch, M. H. "Nitric oxide-releasing S-nitrosothiol-modified xerogels," *Biomaterials* **2009**, *30*, 4494-4502.

30. Nablo, B. J.; Schoenfisch, M. H. "Antibacterial properties of nitric oxide-releasing sol-gels," *J. Biomed. Mater. Res., Part A* **2003**, *67A*, 1276-1283.

31. Marxer, S. M.; Rothrock, A. R.; Nablo, B. J.; Robbins, M. E.; Schoenfisch, M. H. "Preparation of nitric oxide (NO)-releasing sol-gels for biomaterial applications," *Chem. Mater.* **2003**, *15*, 4193-4199.

32. Nablo, B. J.; Chen, T. Y.; Schoenfisch, M. H. "Sol-gel derived nitric-oxide releasing materials that reduce bacterial adhesion," *J. Am. Chem. Soc.* **2001**, *123*, 9712-9713.

33. Akimitsu, N.; Hamamoto, H.; Inoue, R.; Shoji, M.; Akamine, A.; Takemori, K.; Hamasaki, N.; Sekimizu, K. " Increase in resistance of methicillin-resistant *Staphylococcus aureus* to β-lactams caused by mutations conferring resistance to benzalkonium chloride, a disinfectant widely used in hospitals," *Antimicrob. Agents Chemother.* **1999**, *43*, 3042-3043.

34. Hiramatsu, K. "Vancomycin resistance in Staphylococci," *Drug Res. Updates* **1998**, *1*, 135-150.

35. Levy, S. B. "Multidrug resistance: a sign of the times," *New Eng. J. Med.* **1998**, *338*, 1376-1378.

36. Percival, S. L.; Bowler, P. G.; Russell, D. "Bacterial resistance to silver in wound care," *Journal of Hospital Infection* **2005**, *60*, 1-7.

37. Silver, S.; Phung, L. T.; Silver, G. "Silver as biocides in burn and wound dressings and bacterial resistance to silver compounds," *J. Ind. Microbiol. Biotechnol.* **2006**, *33*, 627-634.

38. Suller, M. T. E.; Russell, A. D. "Antibiotic and biocide resistance in methicillin-resistant staphylococcus aureus and vancomycin-resistant enterococcus," *Journal of Hospital Infection* **1999**, *43*, 281-291.

39. Shatalin, K.; Gusarov, I.; Avetissova, E.; Shatalina, Y.; McQuade, L. E.; Lippard, S. J.; Nudler, E. "Bacillus anthracis-derived nitric oxide is essential for pathogen

virulence and survival in macrophages," *Proc. Natl. Acad. Sci. U. S. A.* **2008**, *105*, 1009-1013.

40. Nunoshiba, T.; Derojaswalker, T.; Tannenbaum, S. R.; Demple, B. "Roles of nitric-oxide in inducible resistance of Escherichia-coli to activated murine macrophages," *Infect. Immun.* **1995**, *63*, 794-798.

41. Nunoshiba, T.; Derojaswalker, T.; Wishnok, J. S.; Tannenbaum, S. R.; Demple, B. "Activation by nitric-oxide of an oxidative-stress response that defends Escherichia-coli against activated macrophages," *Proc. Natl. Acad. Sci. U. S. A.* **1993**, *90*, 9993-9997.

42. Poole, R. K. "Nitric oxide and nitrosative stress tolerance in bacteria," *Biochem. Soc. Trans.* **2005**, *33*, 176-180.

43. Tillmann, A.; Gow, N. A. R.; Brown, A. J. P. "Nitric oxide and nitrosative stress tolerance in yeast," *Biochem. Soc. Trans.* **2011**, *39*, 219-223.

44. Husain, M.; Bourret, T. J.; McCollister, B. D.; Jones-Carson, J.; Laughlin, J.; Vazquez-Torres, A. "Nitric oxide evokes an adaptive response to oxidative stress by arresting respiration," *J. Biol. Chem.* **2008**, *283*, 7682-7689.

45. Poole, R. K. "Nitric oxide and nitrosative stress tolerance in bacteria," *Biochem. Soc. Trans.* **2005**, *33*, 176-180.

46. Nunoshiba, T.; Derojaswalker, T.; Wishnok, J. S.; Tannenbaum, S. R.; Demple, B. "Activation by Nitric-Oxide of an Oxidative-Stress Response That Defends Escherichia-Coli against Activated Macrophages," *Proceedings of the National Academy of Sciences of the United States of America* **1993**, *90*, 9993-9997.

47. Husain, M.; Bourret, T. J.; McCollister, B. D.; Jones-Carson, J.; Laughlin, J.; Vazquez-Torres, A. "Nitric oxide evokes an adaptive response to oxidative stress by arresting respiration," *Journal of Biological Chemistry* **2008**, *283*, 7682-7689.

48. Deupree, S. M.; Schoenfisch, M. H. "Morphological analysis of the antimicrobial action of nitric oxide on Gram-negative pathogens using atomic force microscopy," *Acta Biomaterialia* **2009**, *5*, 1405-1415.

49. Dobmeier, K. P.; Schoenfisch, M. H. "Antibacterial properties of nitric oxide-releasing sol-gel microarrays," *Biomacromolecules* **2004**, *5*, 2493-2495.

50. Privett, B. J.; Deupree, S. M.; Backlund, C. J.; Rao, K. S.; Johnson, C. B.; Coneski, P. N.; Schoenfisch, M. H. "Synergy of nitric oxide and silver sulfadiazine against gram-negative, gram-positive, and antibiotic-resistant pathogens," *Mol. Pharmaceutics* **2010**, *7*, 2289-2296.

51. Darwin, K. H.; Ehrt, S.; Gutierrez-Ramos, J. C.; Weich, N.; Nathan, C. F. "The proteasome of Mycobacterium tuberculosis is required for resistance to nitric oxide," *Science* **2003**, *302*, 1963-1966.

52. Miller, C.; McMullin, B.; Ghaffari, A.; Stenzler, A.; Pick, N.; Roscoe, D.; Ghahary, A.; Road, J.; Av-Gay, Y. "Gaseous nitric oxide bactericidal activity retained during intermittent high-dose short duration exposure," *Nitric Oxide-Biol. Chem.* **2009**, *20*, 16-23.

53. Ghaffari, A.; Jalili, R.; Ghaffari, M.; Miller, C.; Ghahary, A. "Efficacy of gaseous nitric oxide in the treatment of skin and soft tissue infections," *Wound Rep. Regen.* **2007**, *15*, 368-377.

54. Ghaffari, A.; Miller, C. C.; McMullin, B.; Ghahary, A. "Potential application of gaseous nitric oxide as a topical antimicrobial agent," *Nitric Oxide-Biol. Chem.* **2006**, *14*, 21-29.

55. Miller, C. C.; Miller, M. K.; Ghaffari, A.; Kunimoto, B. "Treatment of chronic nonhealing leg ulceration with gaseous nitric oxide: A case study," *J. Cutan. Med. Surg.* **2004**, *8*, 233-238.

56. Martinez, J. L.; Baquero, F. "Mutation frequencies and antibiotic resistance," *Antimicrob. Agents Chemother.* **2000**, *44*, 1771-1777.

57. Vasquez, J. E.; Walker, E. S.; Franzus, B. W.; Overbay, B. K.; Reagan, D. R.; Sarubbi, F. A. "The epidemiology of mupirocin resistance among methicillin-resistant Staphylococcus aureus at a veterans' affairs hospital," *Infect. Control Hosp. Epidemiol.* **2000**, *21*, 459-464.

58. Suller, M. T. E.; Russell, A. D. "Antibiotic and biocide resistance in methicillin-resistant Staphylococcus aureus and vancomycin-resistant enterococcus," *J. Hosp. Inf.* **1999**, *43*, 281-291.

59. Suller, M. T. E.; Russell, A. D. "Triclosan and antibiotic resistance in Staphylococcus aureus," *J. Antimicrob. Chemother.* **2000**, *46*, 11-18.

60. Andersson, D. I.; Hughes, D. "Antibiotic resistance and its cost: is it possible to reverse resistance?," *Nat. Rev. Microbiol.* **2010**, *8*, 260-271.

61. Normark, B. H.; Normark, S. "Evolution and spread of antibiotic resistance," *J. Intern. Med.* **2002**, *252*, 91-106.

62. Spellberg, B.; Guidos, R.; Gilbert, D.; Bradley, J.; Boucher, H. W.; Scheld, W. M.; Bartlett, J. G.; Edwards, J. "The epidemic of antibiotic-resistant infections: A call to action for the medical community from the Infectious Diseases Society of America," *Clinical Infectious Diseases* **2008**, *46*, 155-164.

63. LaPara, T. M.; Ghosh, S. "The effects of subtherapeutic antibiotic use in farm animals on the proliferation and persistence of antibiotic resistance among soil bacteria," *Isme Journal* **2007**, *1*, 191-203.

Chapter 5

Microfluidic Nitric Oxide Sensor for Biological Applications

Introduction

Few endogenously produced small molecules are involved in such expansive roles as nitric oxide (NO), a diatomic free-radical. Since being identified in 1987 as the endothelium-derived relaxation factor responsible for regulating vascular tone,[1-3] NO has been the subject of intense scientific interest. Nitric oxide is generated through the conversion of L-arginine to L-citrulline by a class of enzymes known as nitric oxide synthases (NOS).[4-8] Two constitutive isoforms of NOS, neuronal and endothelial NOS, produce NO at pM to nM concentrations in physiological milieu.[9, 10] The inducible NOS isoform, iNOS, expressed by phagocytes during immune system activation, results in much greater NO concentrations (e.g., >10 μM in blood).[11, 12] Nitric oxide has also been implicated in other physiological processes including wound healing,[13-15] angiogenesis,[16-19] and the inhibition of platelet activation.[20-22] As might be expected, the detection and quantification of NO has been and continues to be the subject of intense research.[23-27]

Measuring NO in biological systems is challenging due to NO's reactivity (i.e., short half-life), wide concentration range (pM–10 μM), and sample (i.e., matrix) complexity.[23] Despite these challenges, both direct and indirect analytical methods have been developed for measuring NO in biological samples. Often, NO is more easily quantified by measuring specific oxidative byproducts (e.g., nitrite and nitrate). In this

respect, absorbance or fluorescence may be used upon reaction of NOx with an assay reagent.[12, 28-30] Indeed, the Griess assay is the most widely used approach for measuring NOx and back-calculating NO levels. Unfortunately, NOx levels fluctuate significantly due to diet and other underlying diseases and thus make real-time NO concentration determination in complex media nearly impossible. Alternatively, methods for measuring NO directly include chemiluminescence,[31, 32] electron paramagnetic resonance (EPR) spectroscopy,[24, 31, 33] and electrochemistry.[26] Although direct measurement allows for sensitive and selective NO detection, chemiluminescence and EPR instrumentation is expensive, specialized, and often difficult to adapt to challenging matrices such as whole blood.[26]

Among the direct detection methods, electrochemistry is the most straightforward, inexpensive, and versatile for measuring NO, with a large assortment of available sensor platforms (i.e., sensor style, geometry, material, and size).[23, 24, 26, 27, 33-48] In terms of clinical utility, electrochemical sensors are highly amenable to miniaturization, thus enabling in vivo and ex vivo measurements.[23, 24, 49, 50] One obstacle for measuring NO accurately in biological milieu is interfering species such as nitrite, acetaminophen and ascorbic acid,[23] and thus almost all effective NO sensor designs include a membrane to reduce the diffusion of such interferents to the working electrode. For example, Teflon®, Nafion®, and silicon rubber (SiR) membranes restrict the diffusion of anionic nitrite and larger molecules relative to NO.[42, 44, 50, 51] While these membranes are effective at limiting a select group of interferences, such membranes do not enable selectivity over all of the interfering species encountered in vivo. We recently reported the synthesis of fluorinated

xerogel sensor membranes capable of excluding nitrite, acetaminophen, ascorbic acid, uric acid, ammonia, and dopamine, even at high concentrations (i.e., 100 μM).[45]

The style of electrode platform (i.e., needle-type, planar, microfluidic) is often dependent on the intended measuring environment. Planar macroelectrodes provide excellent sensitivity to NO, but only when large volumes of sample fluid are available. For small sample aliquots (<1 mL), miniaturized sensors are necessary.[41, 47] To measure NO intravascularly, Malinski et al. fabricated a Teflon-coated NO microsensor that was able to track NO in the blood stream of humans in real time before and after the administration of bradykinin.[47] Unfortunately, the clinical success of intravascular sensors is hindered by biofouling (i.e., protein adsorption, platelet adhesion, and clot formation), limiting sensor lifetime to only a few hours. While ex vivo measurements are possible, most current sensor designs require a stirred solution that introduces noise and demands large sample volumes (>1 mL).

In contrast to standalone sensors, microfluidic technology allows for reduced sample volume and minimal sample handling, and thus address many of the shortcomings of existing analytical methodology required in clinical settings.[52, 53] With respect to NO, Spence et al. used microfluidics to measure NO from stimulated endothelial cells with a planar carbon ink electrode fabricated within a polydimethylsiloxane (PDMS)-based microfluidic channel.[54] An unfortunate caveat of using hydrophobic PDMS for microfluidic channel fabrication is an inaccurately low measurement since gases readily diffuse through PDMS.[54] Recognizing this problem, Cha et al. reported the fabrication of a catalytic gold/indium tin oxide microfluidic NO sensor with non-NO-permeable polyethylene tetraphthalate/polyurethane channels, thus minimizing NO loss.[55] Of note,

the design and necessary hand-assembly of this device is not amenable to larger-scale production made possible by photolithographic microfabrication.

Herein, we report the fabrication of a microfluidic NO sensor using standard photolithographic techniques amenable to rapid and inexpensive fabrication. The analytical performance of the device in phosphate buffered saline (PBS) make it ideal for measuring NO in small volumes of complex biological matrices at low concentrations.

5.2 Materials and Methods

(Heptadecafluoro-1,1,2,2-tetrahydrodecyl)trimethoxysilane (17FTMS) was purchased from Gelest (Tullytown, PA). Methyltrimethoxysilane (MTMOS), ascorbic acid, acetaminophen, and sodium nitrite were purchased from Sigma (St. Louis, MO). Nitric oxide (99.5%), nitrogen, and argon gases were obtained from National Welders Supply (Raleigh, NC). Other solvents and chemicals were analytical-reagent grade and used as received. A Millipore Milli-Q UV Gradient A10 System (Bedford, MA) was used to purify distilled water to a final resistivity of 18.2 MΩ·cm and a total organic content of <6 ppb. Whole porcine blood was obtained in 1:10 EDTA from healthy pigs at the Frances Owen Blood Lab (University of North Carolina, Chapel Hill, NC).

5.2.1 Preparation of working electrodes. Planar platinum (Pt) electrodes were fabricated on a glass substrate via photolithography and evaporative metal deposition. Glass substrates (4 × 4 in) were cleaned with distilled water, isopropanol, N_2, and then dried on a hotplate at 95 °C for 5 min. After cooling to RT, photoresist (Microposit S1813, Microchem Corp., Newton, MA) was deposited via spincoating at 3000 rpm for 45 s and then soft-baked at 115 °C for 2 min. The electrode pattern was exposed through a mylar mask for 10 s using a Karl Suss MA6/BA6 mask aligner (hard contact, 100 μm

gap) equipped with a 350 W UV lamp. The pattern was developed in an AZ400 alkaline developer for 1 min, thoroughly rinsed with distilled water, dried with N_2, and post-baked on a hotplate at 115 °C for 2 min. To form a recessed electrode region, the exposed glass was etched in buffered oxide etch (BOE) to a depth of ~150 nm, then rinsed in distilled water and dried with N_2. The exposed glass surface was further cleaned in an oxygen plasma at 100 W for 1 min. To form the electrodes, 10 nm Ti and 150 nm Pt were deposited in a magnetron sputterer. The substrate was soaked in acetone to liftoff the remaning photoresist and excess metal, resulting in patterned electrodes on the glass substrate.

5.2.2 Electrode characterization. To evaluate the sensitivity of the NO sensors, amperometric measurements were performed using a CH Instruments 700 B 8-channel potentiostat (Austin, TX). The electrochemical cell consisted of a microfabricated planar Pt working electrode, an Ag/AgCl reference electrode, and a coiled Pt wire counter electrode.

A saturated NO solution (1.9 mM) was prepared as described previously by purging phosphate-buffered saline (PBS; 0.01 M, pH 7.4) with Ar for 30 min to remove oxygen. Nitric oxide (99.5%) was then bubbled through this solution for at least 30 min.[45] The NO gas was purified before use by passing it a column with KOH pellets to remove trace NO degradation products. Glass substrates containing the sensors were diced into 4 sections, each containing 16 electrodes. The connections between the electrodes and solder-on pads were insulated with S1813. Wires were soldered to the connection pads to allow connection to the potentiostat. The electrodes were polarized at +0.7 V in a stirred solution of PBS until a steady background current was attained (>1 h). Nitric oxide

sensitivity was measured by injecting sequentially increasing aliquots of a saturated NO solution into the PBS, resulting in a measured change in oxidation current. Background noise was measured as the standard deviation of the background current measured at each electrode before injection of NO.

5.2.3 Membrane synthesis and deposition. Working electrode-modified glass substrates were rinsed with distilled water, dried with N_2, and heated to 95 °C for 5 min. After cooling, an adhesion layer of MTMOS was deposited by spin-coating 3 mL of a 1:3 (v:v) dilution of MTMOS in ethanol onto the substrate at 3000 rpm. The fluoroalkoxysilane membrane solution was synthesized via the acid catalyzed hydrolysis and condensation of 17FTMS and MTMOS as reported previously.[45] Absolute ethanol (600 µL), MTMOS (120 µL), 17FTMS (30 µL), distilled water (160 µL), and 0.5 M HCl (10 µL) were added sequentially to a 1.5 mL microcentrifuge tube, mixing vigorously between the addition of each component, and then vortexed for 1 h. Working in 16 electrode batches, 100 µL of the sol solution was pipetted across the working electrodes, and then tilted gently in all directions for 90 s to ensure even coating. The membrane solution was quickly dried by spinning at 600 rpm for 1 min. The xerogel was dried overnight in ambient conditions to facilitate adequate curing. This process was then repeated for the remaining electrodes. Membrane thicknesses were characterized with a profilometer (P15, KLA-Tencor Corp., San Jose, CA).

5.2.4 Microfluidic device fabrication. Reference electrodes were fabricated on the substrate with the working and counter electrodes. The substrate was cleaned, patterned with S1813 photoresist, and plasma-treated as described above. To fabricate reference electrodes, 20 nm Ti and 1.5 µm Ag was deposited in a magnetron sputterer. The

substrate was soaked in acetone to liftoff the remaning photoresist and excess metal, resulting in patterned Ag electrodes. Pseudo-reference electrodes were formed via chemical oxidation of the Ag electrodes by reaction in 50 mM $FeCl_2$ for 15 s, followed by thorough rinsing with distilled water. To form channel walls and insulate electrode connections, KMPR® 1010 was patterned on the substrate. Briefly, KMPR was deposited twice via spin-coating at 500 rpm for 10 sec and 1500 rpm for 45 sec. The substrate was soft-baked at 100 °C for 5 min, exposed to UV light through a mylar mask for 15 sec, and then developed in SU-8 developer for 4 min. After rinsing with distilled water, the substrate was dried with N_2, and hard-baked at 150 °C for 10 min. To complete the assembly of the device, a glass microscope slide with pre-drilled inlet and outlet vias was used as the top lid. A thin layer of KMPR was spin-coated onto the glass slide at 3000 rpm for 45 sec and soft-baked for 5 min at 100 °C to bond the glass slide to the KMPR patterned on the bottom substrate,. The glass slide was then fusion-bonded onto the bottom substrate by clamping the components together with spring clamps and baking at 100 °C for 1 h. The ends of the channel were sealed and 8 mm dia inlet/outlet reservoirs were affixed using a high-strength, chemical-resistant epoxy (Hysol E-120HP; Henkle Corp., Morrisville, NC). Electrical wires were soldered directly to the solder-on pads of each electrode, facilitating an electrical connection.

5.2.5 Microfluidic device characterization. To evaluate the performance of the microfluidic device, the working, counter, and reference electrodes were connected to a CH Instruments 1030A 8-channel potentiostat. By attaching a 1.5 inch length of tygon tubing to the inlet reservoir and filling it with PBS, flow was maintained by gravity alone at a rate of 15 μL/min. The device was polarized for up to 1 h at +0.7 V vs. the AgCl

pseudo-reference electrode by flowing PBS into the device. To calibrate the device, solutions of deoxygenated PBS containing increasing concentrations of NO were added to the sample reservoir. To assess the selectivity of the device, solutions of nitrite, acetaminophen, and ascorbic acid (100 μM in water) were added to the sample reservoir. The sensitivity of the microfluidic device was tested in both anticoagulated whole blood (5 mM EDTA) and simulated wound fluid (10% v/v fetal bovine serum in water). Saturated NO solution was added to 1 mL aliquots of blood and wound fluid, mixed briefly, and added to the sample reservoir. To maintain a flow rate of 15 μL/min when using whole blood, a small vacuum via was applied at the device outlet using a venturi pump.

5.3 Results and Discussion

5.3.1 Working electrode fabrication and characterization. Several types of microfabricated working electrodes have been utilized for NO sensing.[45, 46, 54, 55] For example, Spence and coworkers employed a carbon ink electrode deposited in a PDMS channel and coated with Nafion for selectivity over nitrite.[54] Cha et al. utilized a catalytic gold-hexacyannoferrate layer on a gold/indium tin oxide electrode coated with a gas-permeable membrane as their selective working electrode.[55] The Schoenfisch lab has successfully utilized platinum electrodes for NO sensing via multiple electrode platforms.[45, 46] To simplify the microfabrication process and avoid the use of carbon inks or catalytic layers, platinum electrodes were employed in this study. Microfabricated NO electrodes were fabricated using standard photolithographic techniques and metal evaporation, resulting in 150 nm thick Pt electrodes as measured by a quartz crystal

microbalance. An intermediate 10 nm layer of Ti was added between the glass and Pt layer to improve adhesion of the electrode to the glass surface. The working electrodes were also recessed ~150 nm into the glass substrate via buffered oxide etch (BOE) etching prior to metal evaporation, thus ensuring successful liftoff of excess metal during the fabrication. The general design for the electrode pattern is illustrated in Figure 5.1. To fully elucidate the effect of electrode surface area on the sensitivity and background, electrode widths were varied from 50–1000 μm. The sensitivity of the electrodes was characterized via amperometry in stirred PBS (pH 7.4) by adding aliquots of a saturated NO solution (1.9 mM). As expected, the sensitivity of each electrode scaled linearly with electrode surface area (Figure 5.2). Nitric oxide sensitivity ranged from 0.94 pA/nM for the 50 μm wide Pt electrodes to 17.3 pA/nM for the 1000 μm wide electrodes. Background noise (RMS) also scaled linearly with electrode surface area from 43.2 to 301 pA for the 50 μm and 1000 μm wide electrodes, respectively. Noise for the bare electrode was relatively high, resulting in limits of detection (LOD) ranging from 80-277 nM NO. However, much of the background noise was attributed to inductive coupling of the magnetic stir plate to the planar electrodes, fluctuating PBS levels during convection, and/or lack of a selective membrane.

A commonly employed strategy for enhancing the sensitivity of bare Pt electrodes for NO is platinization, where the electrodeposition of Pt black results in a rough Pt surface with greater surface area.[45] Platinization may be performed by cycling the potential of a Pt electrode immersed in chloroplatanic acid. The deposition of Pt black on the electrode occurs via a 3 step, 8 electron process outline in Scheme 5.1.[56] As expected, platinization of the microfabricated planar Pt electrodes did enhance the

sensitivity to NO in a stirred solution of PBS. However, noise levels were also increased drastically for the larger electrode widths (≥500 μm), resulting in poor LOD for NO. The LOD for electrodes with widths <500 μm was lower for platinized electrodes, demonstrating that modification of electrodes with Pt black would potentially benefit smaller electrodes. A comparison of the sensitivity and LOD for bare and platinized sensors of select widths is provided in Table 5.1. Platinization was not utilized further for this study because of the noise introduced at each electrode. However, the strategy may be utilized for future versions of the NO electrodes if additional sensitivity enhancement is required.

5.3.2 Membrane deposition and characterization. To ensure adequate selectivity for NO over interfering species and reduce background noise, a fluorinated alkoxysilane xerogel membrane (20% 17FTMS-MTMOS) was deposited over the microfabricated electrodes. We previously reported the high selectivity obtainable using 17FTMS membranes when applied via dip-coating to platinum-modified tungsten conical wire electrodes.[45] Of note, this coating method was not feasible for the microfabricated planar Pt electrodes as selective and consistent deposition on only the electrode surface could not be adequately controlled. Instead, a combination of spread and spin-casting were employed. Application of a negative photoresist (S1813) mask was first utilized to allow for selective deposition of the membrane solution over the working, but not the counter and reference electrodes.

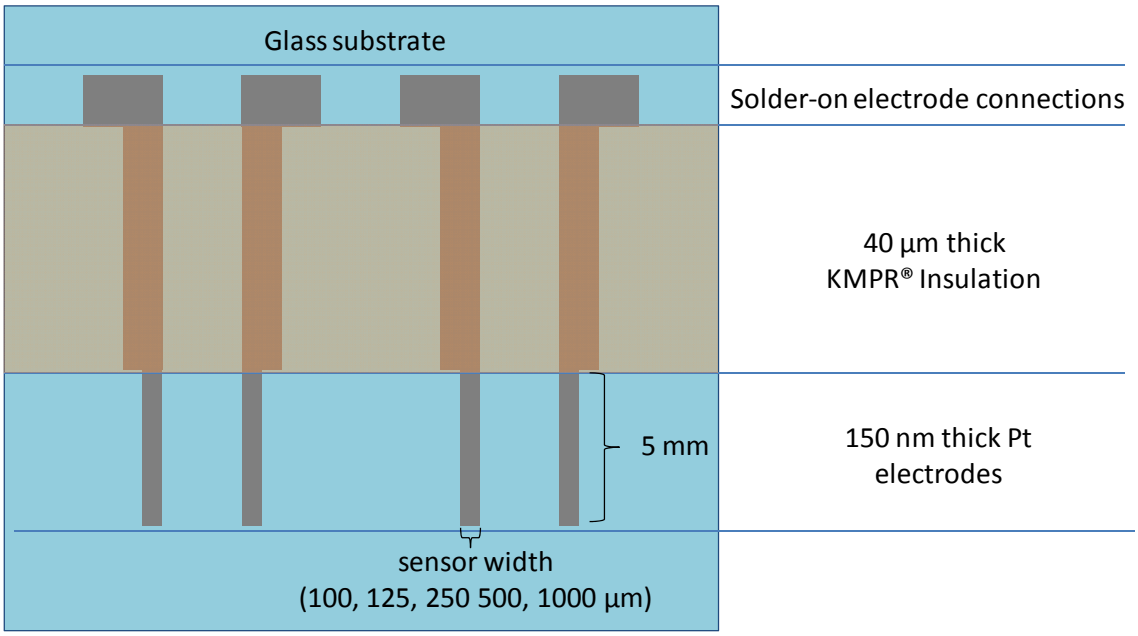

Figure 5.1. Illustration of a Pt working electrode pattern on a glass substrate.

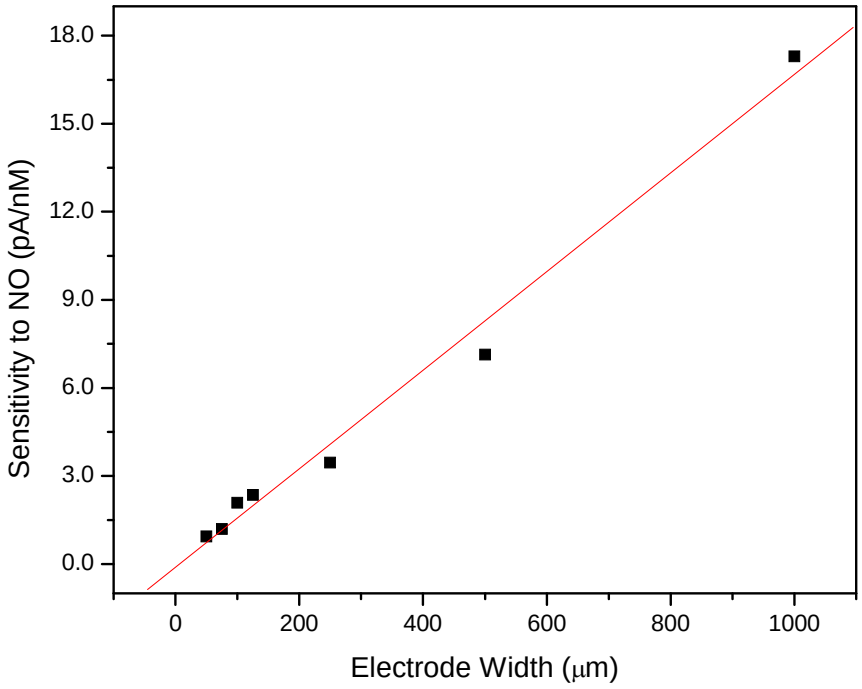

Figure 5.2. The effect of working electrode width on sensitivity to NO ($R^2 = 0.99$).

Scheme 5.1. Electrochemical platinization reactions.

$$Pt^{IV}Cl_6^{2-} + 2e^- \rightleftharpoons Pt^{II}Cl_4^{2-} + 2Cl^- \quad (1)$$

$$Pt^{II}Cl_4^{2-} + 2e^- \rightleftharpoons Pt + 4Cl^- \quad (2)$$

$$Pt^{IV}Cl_6^{2-} + 4e^- \rightleftharpoons Pt + 6Cl^- \quad (3)$$

Table 5.1. Electrode sensitivity and limit of detection for NO as a function of widths between bare platinum (Pt) and platinum-black-coated (PtB) electrode.

	Sensor width							
	75 μm		100 μm		500 μm		1000 μm	
	Pt	PtB	Pt	PtB	Pt	PtB	Pt	PtB
Sensitivity (pA/nM)	1.9	6.3	2.2	5.7	6.1	11	17	26
Limit of Detection (nM)	200	38	260	60	312	820	337	2400

After allowing some of the ethanol to evaporate, thus increasing the solution viscosity, the substrate was spun at 600 rpm to remove excess xerogel solution. Initial testing showed that the ethanol present in the membrane solution slightly dissolved and mixed with the photoresist. As such, S1813 that had incorporated into the xerogel was dissolved during liftoff of the photoresist mask, weakening and cracking parts of the xerogel membrane. Nevertheless, enough of the xerogel membrane remained intact to allow for preliminary testing of an assembled microfluidic device. A second method of deposition was later employed to avoid problems encountered with the ethanol compatibility of the S1813 photoresist. In this method, the counter and reference electrodes were deposited onto the lid of the microfluidic device rather than on the same substrate as the working electrodes to avoid the need for a photoresist mask for the xerogel. Spread casting was utilized to deposit the membrane solution, and the substrate was tilted slightly in all directions to evenly coat the electrodes. This technique ensured that a precise volume of sol solution was deposited on the substrate, resulting in consistent average thicknesses of 500 nm over each electrode as determined by profilometry. The effectiveness of both membrane deposition strategies are discussed below.

Characterization of with respect to sensitivity and selectivity was carried out in a stirred solution of PBS to confirm that the membrane allowed adequate sensitivity to NO and selectivity over interfering species. One immediate benefit of the NO-selective membrane was significant noise reduction observed for non-platinized electrodes. Although the sensitivity of the membrane-coated electrodes was reduced slightly (2.2 to 2.0 pA/nM NO for 100 μm and 17 to 13 pA/nM NO for 1000 μm electrodes), the decreased noise resulted in improved LOD. For example, the LOD observed with the

fluorinated membrane at the 100 and 1000 μm electrodes was reduced by 97 % (260 to 6 nM NO) and 94% (337 to 21 nM NO), respectively. Interestingly, membrane-coated platinized electrodes were characterized by a slow response to NO and significant signal drift. For this reason, platinization was not utilized further to enhance NO electrode sensitivity.

The selectivity of the membrane-coated electrodes for NO over nitrite, ascorbic acid, and actetaminophen was evaluated in a stirred PBS solution. Interferent concentrations used in the study were chosen to be well in excess of the expected physiological concentrations. As expected, the sensitivities of the 100 and 1000 μm electrodes to NO were ~4 orders of magnitude greater than the sensitivities for the interferents, with the exception of ascorbic acid, where the NO response was only ~2.5 orders of magnitude greater than the interferent for the 1000 μm electrodes.

5.3.3 Reference electrode fabrication and characterization. Due to the small size of the microfluidic channel, a traditional solution-based Ag/AgCl reference could not be utilized for this device. Many groups have utilized wire pseudo-reference electrodes in the construction of microfluidic sensors. For example, Spence et al. placed a Pt quasi reference electrode at the solution outlet of their PDMS-based NO measurement device.[54] However, this design was found to be practical only if the distance between the electrode and the outlet reservoir is small enough to minimize electrical resistance. Cha et al. utilized an oxidized silver wire pseudo reference electrode inserted next to the working electrode in the channel, although this approach required careful hand positioning of the electrode during fabrication.[55] More precise positioning and integration of reference electrodes may be attained via microfabrication of the reference electrode within the

microfluidic channel. Typically, this may be achieved by first depositing a silver electrode, and then chemically or electrochemically oxidizing the surface. For example, Heuck and Staufer reported the deposition of silver within a microfluidic channel using a Tollens reagent, where aqueous silver was chemically precipitated onto glass, followed by chemical oxidation with ferric chloride.[57] To attain a thick enough silver layer to prevent disintegration of the electrode during oxidation, multiple deposition steps were necessary, requiring large volumes of the potentially explosive Tollens reagent. Polk et al. pursued an alternative strategy involving evaporative deposition of the silver electrode.[58] Specifically, a substrate with 150 nm thick Ag electrodes was patterned via evaporative deposition. The thickness of the Ag electrodes was increased to 1–5 μm via electroplating, followed by chemical oxidation with ferric chloride. While the electrodes were found to be stable for up to 4 d of continuous use, the measured potentials were not uniform among the entire batch of electrodes, likely owing to inconsistent electrochemical plating.

To simplify the process of reference electrode fabrication, thick films of Ag (~1.5 μm) were deposited onto a thin (10 nm) Ti adhesion layer. Two negative photoresist layers, a liftoff resist (LOR) bottom layer and S1813 top layer, were used to pattern the electrodes (Figure 5.3B). The use of the additional LOR layer resulted in undercutting of the S1813 photoresist. After deposition of the silver layer, the undercut photoresist prevents a connection of the thick silver layer between the electrodes and the excess silver deposited around the electrodes that may result in “dog ears” after liftoff (Figure 5.3A) and peeling of the electrode. To further protect the Ag electrodes from peeling, buffered oxide etch (BOE) was utilized prior to metal deposition to form 1.5 μm deep

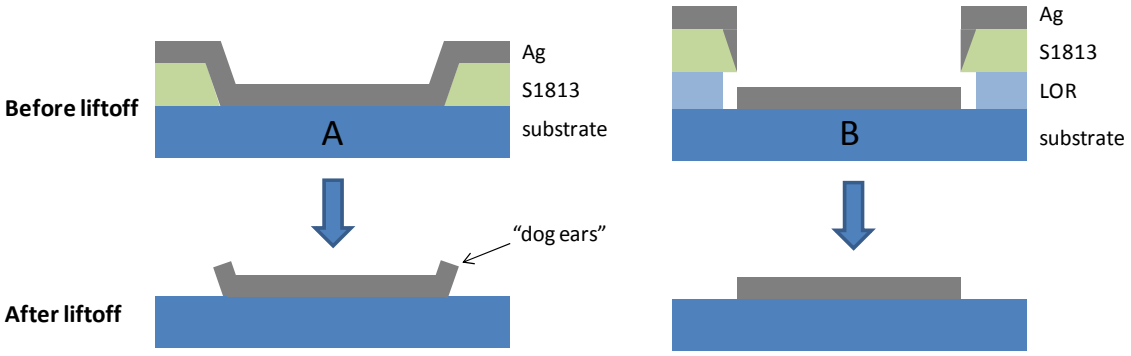

Figure 5.3. Cutaway illustration of reference electrode profile after masking and Ag deposition using A), an S1813 mask only, resulting in "dog ears" after liftoff, and B), a mask composed of both LOR and S1813.

troughs where electrodes could be deposited. The Ag electrodes were then oxidized with ferric chloride prior to assembly of the chip (rather than within the microfluidic channel) to prevent over-oxidation of the Ag by residual ferric chloride that would have been difficult to rinse out of the channel completely.

5.3.4 Microfluidic device assembly. The microfluidic portion of the device was combined with the glass substrate after fabrication of the membrane-coated working electrodes, Pt counter electrodes, and Ag/AgCl working electrodes. Initially, double-sided Kapton® polyimide tape was utilized to form the walls of the microfluidic channel and facilitate attachment of a glass slide as a lid of the channel. Two strips of tape were deposited 3 mm apart across the electrodes so that a portion of each electrode was exposed in the channel. A clean glass slide with via holes at both ends was affixed on top of the tape, forming the microfluidic channel. Flow testing of the device assembled with polyimide tape led to sporadic leakage on some devices. Use of the polyimide tape also resulted in imprecise positioning across the electrodes and difficulty maintaining consistent channel width. To ensure a more precise, leak-free microfluidic channel, a negative photoresist, KMPR, was patterned on the substrate. The KMPR served as both an insulator for the connections between the electrodes and solder-on pads, as well as walls for the microfluidic channel. By precisely controlling spin speed and employing two KMPR depositions, a 40 μm deep, 3 mm wide channel was formed across each set of electrodes (Figure 5.4). A KMPR-coated glass slide with pre-drilled vias was used as the lid of the microfluidic channel. The KMPR on the glass slide was coated on the underside and not exposed with UV prior to assembly, thus allowing fusion bonding to the KMPR deposited on the electrode substrate with only moderate mechanical pressure and heat.

The resulting channel was leak-free upon flow testing and maintained a consistent width across the device. Although only one channel depth and width was utilized for initial studies, flow rate may be controlled by adjusting either parameter. A deep, wide channel was chosen for this design to allow for adequate flow of more viscous biological fluids (e.g., blood and plasma). Hard plastic 8 mm diameter reservoirs attached with epoxy over the inlet and outlet vias provided a means of adding fluids to and removing waste from the microfluidic device (Figure 5.5). A section of tubing attached to the inlet reservoir provided adaquate pressure when filled to drive flow at ~15 μL/min without the need for an external vacuum pump. When using blood and plasma, a variable venturi pump was attached to the outlet via and adjusted to provide a ~15 μL/min flow rate. A photograph of the final microfluidic device with the reservoir tubing installed is shown in Figure 5.6.

5.3.5 Microfluidic device characterization. To characterize performance of the microfluidic NO sensor, the sensitivity and selectivity of the device was tested using constant potential amperometry at a potential of +0.7 V vs. The electrode was polarized in PBS for at most 1 h prior to testing to achieve a steady baseline current. Nitric oxide calibration curves were constructed by adding aliquots of saturated NO to a deoxygenated PBS solution and transferring a small quantity of this solution to the reservoir of the device.

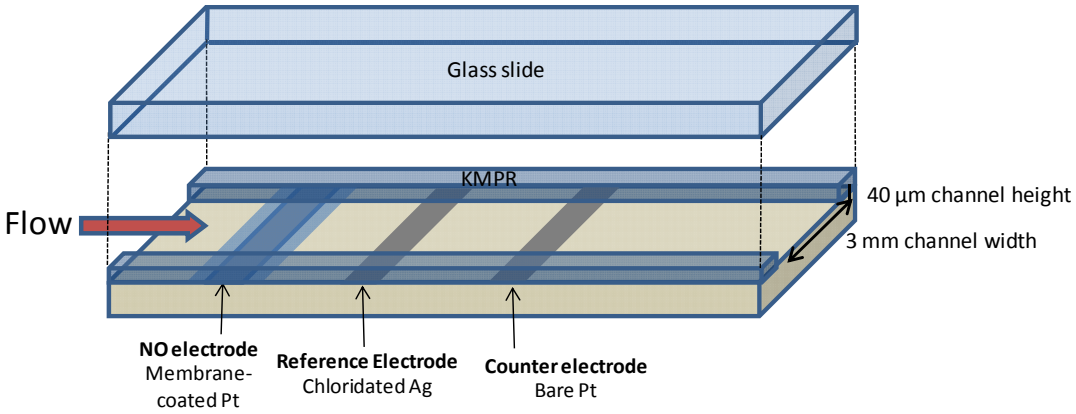

Figure 5.4. Cutaway illustration of microfluidic channel construction.

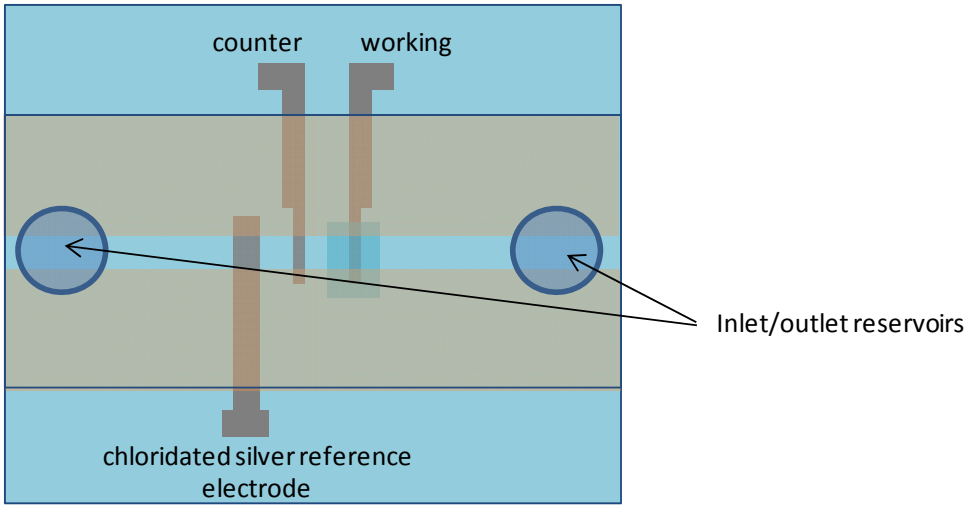

Figure 5.5. Top-view illustration of microfluidic device with placement of inlet and outlet reservoirs.

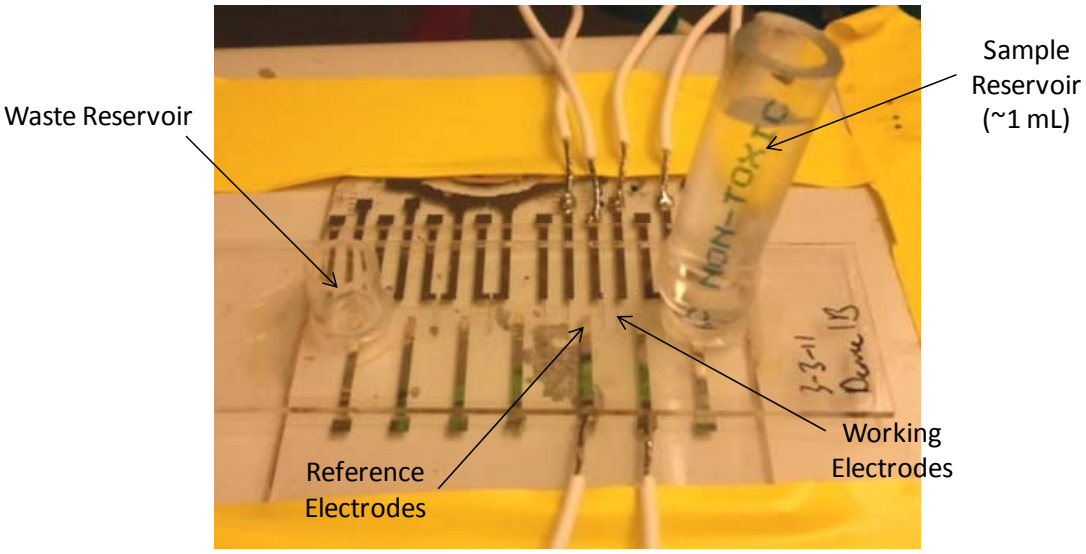

Figure 5.6. Photograph of the microfluidic device with attached sample reservoir.

After the oxidation current stabilized, the NO solution in the reservoir was removed and replaced with a more concentrated NO solution. The real-time NO addition and the NO calibration plot is shown for a 100 μm bare and membrane-coated electrode in Figure 5.7. The sensitivities of the bare and membrane-coated electrodes were measured to be 2.7 and 2.3 pA/nM NO, respectively. As expected, the membrane-coated electrode had a slightly lower sensitivity than the bare electrode due to reduced NO diffusion across the membrane to the electrode surface. The sensitivities for both the bare and coated electrodes were lower for the microfluidic vs. non-microfluidic device because the channel exposes only a portion of the actual electrode area. Despite lower sensitivities, the LODs for both the bare and coated microfluidic electrodes were 590 and 760 pM, ~1 log lower than the same electrodes outside of the microfluidic device. The improvement in the LOD is attributed to lower noise as a result of no convection and/or the elimination of the oscillating magnetic field from the magnetic stir plate. Furthermore, the flow provided to the microfluidic device is driven by either gravity or a venturi pump, preventing the pulsatile noise often encountered for syringe or peristaltic pumps. The selectivity of the microfluidic device over the most common interfering species (i.e., nitrite, acetaminophen, and ascorbic acid) is shown in Figure 5.8. While the bare electrode registered a slight response from nitrite and greater responses from acetaminophen and ascorbic acid, (selectivities of -5, -2.3, and -2.6, respectively), the response from nitrite was undetectable and only slightly detectable for acetaminophen and ascorbic acid (<-6, -4.3, and -3.7, respectively) for devices employing the NO-selective 17FTMS membrane.

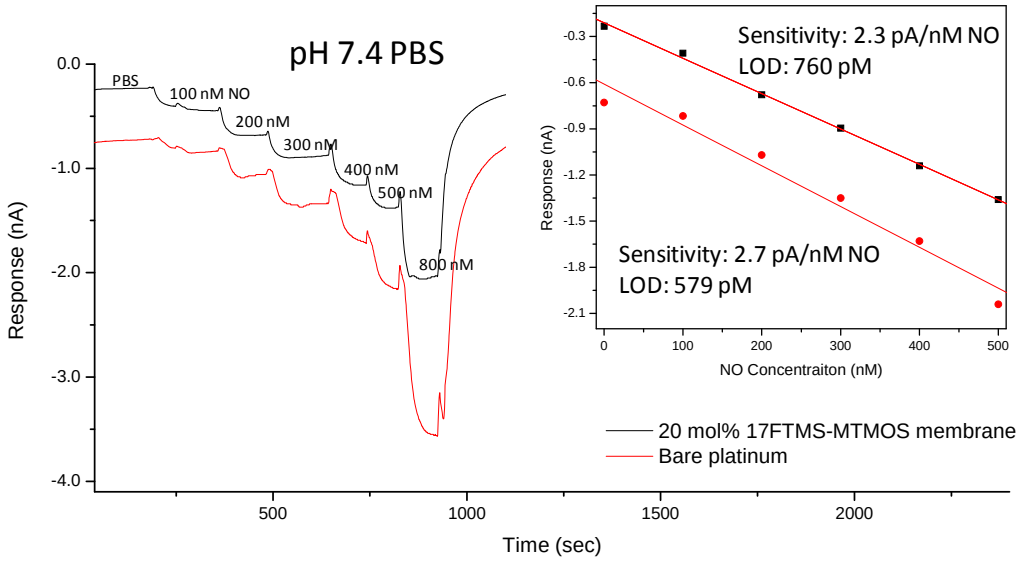

Figure 5.7. Response of bare (gray line) and membrane-coated (black line) microfluidic-based NO sensors to NO in PBS flowing at 15 µL/min. Inset shows NO calibration curves for bare (●) and membrane-coated (■) sensors.

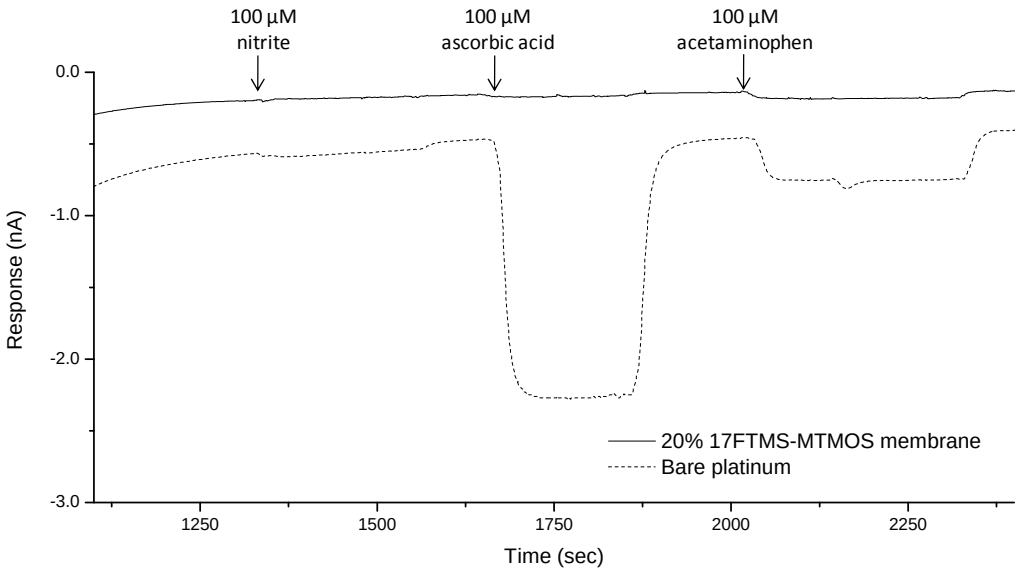

Figure 5.8. Response of bare (dotted line) and membrane-coated (solid line) microfluidic-based NO sensors to interfering species in PBS flowing at 15 µL/min.

5.3.6 Microfluidic NO sensor response in physiological fluids. Since the intended purpose of the microfluidic NO sensor is the detection of NO in biological fluids, the microfluidic NO sensor was next characterized in whole blood and wound fluid, two matrices where NO measurements are clinically useful yet difficult. Indeed, measurement of NO in blood is particularly challenging because of the presence of NO scavengers such as hemoglobin and oxygen. To characterize the sensor response in whole blood, aliquots of an NO solution were added to measured volumes of blood, mixed, and then added to the microfluidic NO sensor where NO was detected at +0.7 V vs. Ag/AgCl. The time elapsed from the injection of NO into the blood aliquot to the addition of the blood to the device did not exceet 10 s. Since blood is more viscous than PBS, a venturi pump was used at the channel outlet to provide a constant flow rate of 15 μL/min. As shown in Figure 5.9, clean blood was initially flowed into the device, followed by blood aliquots with NO concentrations increasing by 5 μM, resulting in detectable and consistent increases in the magnitude of the oxidation current due to NO measured at the working electrode. Upon adding clean blood into the microfludic NO sensor, the current returned to the original baseline level. Although the sensitivity for NO in blood was decreased compared to PBS (56 pA/μM NO in blood vs. 2.3 pA/nM NO in PBS), the reduced noise inherent to the microfluidic sensor reduced the LOD to a biologically-reasonable level of 225 nM. To test the practical lower NO concentration limits of the device, NO concentrations in blood were changed in 500 nM increments (Figure 5.10). In doing so, the sensitivity range of the potentiostat was reduced, resulting in a lower calculated LOD for NO in blood (~50 nM). The resulting LOD of 50 would be well below the required

LOD needed for detecting NO in blood during sepsis, for example, where NO concentrations have been reported to exceed 10 μM.[11, 12, 59]

Since NO is believed to be a potential prognostic biomarker for wound healing progress,[13-15, 60] the operation of the microfluidic NO sensor was also tested in simulated wound fluid (10% fetal bovine serum in water) (Figure 5.11). The resulting LOD was 2 nM, 1-2 orders of magnitude lower than in blood, attributable to the absence of scavenging from blood proteins and hemoglobin.

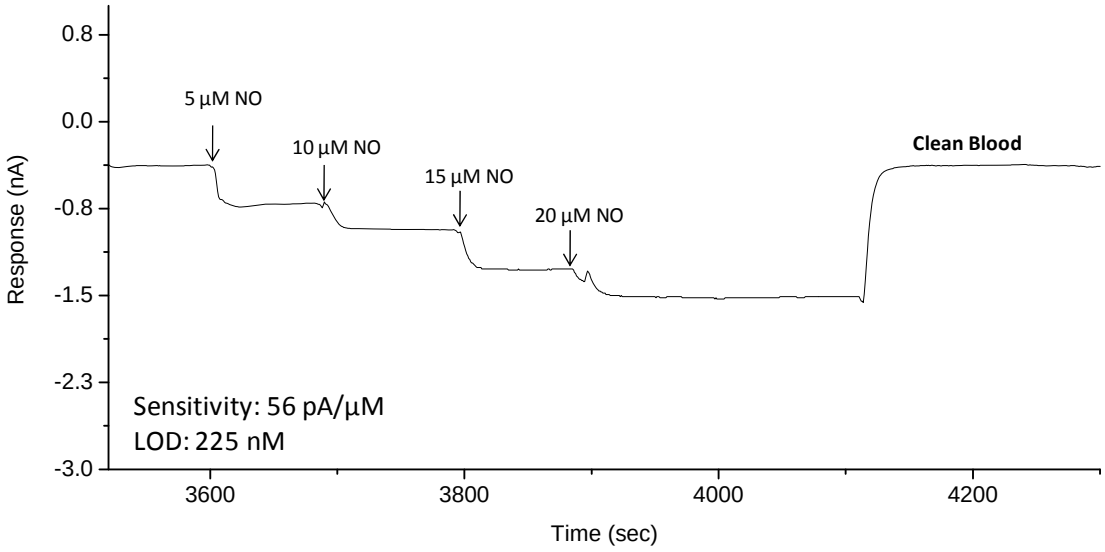

Figure 5.9. Response of membrane-coated microfluidic-based NO sensor to 5 µM increases of NO concentrations in whole blood flowing at 15 µL/min.

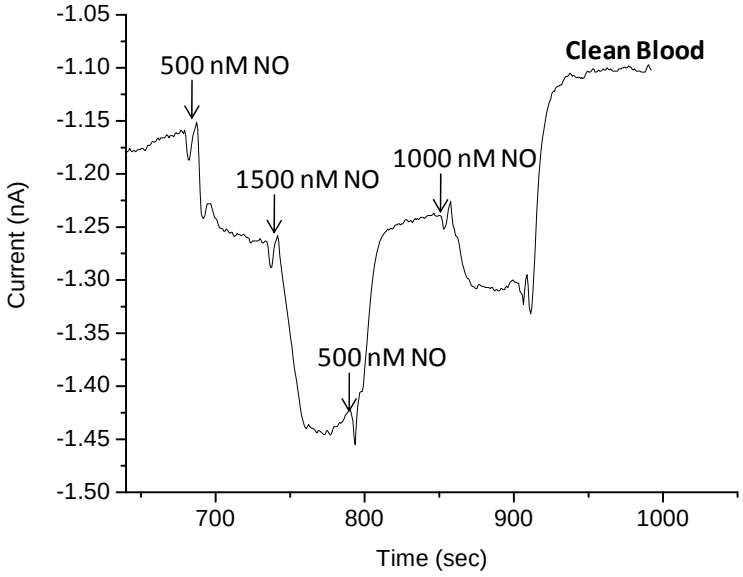

Figure 5.10. Response of membrane-coated microfluidic-based NO sensor to various concentrations of NO in whole blood flowing at 15 μL/min.

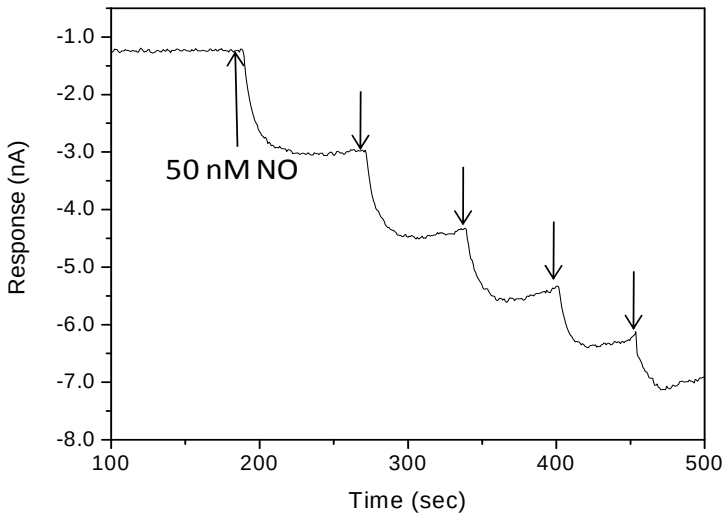

Figure 5.11. Response of membrane-coated microfluidic-based NO sensor to 50 nM increases of NO concentrations in 10% FBS flowing at 15 µL/min.

5.4 Conclusions

The use of a selective fluorinated membrane in combination with an electrochemical microsensor within a microfluidic device enables highly sensitive detection of NO in challenging biological matrices such as blood and simulated wound fluid. In contrast to previously reported devices, the use of standard photolithographic microfabrication techniques makes the assembly highly amenable to rapid, large-scale production. The resulting microfluidic sensor was characterized by excellent sensitivity for NO in PBS, (2.3 pA/nM), and selectivity over interfering species (<-6, -4.3, and -3.7 for nitrite, ascorbic acid, and acetaminophen, respectively). The low background noise levels of the electrochemical microfluidic device resulted in very low LODs for NO in PBS, blood, and simulated wound fluid (760 pM, 50 nM, and 2 nM, respectively). To date, the reported 50 nM LOD for NO in blood is the lowest reported for the direct electrochemical detection of NO. Overall, unlike previous NO detection methods, this device provides a platform for quickly measuring NO directly at very low concentrations in small volumes of biological fluids.

A number of possible applications exist that may be well served by this technology. In the field of skin wounds, the need for tools to assess the progress of wound healing and the efficacy of treatment is significant. Although the role of NO in wound healing has been studied,[61-64] the correlation between NO and prognosis (i.e., whether the wound will heal) is not well understood. The low LOD for NO in wound fluid may aide in more accurate measurement of NO during wound healing. Furthermore, this knowledge may provide a tool for better assessing treatment efficacy. Nitric oxide also plays an important role in the immune response to pathogens.[12, 65, 66] Indeed, NO

concentrations >10 μM have been measured indirectly (using the griess assay) during clinical sepsis. By utilizing the microfluidic NO sensor to measure NO in blood, an improved evaluation of how NO levels change during sepsis may be undertaken. In addition, this device may enable an examination of NO as a potential biomarker for sepsis prognosis.

5.5 References

1. Ignarro, L. J.; Buga, G. M.; Wood, K. S.; Byrns, R. E.; Chaudhuri, G. "Endothelium-derived relaxing factor produced and released from artery and vein is nitric-oxide," *Proc. Natl. Acad. Sci. U. S. A.* 1987, *84*, 9265-9269.

2. Khan, M. T.; Furchgott, R. F. "Similarities of behavior of nitric-oxide (NO) and endothelium-derived relaxing factor in a perfusion cascade bioassay system," *Fed. Proc.* 1987, *46*, 385-385.

3. Rapoport, R. M.; Murad, F. "Agonist-induced endothelium-dependent relaxation in rat thoracic aorta may be mediated through Cgmp," *Circ. Res.* 1983, *52*, 352-357.

4. Ignarro, L. J. *Nitric Oxide: Biology and Pathobiology*; Academic Press: San Diego, 2000.

5. McCleverty, J. A. "Chemistry of nitric oxide relevant to biology," *Chem. Rev.* 2004, *104*, 403-418.

6. Thomas, D. D.; Ridnour, L. A.; Isenberg, J. S.; Flores-Santana, W.; Switzer, C. H.; Donzelli, S.; Hussain, P.; Vecoli, C.; Paolocci, N.; Ambs, S.; Colton, C. A.; Harris, C. C.; Roberts, D. D.; Wink, D. A. "The chemical biology of nitric oxide: Implications in cellular signaling," *Free Radical Biol. Med.* 2008, *45*, 18-31.

7. Wink, D. A.; Mitchell, J. B. "Chemical biology of nitric oxide: Insights into regulatory, cytotoxic, and cytoprotective mechanisms of nitric oxide," *Free Radical Biology and Medicine* 1998, *25*, 434-456.

8. Knowles, R. G.; Moncada, S. "Nitric oxide synthases in mammals," *Biochem. J.* 1994, *298*, 249-258.

9. Zhou, L.; Zhu, D. Y. "Neuronal nitric oxide synthase: Structure, subcellular localization, regulation, and clinical implications," *Nitric Oxide-Biol. Chem.* 2009, *20*, 223-230.

10. Dudzinski, D. M.; Igarashi, J.; Greif, D.; Michel, T. "The regulation and pharmacology of endothelial nitric oxide synthase," *Annu. Rev. Pharmacol. Toxicol.* 2006, *46*, 235-276.

11. Strand, Ø. A.; Leone, A.; Geircksky, K.-E.; Kirkebøen, K. A. "Nitric oxide indices in human septic shock," *Crit. Care. Med.* 2000, *28*, 2779-2785.

12. Ochoa, J. B.; Udekwu, A. O.; Billiar, T. R.; Curran, R. D.; Cerra, F. B.; Simmons, R. L.; Peitzman, A. B. "Nitrogen oxide levels in patients after trauma and during sepsis," *Ann. Surg.* 1991, *214*, 621-626.

13. Luo, J. D.; Chen, A. F. "Nitric oxide: a newly discovered function on wound healing," *Acta Pharmacol. Sin.* 2005, *26*, 259-264.

14. Isenberg, J. S.; Ridnour, L. A.; Espey, M. G.; Wink, D. A.; Roberts, D. D. "Nitric oxide in wound-healing," *Microsurgery* 2005, *25*, 442-451.

15. Soneja, A.; Drews, M.; Malinski, T. "Role of nitric oxide, nitroxidative and oxidative stress in wound healing," *Pharmacological Reports* 2005, *57*, 108-119.

16. Donnini, S.; Ziche, M. "Constitutive and inducible nitric oxide synthase: Role in angiogenesis," *Antioxidants & Redox Signaling* 2002, *4*, 817-823.

17. Morbidelli, L.; Donnini, S.; Ziche, M. "Role of nitric oxide in the modulation of angiogenesis," *Current Pharmaceutical Design* 2003, *9*, 521-530.

18. Al-Ani, B.; Hewett, P. W.; Ahmed, S.; Cudmore, M.; Fujisawa, T.; Ahmad, S.; Ahmed, A. "The release of nitric oxide from *S*-nitrosothiols promotes angiogenesis," *Plos One* 2006, *1*, e25.

19. Kuwabara, M.; Kakinuma, Y.; Ando, M.; Katare, R. G.; Yamasaki, F.; Doi, Y.; Sato, T. "Nitric oxide stimulates vascular endothelial growth factor production in cardiomyocytes involved in angiogenesis," *Journal of Physiological Sciences* 2006, *56*, 95-101.

20. Schoenfisch, M. H.; Mowery, K. A.; Rader, M.; Meyerhoff, M. E. "Improving the biocompatibility of intravascular amperometric oxygen sensors via nitric oxide release," *Book of Abstracts, 216th ACS National Meeting, Boston, August 23-27 FIELD Full Journal Title:Book of Abstracts, 216th ACS National Meeting, Boston, August 23-27* 1998, ANYL-062.

21. Stamler, J. S. "Nitric oxide in the cardiovascular system," *Coronary Artery Dis.* 1999, *10*, 273-276.

22. Marxer, S. M.; Robbins, M. E.; Schoenfisch, M. H. "Sol-gel derived nitric oxide-releasing oxygen sensors," *Analyst* 2005, *130*, 206-212.

23. Privett, B. J.; Shin, J. H.; Schoenfisch, M. H. "Electrochemical nitric oxide sensors for physiological measurements," *Chemical Society Reviews* 2010, *39*, 1925-1935.

24. Bedioui, F.; Villeneuve, N. "Electrochemical nitric oxide sensors for biological samples - Principle, selected examples and applications," *Electroanalysis* 2003, *15*, 5-18.

25. Davies, I. R.; Zhang, X. J. "Nitric oxide selective electrodes," *Methods in Enzymol.* 2008, *436*, 63-95.

26. Hetrick, E. M.; Schoenfisch, M. H. "Analytical chemistry of nitric oxide," *Annu. Rev. Anal. Chem.* 2009, *2*, 409-433.

27. Allen, B. W.; Liu, J.; Piantadosi, C. A. "Electrochemical detection of nitric oxide in biological fluids," *Methods Enzymol.* 2005, *396*, 68-77.

28. Oblak, T. D. A.; Root, P.; Spence, D. M. "Fluorescence monitoring of ATP-stimulated, endothelium-derived nitric oxide production in channels of a poly(dimethylsiloxane)-based microfluidic device," *Analytical Chemistry* 2006, *78*, 3193-3197.

29. Gomes, A.; Fernandes, E.; Lima, J. "Use of fluorescence probes for detection of reactive nitrogen species: A review," *Journal of Fluorescence* 2006, *16*, 119-139.

30. Griess, J. P. "Bemerkungen zu der Abhandlung der HH. Weselsky und Benedikt „Ueber einige Azoverbindungen"," *Ber. Dtsch. Chem. Ges.* 1879, *12*, 426-429.

31. Archer, S. "Measurement of nitric-oxide in biological models," *Faseb Journal* 1993, *7*, 349-360.

32. Mehta, S.; Javeshghani, D.; Datta, P.; Levy, R. D.; Magder, S. "Porcine endotoxemic shock is associated with increased expired nitric oxide," *Critical Care Medicine* 1999, *27*, 385-393.

33. Hurst, R. D.; Clark, J. B. "The utility of the nitric oxide electrochemical sensor in biomedical research," *Sensors FIELD Full Journal Title:Sensors* 2003, *3*, 321-329.

34. Brisby, H.; Ashley, H.; Diwan, A. D. "In vivo measurement of facet joint nitric oxide in patients with chronic low back pain," *Spine* 2007, *32*, 1488-1492.

35. Brovkovych, V.; Stolarczyk, E.; Oman, J.; Tomboulian, P.; Malinski, T. "Direct electrochemical measurement of nitric oxide in vascular endothelium," *J. Pharm. Biomed. Anal.* 1999, *19*, 135-143.

36. Brown, F. O.; Finnerty, N. J.; Lowry, J. P. "Nitric oxide monitoring in brain extracellular fluid: characterisation of Nafion (R)-modified Pt electrodes in vitro and in vivo," *Analyst* 2009, *134*, 2012-2020.

37. Dalbasti, T.; Kilinc, E. "Microelectrode for in vivo real-time detection of NO," *Methods Enzymol.* 2005, *396*, 584-592.

38. Fan, C. H.; Li, G. X.; Zhu, J. Q.; Zhu, D. X. "A reagentless nitric oxide biosensor based on hemoglobin-DNA films," *Anal. Chim. Acta* 2000, *423*, 95-100.

39. Griveau, S.; Dumezy, C.; Seguin, J.; Chabot, G. G.; Scherman, D.; Bedioui, F. "In vivo electrochemical detection of nitric oxide in tumor-bearing mice," *Anal. Chem.* 2007, *79*, 1030-1033.

40. Hart, C. M.; Kleinhenz, D. J.; Dikalov, S. I.; Boulden, B. M.; Dudley, S. C., Jr. "The measurement of nitric oxide production by cultured endothelial cells," *Methods Enzymol.* 2005, *396*, 502-514.

41. Malinski, T.; Mesaros, S.; Patton, S. R.; Mesarosova, A. "Direct measurement of nitric oxide in the cardiovascular system," *Physiological Research* 1996, *45*, 279-284.

42. Malinski, T.; Taha, Z. "Nitric-oxide release from a single cell measured insitu by a porphyrinic-based microsensor," *Nature* 1992, *358*, 676-678.

43. Oh, B. K.; Robbins, M. E.; Schoenfisch, M. H. "Development and characterization of nitric oxide microsensor for surface nitric oxide measurements from NO-releasing sol-gels," *Abstracts, 56th Southeast Regional Meeting of the American Chemical Society, Research Triangle Park, NC, United States, November 10-13* 2004, GEN-332.

44. Oh, B. K.; Robbins, M. E.; Schoenfisch, M. H. "Planar nitric oxide (NO)-selective ultramicroelectrode sensor for measuring localized NO surface concentrations at xerogel microarrays," *Analyst* 2006, *131*, 48-54.

45. Shin, J. H.; Privett, B. J.; Kita, J. M.; Wightman, R. M.; Schoenfisch, M. H. "Fluorinated xerogel-derived microelectrodes for amperometric nitric oxide sensing," *Analytical Chemistry* 2008, *80*, 6850-6859.

46. Shin, J. H.; Weinman, S. W.; Schoenfisch, M. H. "Sol-gel derived amperometric nitric oxide microsensor," *Analytical Chemistry* 2005, *77*, 3494-3501.

47. Vallance, P.; Patton, S.; Bhagat, K.; Macallister, R.; Radomski, M.; Moncada, S.; Malinski, T. "Direct measurement of nitric-oxide in human-beings," *Lancet* 1995, *346*, 153-154.

48. Zhang, X. J. "Real time and in vivo monitoring of nitric oxide by electrocehmical sensors - From dream to reality," *Frontiers in Bioscience* 2004, *9*, 3434-3446.

49. Cha, W. S.; Anderson, M. R.; Zhang, F. H.; Meyerhoff, M. E. "Amperometric S-nitrosothiol sensor with enhanced sensitivity based on organoselenium catalysts," *Biosensors & Bioelectronics* 2009, *24*, 2441-2446.

50. Zhang, X. J.; Cardosa, L.; Broderick, M.; Fein, H.; Lin, J. "An integrated nitric oxide sensor based on carbon fiber coated with selective membranes," *Electroanalysis* 2000, *12*, 1113-1117.

51. Wang, S.; Lin, X. "Electrodeposition of Pt-Fe(III) nanoparticle on glassy carbon electrode for electrochemical nitric oxide sensor," *Electrochim. Acta FIELD Full Journal Title:Electrochimica Acta* 2005, *50*, 2887-2891.

52. Yager, P.; Edwards, T.; Fu, E.; Helton, K.; Nelson, K.; Tam, M. R.; Weigl, B. H. "Microfluidic diagnostic technologies for global public health," *Nature* 2006, *442*, 412-418.

53. Cai, X. X.; Klauke, N.; Glidle, A.; Cobbold, P.; Smith, G. L.; Cooper, J. M. "Ultra-low-volume, real-time measurements of lactate from the single heart cell using microsystems technology," *Analytical Chemistry* 2002, *74*, 908-914.

54. Spence; Dana, M.; Torrence; Nicholas, J.; Kovarik; Michelle, L.; Martin; Scott, R. "Amperometric determination of nitric oxide derived from pulmonary artery endothelial cells immobilized in a microchip channel," *The Analyst* 2004, *129*, 6.

55. Cha, W.; Tung, Y.-C.; Meyerhoff, M. E.; Takayama, S. "Patterned electrode-based amperometric gas sensor for direct nitric oxide detection within microfluidic devices," *Anal. Chem.* 2010, *82*, 3300-3305.

56. Feltham, A. M.; Spiro, M. "Variation of area of platinized platinum-electrodes with deposition potential at constant mass degree of platinization," *Journal of Electroanalytical Chemistry* 1972, *35*, 181-192.

57. Heuck, F.; Staufer, U. "Silver/silver-chloride electrode fabrication in closed micro-fluidic capillaries," *Microelectron. Eng.* 2010, *87*, 1383-1385.

58. Polk, B. J.; Stelzenmuller, A.; Mijares, G.; MacCrehan, W.; Gaitan, M. "Ag/AgCl microelectrodes with improved stability for microfluidics," *Sensors and Actuators B-Chemical* 2006, *114*, 239-247.

59. Brovkovych, V.; Stolarczyk, E.; Oman, J.; Tomboulian, P.; Malinski, T. "Direct electrochemical measurement of nitric oxide in vascular endothelium," *J. Pharm. Biomed. Anal.* 1999, *19*, 135-143.

60. Boykin, J. V. "Wound nitric oxide bioactivity A promising diagnostic indicator for diabetic foot ulcer management," *Journal of Wound Ostomy and Continence Nursing* 2010, *37*, 25-32.

61. Witte, M. B.; Barbul, A. "Role of nitric oxide in wound repair," *The American Journal of Surgery* 2002, *183*, 406-412.

62. Stallmeyer, B.; Kampfer, H.; Kolb, N.; Pfeilschifter, J.; Frank, S. "The function of nitric oxide in wound repair: Inhibition of inducible nitric oxide-synthase severely impairs wound reepithelialization," 1999, *113*, 1090-1098.

63. Schwentker, A.; Vodovotz, Y.; Weller, R.; Billiar, T. R. "Nitric oxide and wound repair: role of cytokines?," *Nitric Oxide* 2002, *7*, 1-10.

64. Rizk, M.; Witte, M. B.; Barbul, A. "Nitric oxide and wound healing," *World Journal of Surgery* 2004, *28*, 301-306.

65. Dhillon, S. S.; Mahadevan, K.; Bandi, V.; Zheng, Z. L.; Smith, W.; Rumbaut, R. E. "Neutrophils, nitric oxide, and microvascular permeability in severe sepsis," *Chest* 2005, *128*, 1706-1712.

66. Kirkebøen, K. A.; Strand, Ø. A. "The role of nitric oxide in sepsis – an overview," *Acta Anaesthesiol. Scand.* 1999, *43*, 275-288.

Chapter 6

Summary and Future Research Directions

6.1 Summary

The efficacy of superhydrophobic and NO-releasing surfaces, the fabrication and characterization of a microfluidic NO sensor, and the evaluation of bacterial resistance to exogenous NO was described in the preceding chapters. In Chapter 2, the efficacy of NO-releasing xerogel surfaces against the pathogenic fungus *C. albicans* was evaluated using three adhesion and viability assays. In the first assay, a parallel plate flow cell was utilized to quantify cellular adhesion to the surfaces as a function of NO release. The adhesion of *C. albicans* to the coatings with the highest NO fluxes was reduced by 52% compared to control (non-NO-releasing) surfaces. The viability of the adhered fungus was characterized via nucleic acid staining in combination with fluorescence microscopy. Cell death was observed after 11 h of fungal exposure to the surface with the highest NO flux. The reduction in viability due to NO was confirmed using a quantitative viability assay where cells were adhered to control and NO-releasing substrates, incubated in PBS for 15 h, removed from the surface via sonication, and then enumerated via plating on nutrient agar. The viability of fungal cells exposed to the highest flux of NO was reduced by 42% versus cells exposed to the lowest flux of NO. Biofilms of *C.*

albicans often result after initial adhesion to a surface and are notoriously difficult to treat. Thus, the efficacy of the NO-releasing xerogels against biofilm development was studied by incubating NO-releasing and control surfaces in a bacteria/nutrient broth suspension for 2 d. Environmental scanning electron microscopy was used to interrogate these substrates; much less biofilm formation was observed at the NO-releasing surfaces. The amount of biofilm was reduced even further upon combining NO release with sub-therapeutic doses of silver sulfadiazine.

The synthesis of superhydrophobic surfaces composed of fluorinated silica colloids doped into a fluorinated xerogel was described in Chapter 3. The surface topography was assessed via both SEM and AFM, and revealed a coating composed of both micro- and nano-structured features. The resulting interface was characterized by having a static water contact angle of >165°. The coating was stable after no change in the static water contact angle of the coating was measured after 15 d of immersion in distilled water. Using a combination flow cell and sonication viability assay, the ability of the coating to resist the adhesion of *P. aeruginosa* and *S. aureus* was described in PBS. These superhydrophobic surfaces reduced the adhesion of both bacteria by ~2 orders of magnitude vs. control surfaces.

Studies investigating the likelihood that exogenous NO release may foster the emergence of NO-resistance in bacteria were described in Chapter 4. Several gram-positive and gram-negative bacteria species were exposed to both repeated sub-therapeutic doses of NO (serial passage mutagenesis) and single bactericidal doses of NO (spontaneous mutagenesis) from NO-releasing nitrosothiol particles. No significant increase in NO resistance was observed for bacteria during the spontaneous mutagenesis

or the serial passage mutagenesis assays. While this study is by no means comprehensive in the types of NO-releasing materials and associated NO release kinetics available, it provides a blueprint for future testing of bacterial resistance to NO.

The fabrication and characterization of a microfluidic electrochemical NO sensor for physiological measurements was presented in Chapter 5. Using standard photolithographic methods, working, counter, and reference electrodes were patterned onto a glass substrate. Microfluidic channels were then positioned across the electrodes along with a lid with access ports to fabricate a device capable of selectively measuring NO in small sample volumes (< 1 mL). The device was characterized in PBS with a limit of detection (LOD) of 760 pM and >4 orders of magnitude selectivity for NO over common interfering species (e.g., nitrite, ascorbic acid, and acetaminophen). The ability to determine NO levels in whole blood and simulated wound fluid was demonstrated with LODs for NO of 50 and 2 nM, respectively, making it well suited for potential clinical measurements.

6.2 Future research directions

Future studies related to the efficacy of NO-releasing surfaces against fungal adhesion, proliferation, and biofilm formation should focus on increasing the NO-release capabilities of these xerogels. To this end, Storm and Schoenfisch are developing methods to pre-modify the aminosilanes precursors prior to xerogel synthesis and deposition, thus maximizing the amount of NO available for release.[1] By increasing the NO release rate and amounts, it is hypothesized that the bactericidal efficacy would be

further enhanced. A study is also planned to utilize the enhanced permeability afforded by the pre-NO-modified coating for electrochemical glucose sensor membranes. It has been previously demonstrated that NO release reduces fibrous encapsulation and enhance angiogenesis surrounding implants.[2-5] Thus, NO-releasing glucose sensor membranes may enhance the clinical utility of implanted glucose sensors by increasing glucose delivery and diffusion to the electrode.

Future studies related to fluorinated silica colloid-based superhydrophobic coatings should be aimed at improving the scratch-resistance and robustness of the coatings on a variety of surfaces including glass, polymers, and metals. Development of the coatings for use on medical devices would necessitate in vivo biocompatibility studies where coated implants are intentionally seeded with bacteria. Studies in our lab are currently planned to evaluate the antimicrobial efficacy of superhydrophobic surfaces in combination with surface-released NO. By doping NO-releasing nanoparticles into the superhydrophobic coating,[6-9] NO-releasing superhydrophobic surfaces may be possible. The combination of NO release with a superhydrophobic surface may more significantly enhance antimicrobial efficacy by killing any microbes that do manage to adhere to the superhydrophobic surfaces. Future work should also explore the suitability of the superhydrophobic coatings for other applications including biofouling reduction on boat hulls,[10] water distribution pipes,[11] and anti-icing surfaces for aircraft.[12]

While no increased NO resistance was observed in the resistance assays for a select number of bacteria tested, it is well known that the development of resistance to antimicrobials depends on both the type of bacteria and the conditions of exposure (i.e., antimicrobial concentration and kinetics, growth conditions, time of exposure).[13] Future

studies must thus focus on the evaluation of other NO-releasing materials that are being developed for possible clinical use, as well as expanding the range of microbial species utilized in the tests. Should an increase in NO-resistance be observed, genetic analysis should be undertaken to identify if DNA mutations or changes in RNA expression are responsible. Such information would be useful for optimizing NO-releasing therapeutics and identifying synergistic NO/drug combinations that would reduce the likelihood of developing further bacterial resistance.

Lastly, the developed microfluidic electrochemical NO sensor should be further evaluated in real samples. Toward this end, future work will focus on the optimization of device parameters (e.g., electrode size, microfluidic geometry, and membrane thickness) to improve the sensitivity and selectivity of the device in biological matrices such as blood and wound fluid. Subsequent work should evaluate the capabilities of the device in determining the time course of NO in various physiological processes such as wound healing and sepsis. Studies are already planned to utilize the microfluidic NO sensor for measuring changes in NO concentration in a porcine sepsis model and evaluating the efficacy of NO measurements as a diagnostic and prognostic biomarker for sepsis. Nitric oxide may also be a useful biomarker for evaluating the progress of wound healing and associated treatments.[14, 15] Future studies must be designed to understand the time course of NO during the stages of wound healing and during the course of therapeutic treatment. By varying the device fabrication parameters (i.e., microfluidic geometry, membrane composition, and electrochemical technique), the device may be utilized for measuring multiple analytes to give a better diagnosis. For example, by adding the ability to detect

nitrate, nitrate, nitrosothiols oxygen, glucose, and lactate, a field portable comprehensive diagnostic device may be fabricated.

By making slight modifications to the device, the NO sensor could also be used to evaluate NO-releasing therapeutics such as nanoparticles, dendrimers, small molecules, and polymers. Results from a report in preparation by Hunter et al. demonstrate that electrochemical detection of NO is superior in terms of sensitivity to traditional NO measurement techniques (i.e., Griess assay and chemiluminescence), especially in complex nutrient broths and physiological milieu.[16] By adapting the microfluidic NO sensor described in Chapter 5 to measure NO-releasing materials in situ, NO release in complex media may be accurately assessed.

6.3 Conclusions

As the demand for implanted medical devices increases, the development of creative strategies for preventing microbial adhesion and proliferation on medical devices will be critical. Novel surfaces that release antimicrobials that are biocidal via multiple mechanisms (i.e., NO) may allow for more effective antimicrobial coatings that do not foster resistance. Passive strategies such as superhydrophobic coatings are particularly important because they do not foster antimicrobial-resistant microbes. In addition, superhydrophobic surfaces may be applied to solve other commercial problems such as preventing the fouling of marine hulls, water pipes, and condenser coils, and preventing condensation and ice buildup on optical and aircraft surfaces. The demand is also increasing for diagnostic tools that diagnose and monitor treatment progress of diseases. Sensors that measure NO, a biomolecule implicated in immune response to infection,

may play a key role in the diagnosis and prognosis of several conditions including sepsis, wound healing, cancer, and neurodisorders. By allowing measurements to be performed in small volumes of fluid, microfluidic NO sensors may enable more rapid bedside diagnosis. These devices may also serve as platforms for evaluating NO-releasing therapeutics in vitro and during clinical use.

6.4 References

1. Storm, W. L.; Schoenfisch, M. H. "Enhanced nitric oxide storage and glucose permeability of pre-diazeniumdiolated xerogels," In preparation.

2. Schoenfisch, M. H.; Nablo, B. J.; Robbins, M. E.; Butler, R. D.; Klitzman, B. "Nitric oxide release as a means for improving the tissue-compatibility of in vivo subcutaneous glucose biosensors.," *Abstracts of Papers of the American Chemical Society* **2004**, *228*, U159-U160.

3. Shin, J. H.; Schoenfisch, M. H. "Improving the biocompatibility of in vivo sensors via nitric oxide release," *Analyst* **2006**, *131*, 609-615.

4. Hetrick, E. M.; Prichard, H. L.; Klitzman, B.; Schoenfisch, M. H. "Reduced foreign body response at nitric oxide-releasing subcutaneous implants," *Biomaterials* **2007**, *28*, 4571-4580.

5. Shin, J. H.; Marxer, S. M.; Schoenfisch, M. H. "Nitric oxide-releasing sol-gel particle/polyurethane glucose biosensors," *Anal. Chem. FIELD Full Journal Title:Analytical Chemistry* **2004**, *76*, 4543-4549.

6. Riccio, D. A.; Nugent, J. L.; Schoenfisch, M. H. "Stöber synthesis of nitric oxide-releasing *S*-nitrosothiol-modified silica particles," *Chemistry of Materials* **2010**, *23*, 1727-1735.

7. Hetrick, E. M.; Shin, J. H.; Paul, H. S.; Schoenfisch, M. H. "Anti-biofilm efficacy of nitric oxide-releasing silica nanoparticles," *Biomaterials* **2009**, *30*, 2782-2789.

8. Hetrick, E. M.; Shin, J. H.; Stasko, N. A.; Johnson, C. B.; Wespe, D. A.; Holmuhamedov, E.; Schoenfisch, M. H. "Bactericidal efficacy of nitric oxide-releasing silica nanoparticles," *ACS Nano* **2008**, *2*, 235-246.

9. Shin, J. H.; Metzger, S. K.; Schoenfisch, M. H. "Synthesis of nitric oxide-releasing silica nanoparticles," *J. Am. Chem. Soc.* **2007**, *129*, 4612-4619.

10. Genzer, J.; Efimenko, K. "Recent developments in superhydrophobic surfaces and their relevance to marine fouling: a review," *Biofouling* **2006**, *22*, 339-360.

11. Blossey, R. "Self-cleaning surfaces - virtual realities," *Nat. Mater.* **2003**, *2*, 301-306.

12. Saleema, N.; Farzaneh, M.; Paynter, R. W.; Sarkar, D. K. "Prevention of ice accretion on aluminum surfaces by enhancing their hydrophobic properties," *Journal of Adhesion Science and Technology* **2010**, *25*, 27-40.

13. Martinez, J. L.; Baquero, F. "Mutation frequencies and antibiotic resistance," *Antimicrob. Agents Chemother.* **2000**, *44*, 1771-1777.

14. Schwentker, A.; Vodovotz, Y.; Weller, R.; Billiar, T. R. "Nitric oxide and wound repair: role of cytokines?," *Nitric Oxide* **2002**, *7*, 1-10.

15. Witte, M. B.; Barbul, A. "Role of nitric oxide in wound repair," *The American Journal of Surgery* **2002**, *183*, 406-412.

16. Hunter, R. A.; Coneski, P. N.; Privett, B. J.; Schoenfisch, M. H. "Quantitative methodologies for nitric oxide measurement in biological media," In preparation.